THE INFLUENCE OF LENGTH CHANGE SPEED AND DIRECTION ON

DYNAMIC FUNCTION POTENTIATION IN FAST MOUSE MUSCLE

Daniel Caterini, BKin

Submitted in partial fulfillment of the requirements for the degree of
Master of Science in Applied Health Sciences
(Kinesiology)

Under the supervision of Rene Vandenboom, Ph.D

Faculty of Applied Health Sciences, Brock University

St. Catharines, Ontario

ABSTRACT

The purpose of this study was to test the hypothesis that the potentiation of dynamic function was dependent upon both length change speed and direction. Mouse EDL was cycled in vitro ($25°$ C) about optimal length (L_o) with constant peak strain ($\pm$ 2.5% L_o) at 1.5, 3.3 and 6.9 Hz before and after a conditioning stimulus. A single pulse was applied during shortening or lengthening and peak dynamic (concentric or eccentric) forces were assessed at L_o. Stimulation increased peak concentric force at all frequencies (range: 19 ± 1 to $30 \pm 2\%$) but this increase was proportional to shortening speed, as were the related changes to concentric work/power (range: -15 ± 1 to 39 ± 1 %). In contrast, stimulation did not increase eccentric force, work or power at any frequency. Thus, results reveal a unique hysteresis like effect for the potentiation of dynamic output wherein concentric and eccentric forces increase and decrease, respectively, with work cycle frequency.

ACKNOWLEDGEMENTS

I would like to thank everyone who positively influenced my time here at Brock. It was the support and encouragement from faculty and friends that aided in the completion of this document. Specifically, I want to thank Dr. Rene Vandenboom as his passion for his work was truly inspirational. His meticulous work habits and constructive suggestions have not only aided in my development and maturation as a student, but as an individual as well. I would also like to thank Bill Gittings (M.Sc) as his countless hours devoted to training, as well as collaborating in lab were fundamental to my work. Bill represents an exemplary model of a leader, coworker and friend. Also, my committee members; Dr. Sullivan, Dr. Roy and Dr. Grange, were very approachable and offered helpful suggestions which assisted in fine tuning this document. Their kindness and patience were much appreciated and will not be forgotten.

Furthermore, a thank-you must also be extended to Dr. Stull and colleagues at the University of Texas Southwestern Medical School for generously analyzing myosin RLC phosphate content for us.

Finally, I would like to thank my fellow graduate students as each day brought exciting and rewarding experiences together. Their support both in and out of the lab was most comforting, and assisted in completion of this degree.

TABLE OF CONTENTS

LIST OF ABBREVIATIONS

EDL = Extensor digitorum longus

WT, KO = Wildtype, Knockout

skMLCK, CaM = Myosin Light Chain Kinase, Calcium-Calmodulin

RLC, ELC = Regulatory/ Essential Light Chain

MHC = Myosin Heavy Chain

LMM, HMM = Light, Heavy Meromyosin

S1, S2 = Subfragment-1, 2

Tm, Tn = Tropomyosin, Troponin

EC-C = Excitation-Contraction Coupling

SR = Sarcoplasmic Reticulim

DHPR, RyR = Dihydropyridine Receptor, Ryanodine Receptor

$\mathbf{P_o, P_t}$ = Peak Tetanic Force, Peak Twitch Force

$\mathbf{V_{max}, V_o}$ = Maximal Shortening Velocity, Unloaded Shortening Velocity

+dP/dt, -dP/dt = Rate of Force Development, Relaxation

SID = Shortening-Induced Deactivation

PTP = Post-Tetanic Potentiation

$\mathbf{Ca^{2+}}$ = Calcium

$\mathbf{P_i}$ = Inorganic Phosphate

CS = Conditioning Stimulus

LFF = Low Frequency Fatigue

MLCP = Myosin Light Chain Phosphatase

$\mathbf{L_o}$ = Optimal Muscle Length

$\mathbf{f_{app}, g_{app}}$ = Forward and Reverse Rate Constants of Crossbridge Formation

LIST OF TABLES

LIST OF FIGURES

INTRODUCTION

The muscular system is unique in its ability to respond and adapt to environmental stressors. Skeletal muscle, in particular, performs many important functions as it provides thermogenic assistance to aid in heat loss, offers storage reserves for nutritional intake, as well as plays a vital role in locomotion by shortening against a definite load, thus performing work. In contracting muscles the binding of myosin heads to active sites on the thin filament, and subsequent energy release results in translation of the myosin heads along the thin filament, thereby generating positive work. Such actomyosin interaction and subsequent ATP hydrolysis causes an increase in potential energy within the muscle which results in energy being released as heat, or converted into kinetic energy for work. Therefore, the movement of myosin along the thin filament is a result of mechanical work generated by the energy released during chemical reactions within a muscle fiber. However, this alone does not ensure optimal force production. A concept derived from the early crossbridge model of Huxley (1957) can be used to explain this mechanism. In essence, muscle contraction stems from the transition of crossbridges from non-force generating, to force generating states. An increase in the population of crossbridges in a force generating state will maximize force output (Sweeney and Stull, 1990). Conversely, with a greater percentage of crossbridges in a non-force generating state, a muscle fiber will experience reduced force output, as well as total work generated. Thus, increases in the population, and duration that crossbridges spend in a force generating state will in turn augment net work production.

Interestingly, in response to previous contractile activity, striated skeletal muscle demonstrates a remarkable ability to transiently enhance its performance. Previous work with skinned and isolated skeletal muscles have demonstrated that the regulatory light chain (RLC) of myosin is phosphorylatable (Morgan, Perry, and Ottaway, 1979; Perrie, Smillie, and Perry, 1973), and that this corresponds with previous contractile activity, thereby providing force enhancing, or "potentiating" effects (Manning and Stull, 1979; Manning and Stull, 1982). Potentiation of force is therefore a mechanism by which the inhibition of contractile performance by fatigue may be reduced. Early studies by Manning and Stull demonstrated that peak isometric twitch force (P_t) can be increased after a tetanic stimulation, and that this was correlated to the phosphorylation of the RLC. These findings suggest that a potential fatigue resisting mechanism may exist within fast-twitch skeletal muscle fibers. This phenomenon is known as posttetanic potentiation (PTP), and exhibits a positive temporal correlation between RLC phosphorylation-dephosphorylation and the potentiation of peak twitch tension (Close and Hoh, 1968; Manning and Stull 1982). The physiological basis for this mechanism stems from the modulation of crossbridge kinetics after an initial contractile performance (MacIntosh, 2003).

Skeletal muscle is therefore capable of increasing RLC phosphate content (Manning and Stull, 1979: 1982), while coincidently augmenting work and power output (Grange, Vandenboom, and Houston, 1995; Grange, Vandenboom, Xeni, and Houston, 1998; Abbate et al., 2000; MacIntosh and Bryan, 2002; Xeni et al., 2011) when contractile activity is preceded by an appropriate conditioning contraction. The concomitant potentiation of work and power can be attributed to an increase in the

transition of crossbridges in a force generating state (f_{app}), increased sensitivity to Ca^{2+} (Persechini, Stull, and Cooke, 1985; Metzger, Greaser, and Moss, 1989; Sweeney and Stull 1990), as well as an altered rate of myosin's association with actin (Manning and Stull, 1982). Ultimately, PTP may allow greater force to be generated at a lower Ca^{2+} activation level, masking the effects of fatigue at low frequencies of stimulation as well as temporarily restoring force to near pre-fatigue levels (Fowles and Green, 2003). Although it is clear that RLC phosphorylation in striated skeletal muscle is not regulatory, this putative phenomenon may modulate contractility such that "normal" performance may be enhanced.

Taken together, it is evident that muscle performance is highly plastic due to its inherent ability to respond to external stressors. Contractile activity may be modulated depending on the concentration of intracellular metabolites, as well as structural modifications. Although RLC phosphorylation is not required for contraction in striated skeletal muscle, its effects may assist in reducing force deficits present during fatigue and increasing net work output, suggesting a modulatory role for its existence. To date, much of our understanding of PTP has been derived from isometric fiber studies, using a range of submaximal stimulation frequencies to examine these unique properties. Although this research has been essential in defining the mechanistic basis for potentiation, it lacks physiological relevance as skeletal muscles *in vivo* are better represented by a dynamic model. Grange and colleagues have explored physiological function, and the effects of potentiation during length changes simulating dynamic activation in isolated fast-twitch skeletal muscle of mice. Notably, previous studies suggested that the extent of fiber displacement, as well as the work and power output are significantly potentiated after a

conditioning stimulus (CS) which elicited a five-fold elevation in RLC phosphate content (Grange et al., 1995). Such enhancements can be depicted as an upward shift in the force-displacement and force-velocity relationships, coinciding with potentiation of isometric force and maximal rate of isometric force development ($+dF/dt_{max}$).

In order to further elucidate a functional purpose for RLC phosphorylation *in vivo*, examination of work and power output during cyclic contractions is warranted (Grange et al., 1998). Considering locomotion is a result of the mechanical work generated by skeletal muscle, and the speed of locomotion depends on the mechanical power output, these measures are excellent indicators of physiological contractile performance (Allen, lamb and Westerblad, 2008). From a performance perspective, an important functional property of skeletal muscle is not its peak tetanic force, but rather the peak power it is capable of producing while being constrained by load and speed. Therefore, the inhibition of force by fatigue can significantly affect the maximal work performed, and power produced during a work cycle. Therein provides merit for understanding how modulation of contractile mechanics can affect locomotor performance. Identifying a mechanism by which a muscle is capable of reducing the inhibition of work and power, and thus augmenting performance may be highly significant for physiological function.

REVIEW OF LITERATURE:

2.0.0 Background

It is important to understand the biochemical basis upon which muscle contraction, cellular fatigue and myosin regulatory light chain phosphorylation occur to understand exactly how they affect function. Excitation at the neuromuscular junction and subsequent crossbridge cycling is the basis of skeletal muscle contraction. Briefly, the binding of Ca^{2+} to troponin C removes steric blocking and allows the myosin head to bind with active sites on the thin filament (Gordon, Homsher, and Regnier, 2000). The resulting interaction between myosin heads and the thin filament allows for the conversion of potential energy into mechanical work via ATP hydrolysis.

Early studies have determined that the regulatory light chains of myosin are capable of phosphorylation after tetanic stimulation, and that this corresponds to transient increases in isometric force production (Perrie et al., 1973; Manning and Stull, 1979; 1982). In fast twitch fibers of skeletal muscle, skeletal muscle myosin light chain kinase (skMLCK), a specific Ca^{2+} calmodulin-dependent kinase, is responsible for RLC phosphorylation. skMLCK phosphorylates the RLC at serine site 15, adding a phosphate to the RLC tail. This structurally modifies the myosin head, causing a disruption in its ordered array along the thick filament backbone (Ritz-Gold, Cooke, Blumenthal, and Stull, 1980; Yang, Stull, Levine and Sweeney, 1998). Ablation of the skMLCK gene prevents RLC phosphorylation (Zhi et al., 2005). Observations in skMLCK knockout mice demonstrated a failure to reproduce the structural modifications and the potentiation of peak twitch force commonly seen in wild types (Zhi et al., 2005; Gittings et al., 2011).

Fig.1- Phosphorylation of the myosin regulatory light chain
(A) The native (unphosphorylated) myosin motor protein is depicted with inactive skeletal muscle myosin light chain kinase (skMLCK$_i$). (B) The same Ca^{2+} signal which regulate crossbridge binding, and thus contractile activity also activates skMLCK from its inactive form (skMLCK$_i$ → skMLCK$_a$). An activated kinase transfers a phosphate group from ATP to serine site 15 on the RLC of myosin. (C) In opposition to skMLCK activity, unregulated activity of protein phosphatases (PP1) removes the phosphate, thus dephosphorylating the RLC. (D) As a result, net phosphate content of the RLC depends on a balance between kinase and phosphatase activity.
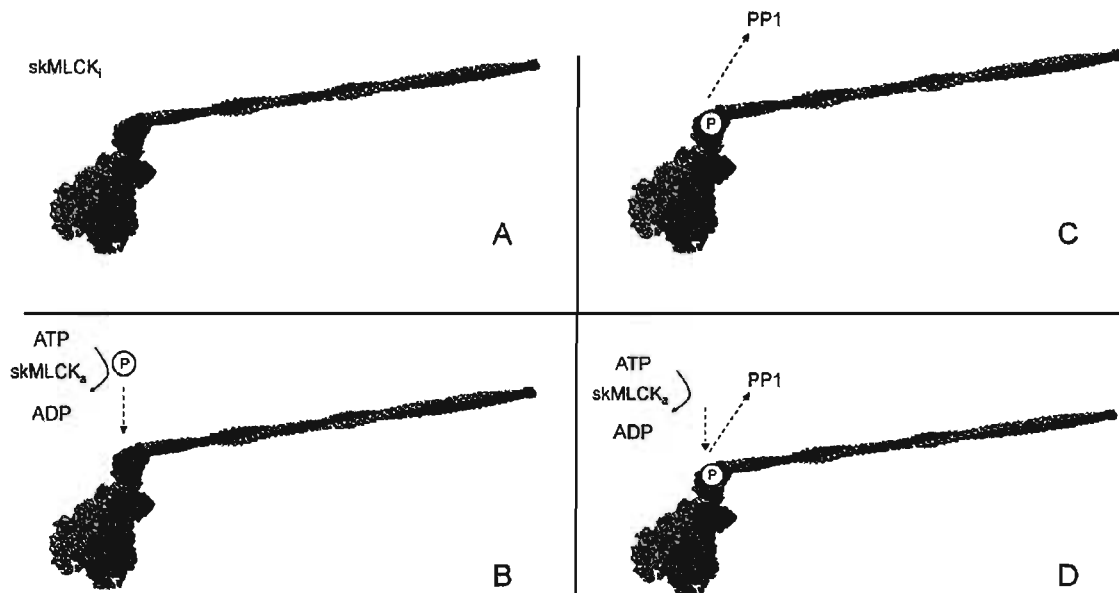
The functional benefit of the conformational change that occurs with phosphorylation is a shift of myosin heads into a more favourable position for binding, thereby enhancing the ability to form strongly bound crossbridges with the thin filament. As a result of this structural change, RLC phosphorylation is thought to improve the Ca^{2+} sensitivity of the contractile apparatus by shifting the force-pCa curve to the left. This increase in Ca^{2+} sensitivity will modulate performance by allowing enhanced force production during fatigue when Ca^{2+} sensitivity is compromised due to accumulation of metabolic by-products (Allen et al., 2008; Fitts 2008).

Ultimately, the effect of increasing force and displacement per stimulus will enhance total work performed by the contractile apparatus as work is the product of force

and displacement. Accordingly, rodent fast-twitch muscle exhibited elevations in dynamic force, work and power output with myosin RLC phosphorylation (Grange et al., 1995; Grange et al., 1998; MacIntosh and Bryan, 2002; Vandenboom et al., 2011). Major efforts have thus been made in identifying the significance of RLC phosphorylation *in vivo*. As a result, this review will dissect contemporary knowledge on the molecular basis for PTP, examining the biochemical and structural characteristics associated with muscle contraction and RLC phosphorylation.

2.1.0 Myosin microanatomy and function

The thick filament is a bipolar polymer of the motor protein myosin (Gordon et al., 2000). Each thick filament sits equidistant between Z-lines, and is anchored in place by binding to a number of structural proteins (Vandenboom 2004). Upon interacting with actin, thick and thin filaments form a strong bond, ultimately producing force and sarcomere shortening (Huxley 1957). Thus, the contractile protein myosin is an ATPase which hydrolyzes ATP to provide energy to perform work when the thick filament slides along the thin filament (Rayment 1996).

Myosin refers to a family of motor proteins with many isoforms. Within skeletal muscle the myosin II isoform is predominate, dissociating into six polypeptide chains in strong denaturing solutions. Myosin II is composed of two heavy chains (molecular weight of ~ 200 kDa), and four light chains (two essential and two regulatory) with molecular weights ranging from ~ 15 to 25,000 kDa (Gordon et al., 2000; Vandenboom 2004). Dimerization of the two structurally similar heavy chains forms a highly asymmetrical molecule with a distinct "head" and "tail" region (Vandenboom 2004).

Under electron microscopy, Lowey and colleagues determined that myosin and its proteolytic fragments can be visualized. Lowey et al., (1969) suggests that the tail region of myosin can be fragmented into heavy meromyosin (HMM), and light meromyosin (LMM) segments. The HMM component can be further split by proteolytic enzymes into a globular head termed subfragment-1 (S1), and a short helical structure tail region considered subfragment-2 (S2) (Lowey et al., 1969). The role of LMM appears to be structural in maintaining organization of the thick filament (Lowey et al., 1969). In comparison, HMM contains essential components required for the formation and cycling of crossbridges. For example, the S2 region is able to bend reversibly away from the axis of the thick filament and bridge the gap between the actin and myosin filaments. As a result, the myosin molecule is designed such that it can readily adjust its length to that required for interaction with actin.

Fig.2. Lowey et al., (1969)- Light and heavy chain components of myosin
Displayed are light meromyosin (LMM) and heavy meromyosin (HMM) components. The myosin heavy chain can is composed of a globular head (S1), containing regulatory and essential light chains (RLC, ELC) as well as a rod like tail (S2).
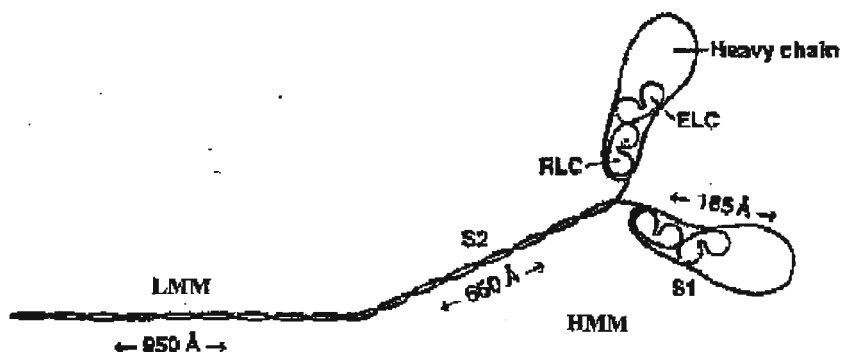
Gordon et al., (2000) suggested that the S1 head is a large globular region which binds to one pair of myosin light chains. The S1 head can be further divided into three

fragments; the N (amino) terminal region (25 kDa), a central/lower region (50 kDa), as well as a C (carboxyl) terminal or upper region (50 kDa). Sweeney, Bowman, and Stull (1993) suggested that the C-terminal region of the myosin heavy chain forms a coiled α-helical rod, separating near the N-terminal to form two globular head regions. Each corresponding head region contains an Mg-ATP binding and hydrolysis site, as well as an actin binding site (Sweeney et al., 1993). The globular S1 region of myosin may function as an actin activated ATPase, however the region containing myosin light chains is critical for the transduction of energy from hydrolysis of ATP into rapid movement (Lowey, Waller, and Trybus, 1993).

Fig. 3. Rayment (1996)- Myosin S1 head and light chain subunits
A closer examination of the subdivisions within the S1 head. This figure highlights the position of both regulatory and essential light chains, as well the nucleotide binding pocket which is located near the 50 kDa cleft. During crossbridge cycling, the lower domain of the S1 head forms a weak interaction with actin and only when strongly bound does the upper domain interact with actin.
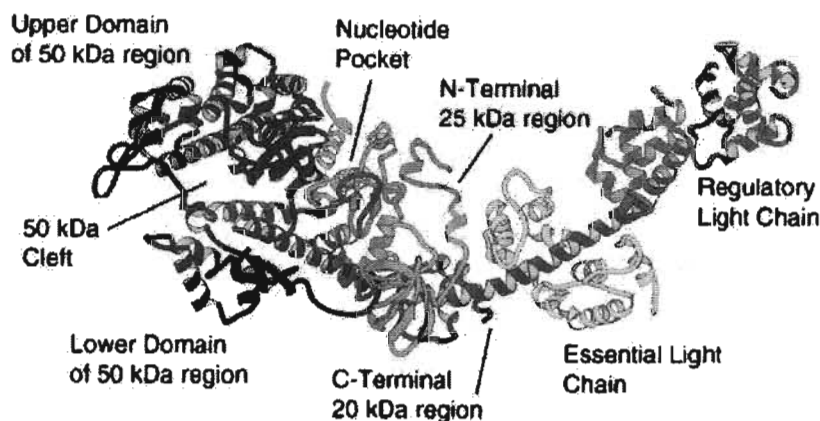
The myosin light chains attach to the N-terminal region and play a significant role in the force generating power stroke (Rayment et al., 1993; Sweeney et al., 1993; Vandenboom 2004). Essential light chains (ELC) can be isolated after an alkali treatment, and are considered a necessary component for stability of the myosin head (Sweeney et al., 1993). Alternatively, an additional light chain is capable of being phosphorylated and

is referred to as the regulatory light chain (RLC) (Perrie et al., 1973). Although both light chain subunits contribute to the structure of the myosin motor, the RLC has also been shown to modulate crossbridge kinetics during contraction (Vandenboom, Xeni, Bestic, and Houston 1997), and thus will be examined more thoroughly in section 2.6.3. The RLC provides primary regulation of muscle contraction in smooth muscle (hence, regulatory), as well as functions to modulate Ca^{2+} activation in mammalian striated muscle (Sweeney et al., 1993). Alteration of contractile performance occurs when Ca^{2+}-calmodulin binds to myosin light chain kinase, activating the enzyme. As a result, serine residue 15 on the RLC is phosphorylated by the active kinase (Sweeney et al., 1993), however this interaction will be examined with greater detail in section 2.6.0.

2.2.0 Excitation contraction-coupling

Dulhunty, (2006) defines excitation contraction-coupling (EC-C) as the process linking the action potential (excitation) with cross-bridge cycling and contraction in striated muscles. The following section will examine the putative mechanism which results in skeletal muscle contraction.

Skeletal muscle contraction begins as an action potential originating from the central nervous system. This signal reaches an alpha motor neuron in the anterior horn of the spinal cord, then transmits down the axon. Transmission of this signal from the motor neuron terminal to the motor end plate is accomplished through a calcium (Ca^{2+}) influx causing synaptic vesicles in the terminal to release neurotransmitter acetylcholine into the extracellular space. Upon acetylcholine binding to nicotinic receptors/ activating ligand-gated sodium ion channels, the muscle membrane triggers an action potential which

continues along the sarcolemma and down transverse-tubules (t-tubules (Allen et al., 2008). This is considered the beginning of EC-C, a process that occurs between the boundaries of the t-tubules, and the intracellular sarcoplasmic reticulum (SR) (Dulhunty, 1992). Depolarization of the membrane represents an action potential which induces a voltage driven conformational change in the t-tubule voltage sensor, also known as the L-type Ca^{2+} channel (Balog, 2010; Lamb, 2009; Zhi et al., 2005; Dulhunty, 1992; Schneider and Chandler, 1973). Depolarization activates the L-type voltage-dependent Ca^{2+} channel (i.e. dihydropyridine receptor, or DHPR) in the t-tubule, which is in close proximity to Ca^{2+} release channels known as the ryanodine receptor (RyR). Action potentials are sensed by the DHPR, and thus opening of the RyR triggers a Ca^{2+} efflux from the SR (Balog, 2010; Lamb, 2009; Allen et al., 2008; Zhi et al., 2005; Gordon et al., 2000; Ashley, Milligan, and Lea, 1991) therefore leading to an increase in free myoplasmic Ca^{2+}, which goes on to bind to Troponin C (TnC) activating the thin filament (Allen et al., 2008). Ca^{2+} binding to TnC on the actin filament allosterically modulates Tropomyosin (Tm) by causing it to roll off of myosin binding sites, allowing myosin crossbridges to bind and generate muscle tension creating a myofibrillar complex (Vandenboom, 2004; Gordon et al., 2000; Ashley et al., 1991). This complex ultimately enables myosin to transduce the free energy provided by the hydrolysis of ATP into mechanical work, resulting in force development (Vandenboom, 2004; Ashley et al., 1991).

Fig. 4. Chin (2005)- Excitation-Contraction Coupling (EC-C)
Displayed is the depolarization of the plasma membrane and the t- tubule system. The t-tubule system carries the signal to the interior of the fibre where the DHPR detects the change in membrane potential and transmits the signal to the RyR. Release of Ca^{2+} from the SR into the myoplasm results in actin-myosin interaction, fiber shortening, and force production.
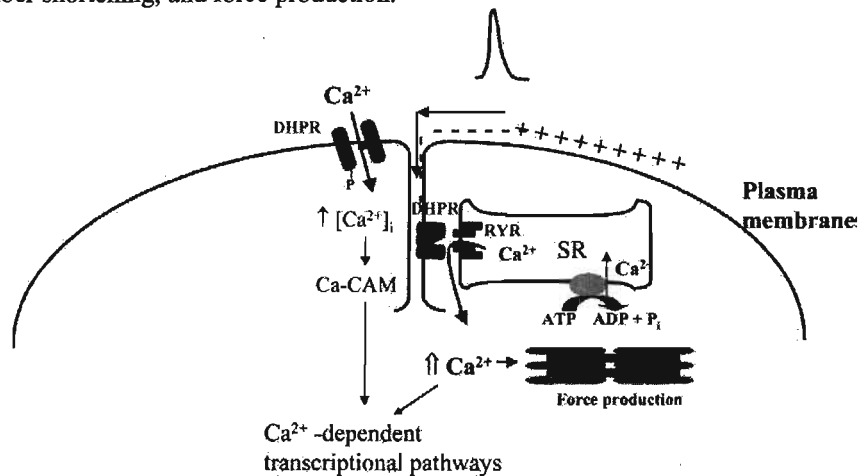
Legend – calcium (Ca^{2+}); depolarization of the membrane (- - + +); dihydropyridine receptor (DHPR); ryanodine receptor (RYR); sarcoplasmic reticulum (SR); calcium-calmodulin complex (Ca-CAM).

Close, (1972) suggests that EC-C ends after the relaxation of activated crossbridges, and subsequent re-sequestration of Ca^{2+} back into the SR. Once impulses from the alpha motor neuron cease, intracellular Ca^{2+} decreases causing Tm to roll back over the binding sites, subsequently blocking myosin heads. Force levels will decrease as Ca^{2+} is actively pumped back into the SR by Ca^{2+}-activated ATPase activity.

2.3.0 Crossbridge cycling

Regulation of crossbridge cycling and subsequent interactions between actin and myosin depends on the structural protein Tropomyosin. In a relaxed state, proteins such as Tm, TnC, Troponin I (TnI), and Troponin T(TnT) act as a steric blocking device, inhibiting actomyosin ATPase activity in the absence of Ca^{2+} (blocked state) (Gordon et al., 2000). After excitation, Ca^{2+} from the SR binds to TnC allowing Tm to uncover

strong hydrophobic binding sites for myosin on actin by a modified steric blocking mechanism (Gordon et al., 2000). Upon Tm movement, the thin filament would be in a closed position as binding sites are partially exposed, allowing for crossbridge binding which increases the affinity of actin for myosin (Gordon et al., 2000). In the early stages of force development crossbridges formed are considered to be weakly bound with myosin heads, having a low affinity for actin (Vandenboom, 2004; Gordon et al., 2000). These weakly bound crossbridges exert a positive effect on thin filament activation by improving the affinity for Ca^{2+} and more crossbridge binding. As this process continues myosin and actin develop stronger bonds, allowing additional crossbridges to form and displace Tm further away from actin binding sites (open state)(Vandenboom, 2004; Gordon et al., 2000). Crossbridges, now strongly bound, can generate force and perform work against the thin filament in the form of a power stroke (Vandenboom, 2004). Elevated myoplasmic concentrations of Ca^{2+} are vital to maintaining this process. When Ca^{2+} concentrations lower, the muscle is relaxed by a reversal of these changes that shift the thin filament back towards the blocked state (Vandenboom, 2004; Gordon et al., 2000; McKillop and Geves, 1993). Therefore, thin filament activation is initially highly dependent on Ca^{2+} release and subsequent interactions with the Tn complex. However, it is the cooperativity of both Ca^{2+} binding and strongly bound crossbridges that is likely responsible for greatest thin filament activation. This proposal suggests that strongly attached crossbridges act as a feed forward signal, enhancing the binding of additional crossbridges on neighboring actin-Tm units in an allosteric manner (Gordon et al., 2000; Squire and Morris, 1998; McKillop and Geves, 1993). As a result, strong crossbridge

binding promotes additional crossbridges to form, thus further activating the thin filament without significantly enhancing Ca^{2+} binding to TnC.

The motility of a myosin head is based upon the hydrolysis of ATP. Once strongly bound, ATP is hydrolyzed releasing inorganic phosphate (P_i), as well as ADP. The transduction of energy released by ATP hydrolysis into mechanical force occurs during product release (ADP and P_i) (Vandenboom, 2004: Gordon et al., 2000; Rayment et al., 1993). Free energy released from hydrolysis is trapped by the myosin head, and is eventually released as mechanical work during the crossbridge power stroke (Vandenboom, 2004) (*See following section*). Furthermore, the by-products of ATP hydrolysis subsequently induce structural changes that affect crossbridge attachment and force production (Vandenboom, 2004; Rayment et al., 1993). It is important to note that accumulation of these by-products as a result of this process may have significant consequences on contractile activity, if muscular work in maintained for a prolonged period of time (i.e., fatigue).

Upon considering the putative EC-C mechanism, one should examine the resultant effects crossbridge binding has on Ca^{2+} sensitivity. As previously addressed, a Ca^{2+} influx from the SR initiates contractile movement by binding to TnC, ultimately leading to the weak binding of crossbridges as seen in skinned fiber studies (Persechini et al., 1985; Sweeney and Stull, 1986). Newly formed crossbridges positively affect thin filament activation by improving its affinity for Ca^{2+} and additional crossbridge binding (Vandenboom, 2004; Gordon et al., 2000). This can increase the number of crossbridges in the strong binding state, away from the myosin thick filament and towards the actin thin filament. Eventually crossbridge formation leads to the rearrangement of myosin

heads and initiation of the power stroke (Vandenboom, 2004; Gordon et al., 2000; McKillop and Geeves, 1993), indicating an increase in the sensitivity of the contractile unit to Ca^{2+} (Metzger et al., 1989; Sweeney and Stull, 1990). Brenner (1986) suggested that the position and shape of the force-pCa relationship is a result of Ca^{2+} modulation to the proportion of crossbridges, which are in a strongly bound force producing state. Metzger et al., (1989) demonstrated that the shape and position of the force-pCa relationship was significantly altered without any affect on a fiber's isometric force redevelopment rate (K_{tr}-pCa). Alterations in Ca^{2+} sensitivity of steady-state isometric force may therefore be attributed to the effects of phosphorylated myosin on the thin filament (Persechini et al., 1885; Metzger et al., 1989). Other factors, such as temperature, muscle length and accumulation of metabolic by-products can affect Ca^{2+} sensitivity by delaying the power stroke and the number of crossbridges in a force-producing state. Therefore, force generation by the contractile unit is highly susceptible to environmental adaptations.

In summary, the physiological events responsible for regulation of crossbridge cycling are highlighted below (as reviewed by Vandenboom, 2004): initially the binding of Ca^{2+} to TnC causes Tm to roll off of the actin binding sites on the thin filament. However, even in the presence of Ca^{2+}, a sufficient number of crossbridges must be strongly bound to move Tm to a position where actin and myosin can bind freely, activating the ATPase (Gordon et al., 2000). In an early state, a myosin head is weakly bound to actin as ATP is hydrolyzed. Hydrolysis increases myosin's affinity for actin, allowing for additional weak myosin interactions to occur with actin. Once ATP is hydrolyzed the myosin head ejects P_i, releasing free energy in the form of mechanical

work (power stroke). This rearranges the myosin head and allows for strong binding to actin, which in turn causes movement of the head along the thin filament, therefore pulling Z-lines closer together to produce force. Following the power stroke, ADP is released from the myosin head allowing ATP to rebind, relinquishing the strong binding between myosin and actin. ATP becomes hydrolyzed once more upon binding to the myosin head. This releases free energy which is used to reverse the structural changes that occurred during the power stroke, leaving myosin prepared to repeat the cycle again (Vandenboom, 2004; McKillop and Geeves, 1993).

2.3.1 Power stroke

Early research has led to the belief that force generation and filament sliding is a result of the globular myosin head region tilting towards the actin filament (Huxley, 1969). Irving et al., (1995) confirmed this proposed theory, using fluorescence polarization to detect changes in the orientation of the light chain region of the myosin head. Their results suggest that the myosin head changes its orientation relative to the filament axis during an instantaneous elastic response to filament sliding (Irving et al., 1995). Additional tilting motions accompany the rapid transition between states of the crossbridge cycle associated with active force generation. Thus, it is commonly accepted that crossbridge formation occurs as a result of the head projecting away from the thick filament backbone, generating force and filament sliding by interacting with specific binding regions on the thin filament (Gordon et al., 2000). However, translocation of the S1 head can vary depending on its nucleotide state. Vandenboom (2004) speculated that any change in the S1 shape due to a change in bound nucleotide, or changes in the light chain (i.e. RLC phosphorylation) can cause a release of the S1 head from the ordered

structure on the backbone. As a result, RLC phosphorylation would reduce S1's association with the thick filament backbone, shifting crossbridges into closer proximity of thin filament binding sites. Under such conditions the physiological role of RLC phosphorylation in mammalian skeletal muscle is modulatory.

It seems plausible that a means of communication exists between filaments, synchronizing the S1 position with association to actin. Rayment et al., (1993) suggested that each S1 head has a narrow cleft that serves this purpose. The cleft extends from under the nucleotide binding site, to the end of the head, acting as a means of communication between the nucleotide binding site and the actin binding site (Rayment et al., 1993). This cleft splits the S1 head into two domains (upper and lower), playing an intricate role in the sequential process of shifting to a strong binding state from a weak binding state (Rayment et al., 1993; Holmes Angert, Kull, Jahn, and Schrider, 2003; Risal et al., 2004). The lower domain initially forms a weak interaction with the actin filament, whereas the upper domain has no contact with actin (Holmes et al., 2003). When strongly bound, the upper domain comes into contact with the actin surface. This transformation has been shown to affect the rate of actin-activated ATPase activity (Holmes et al., 2003). Thus, myosin crossbridges can develop either weak or strong interactions with the thin filament. Figure 5 provides an illustration of the various proposed stages of actomyosin interaction during crossbridge cycling. Initially, when myosin binds to actin there is a weak relationship. The pre-power stroke phase (weak binding) corresponds biochemically to the ADP/P_i - ATP transition state (see Fig 5. state b/c) (Rayment et al., 1993; Holmes et al., 2003; Risal et al., 2004; Fitts, 2008). During this phase, S1 is in a

"primed" lever arm position (~90° to the actin filament axis), and the cleft is open. Closure of the cleft is considered a way to lower the affinity of actin for myosin's phosphate, allowing it to be released (Rayment et al., 1993; Holmes et al., 2003; Risal et al., 2004). Upon releasing P_i (Fig 5. state d), the crossbridge state transforms into a strongly bound high force state, and performs a power stroke (Fitts, 2008). Release of the phosphate is what triggers the power stroke, reversing the conformational change which originally occurred (Fig 5. state e) (Rayment et al., 1993). Discharge of a phosphate is followed by ADP release, followed by another ATP binding. The strongly actin-bound, nucleotide-free conformation of S1 that results is known as the rigor state (Fig 5. state a) (Risal et al., 2004). Initial binding of ATP to S1 at the beginning of a new ATPase cycle results in the dissociation of myosin from actin, a step that may be attributed to the partial opening of the cleft (Risal et al., 2004).

Fig. 5. Fitts (2008). A Mechanochemical scheme for actomyosin crossbridges cycling
States *a- f* represent the various stages of the crossbridge cycle. Starting from the rigor complex (*state a*), ATP binds to rapidly dissociate the complex, and the lever arm is "reprimed" to the pre-power stroke position (*state b*). This is followed by hydrolysis. With ADP and P_i attached, myosin rebinds to actin, initially weakly (*state c*) and then strongly (*state d*). Binding induces the dissociation of P_i and the power stroke (*state e*). The completion of the tail swing (*state f*) is followed by ADP release to return to the rigorlike complex (*state a*).
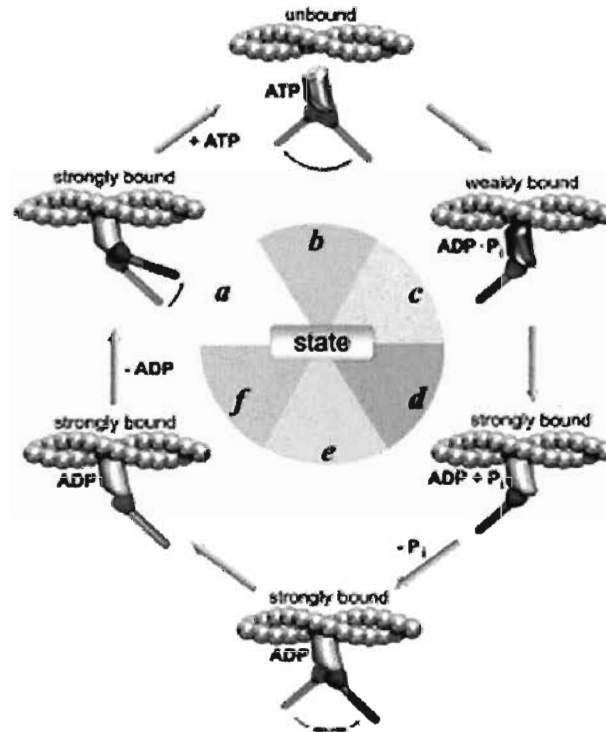
This multi step process briefly outlines the binding of myosin to actin, highlighting the importance of nucleotide binding above the myosin S1 cleft. Opening and closure of the cleft dictates the ensuing actions of the myosin head. Cleft opening and subsequent ATP binding will allow the S1 head to shift or rotate toward actin, interrupting the ordered array along the thick filament backbone. This ultimately increases the chance of a strong actomyosin bond and corresponding power stroke. An increase in strongly bound myosin heads during contraction results in more force at a given submaximal concentration of Ca^{2+}. This also increases the rate crossbridges shift from a non-force producing state (g_{app}), to a force producing state (f_{app}) (Sweeney and Stull, 1990; Hodgson, Docherty, and Robbins, 2005). Fitts (2008) suggests that during

isometric contraction, strongly bound states (d,e,f and a) are most prominent. Conversely, during isotonic shortening crossbridges are strongly bound for approximately 5% of the cycle. This offers evidence as to why higher forces can be attained during isometric contraction in comparison to concentric as observed in the force-velocity relationship.

2.4.0 Fatigue in skeletal muscle

Muscle fatigue is characterized as a loss of power that results from a decline in both force and velocity (Fitts, 2008). However, distinguishing fatigue from muscle weakness or damage is important as the loss of power output associated with fatigue is reversible following adequate rest (Fitts, 1994).

Fatigue has been observed in both animals and humans during endurance exercise, as well as high-intensity and short duration exercise. Reductions in contractile performance associated with fatigue include a decline in both twitch and tetanic force, maximal shortening velocity, and peak power output (Fitts, 2008). Isometric twitches and tetani are often used as indicators of fatigue as P_t generally decreases, and peak tetanic force (P_o) is an indicator of the severity (Fitts, 1994). Therefore, general outcomes of fatigue in fast-twitch skeletal muscle are the reduction of both P_t, and P_o. In addition, prolonged contraction and half-relaxation times, as well as decreases in $+dP/dt$ and rate of tension decline ($-dP/dt$) are also characteristics that need to be taken into consideration (Fitts, 2008). Collectively, the terms $+dP/dt$ and $-dP/dt$ refer to the most rapid rate at which force develops or declines when stimulated. Reductions in P_t, as well as prolonged contraction and relaxation times may be most prominent early in fatigue, representing a decrease in the amplitude and increase in the duration of intracellular Ca^{2+} release (Allen et al., 1995; 2008). Decreases in P_o may be explained by a decline in force per

crossbridge, as well as the number of strongly bound crossbridges, and is associated with the later stages of fatigue (Allen et al., 1995; 2008). Late onset of fatigue may therefore be attributed to a decline in the amplitude of Ca^{2+} release, as well as the corresponding myofibrillar Ca^{2+} sensitivity. This well known characteristic of skeletal muscle fibers is depicted in figure 6.

Fig. 6. Fitts (2008)- Force-pCa relationship during fatigue
Illustrated is P_o plotted against pCa (normalized to the force obtained in pCa 4.5 and 30°C at both concentrations of P_i). Each data point represents the mean ($\pm$SD) force at each pCa level. Curves represent data from separate groups of fibers (filled, no added Pi; empty, 30 mM Pi added).
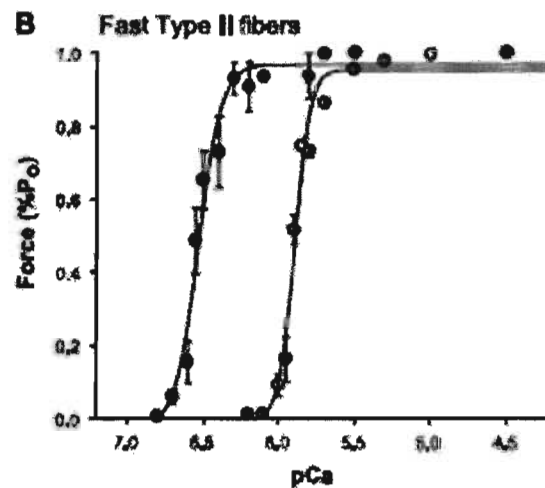
Illustrated is the corresponding shift to the right in the force-pCa curve during fatigue. As a result of this shift, elevated amounts of free Ca^{2+} are required to achieve a given force. If the amplitude of Ca^{2+} transients remains high (saturating levels), peak force will not be affected by the reduced Ca^{2+} sensitivity. However, at submaximal Ca^{2+} concentrations the effect of reduced sensitivity will undoubtedly be more evident.

Although fatigue may have profound effects on contractile function, for the purpose of this review an in depth analysis will not be conducted as the contribution from fatigue was minimal in the proceeding experiments.

2.4.1 Experimental models of study

The specific properties of skeletal muscle may be examined in a variety of ways, all of which provide advantages and disadvantages. Upon analyzing physiological events such as fatigue or potentiation, it is important to consider the parameters of each model, as one approach may be more favourable than another. An ideal model of study closely mimics the physiological environment in which a muscle lives and functions. Correspondingly, Allen et al., (2008) suggests that an *in situ* model is the "gold standard" for examining fatigue in mammals. This model replicates physiological conditions in which the muscle thrives. An *in situ* approach can be considered an intermediate between *in vivo*, and *in vitro* models. This model is based on conducting examinations within a whole intact organ under perfusion, where the blood and nutrient supply remain constant. Although this model requires complex surgical procedures, it would be most favourable as it provides control over the activation of the muscle, yet still operates within a natural environment.

In comparison an isolated whole muscle model (*in vitro*) includes more simplistic surgical procedures as the whole muscle is completely excised, therefore also eliminating the chance for central fatigue. Brown, Cheng and Loeb, (1998) suggest that whole muscle preparations produce better contractions at physiological sub-tetanic stimulation frequencies. However, because of the absence of circulation these preparations often develop diffusion gradients of O_2, K^+, and other metabolites. CO_2, H^+ and lactate may also accumulate in extracellular space until a diffusion gradient sufficient to allow for the flow out of the preparation develops. As a result the mechanisms of fatigue and potentiation may be influenced by the presence of extracellular gradients, a factor that

could also affect the administration of ions and metabolites. Furthermore, Barclay (2005) suggests that hypoxia is a common fate of isolated mouse or rat muscle during prolonged contractile activity. However, for moderate intensity workloads a constant supply of oxygen should be sufficient to sustain activity (Barclay, 2005). In most cases lowering the temperature of the solution bathing the muscle, as well as reducing the muscle's radius (by lengthening the muscle) will enhance oxygen diffusion. Although stimulation of the muscle is not signaled by the alpha motor neuron, this model permits incubations at higher temperatures than other models (i.e. skinned/single fiber), which is a critical factor when observing fatigue and/or potentiation.

Skinned fibers are also commonly used as a result of their ability to study myofibrillar properties such as SR Ca^{2+} release/uptake. To allow direct control of the solution bathing the contractile apparatus, the sarcolemma is chemically or mechanically removed. Under these circumstances precise solutions can be applied, making it is possible to observe the effects of altering intracellular ions and metabolites. Furthermore, the structural integrity of the myofilament lattice is maintained, allowing force and velocity parameters to still be measured (Persechini et al., 1985). This model is advantageous over isolated intact muscles as the latter may not adequately control for all variables that affect force development (i.e. Ca^{2+} transients). However, the functional relevance of this model pertaining to fatigue and potentiation *in vivo* is questionable. In addition, skinned fiber preparations cannot survive at physiological temperatures, thus significantly affecting observations of potentiation.

2.5.0 Contractile mechanics

Force production within skeletal muscle is highly dependent on structural, as well as biochemical alterations within the contractile apparatus. One of the most common observations is the length-tension (L-T) relationship of contractile material. This relationship reflects the fact that tension generation in skeletal muscle is a direct function of the magnitude of overlap between thick and thin filaments. An important consideration, however, is the fact that properties associated with the L-T relationship refer to a muscle in the isometric state. Accordingly, the tension within an inactive muscle at resting length is zero, and will increase proportionally as the muscle lengthens (Close 1972). Thus, linear increases in tension will correspond with an increase in length until a steady state (L_o) is reached. The term L_o suggests that there is maximal overlap of thick and thin filaments, as well as decreased interfilament spacing which will augment f_{app} (Close 1972; Sweeney and Stull 1990). As suggested by Yang and colleagues (1998), when the thick filament is in closer proximity to its thin filament binding sites, additional weak crossbridge interactions may be formed. In turn, this will ease the transition from non-forcing producing to force producing states. However, fiber lengths surpassing that of L_o will begin producing a linear decline in tension as the position of thick and thin filaments is beyond that of optimal overlap. Similarly, excessive sarcomere shortening restrains optimal force production as well by thick filaments sliding towards the H-zone. At extremely short lengths, the thin filaments may collide with the Z-line, interfering with force production causing tension to fall (Close, 1972).

Fig.7. (Gordon et al., 1966)- Length-Tension relationship
Displayed is the corresponding curve which represents the isometric force (% of max) associated with fluctuations in sarcomere length. At very short sarcomere lengths (µm), the ability to produce force is minimal. As length increases, relative force increases until a plateau is reached (optimal filament overlap). Thereafter, force steadily declines as filaments continue to slide away from the optimal overlap region.
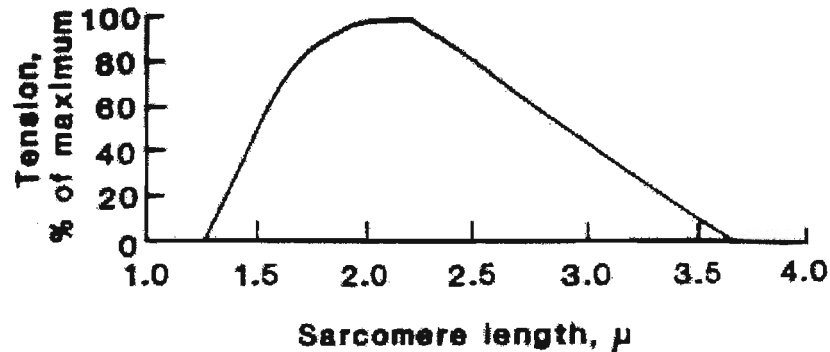
Therefore, an ideal range exists where sarcomere length translates into optimal overlap of thick and thin filaments, resulting in peak force production. It is relevant to also identify the differences in this relationship when comparing maximal and submaximal stimulation frequencies. Notably, with maximal stimulation, the L_o corresponding to optimal filament overlap appears at a shorter length than recorded with submaximal activation (i.e. twitch or low frequency stimulation). This may be due to the changes in Ca^{2+} sensitivity associated with submaximal activation as interfilament spacing decreases with increased length, therefore compensating for a reduced number of crossbridges. This accounts for the shift in the plateau of active force for twitch/ sub maximal stimulations (Rassier, MacIntosh and Herzog, 1999).

Upon examining the relationship between interfilament spacing and force production an additional association exists between force and intracellular Ca^{2+} concentration, suggesting that sarcomere lengthening may augment force as a result of Ca^{2+} sensitivity. It is well established that a sigmoidal relationship exists between

intracellular Ca^{2+} concentrations, and the relative amount of force that can be produced. Once maximal force has been reached the intracellular Ca^{2+} concentration is saturated on TnC, and further increases in Ca^{2+} will not result in additional increases in force. However, a uniform decline in intracellular Ca^{2+} will cause force to subsequently decline as well. Allen and Moss, (1987) observed this relation in comparison to length changes within the muscle. The authors determined that various changes in sarcomere length will affect the force produced, and possibly the sensitivity to Ca^{2+}. As a result, when length is reduced, the force-pCa relationship will shift to the right. Therefore, a greater Ca^{2+} concentration will be necessary to elicit the same force that would normally be produced at a longer length. In contrast, increasing sarcomere length induces a leftward shift of the curve and enhances contractile sensitivity to Ca^{2+} (Allen and Moss, 1987). Stevenson and Williams (1982) suggests that such variability in the force-pCa relationship by changes in sarcomere length reduces as temperature decreases in mammalian skeletal muscle fibers (i.e. 3° C vs. 35° C). It is of interest to also note that Ca^{2+} transients are not altered by length changes in mammalian single fiber preparations, as neither resting, nor tetanic intracellular Ca^{2+} concentration were significantly altered by deviations in muscle length (Balnave and Allen, 1996). Therefore, increases in force development at long lengths can be attributed to the enhancement in bound crossbridges along the thin filament when compared to shorter lengths. Such an attractive observation may be, in part, due to increased S1 binding to actin and therefore strong crossbridge formation for a given level of Ca^{2+} (Gordon et al., 2000). A reciprocal outcome is increased thin filament activation by strong crossbridge binding, resulting in additional crossbridges attached for a given Ca^{2+} concentration. This would ultimately be defined as an apparent increase in Ca^{2+}

sensitivity. Yang et al., (1998) suggested an increase in the force producing capability confirms length dependence of Ca^{2+} sensitivity on tension development in skeletal muscle. Interestingly, skeletal muscles also possess other intrinsic abilities to augment force-Production as a result of previous contractile activity. Phosphorylation of the myosin RLC in skinned rabbit psoas fibers disorders the surface arrangement of myosin heads, increasing the radius they extend into the interfilament space (Levine et al., 1996). These observations coincide with the increase in Ca^{2+} sensitivity in skinned fibers demonstrated by Persechini and colleagues (1985) with RLC phosphorylation. Phosphorylation would therefore result in a leftward shift of the force-pCa curve, indicating the increased sensitivity of the contractile apparatus to Ca^{2+} at shorter sarcomere lengths. However, the proposed length-dependent relationship of potentiation suggests that improved Ca^{2+} sensitivity induced by RLC phosphorylation diminishes as muscle length increases (Rassier and MacIntosh, 2000). Considering Ca^{2+} transients are not altered with length changes (Balnave and Allen 1995), force production must be augmented by a decrease in interfilament spacing, subsequently enhancing crossbridge binding. Thus, RLC phosphorylation may mimic the effect of decreasing interfilament spacing in muscle fibers at more physiological lengths than at longer lengths. This may function by enhancing the rate of transition of crossbridges into force generating states (f_{app}) and therefore the level of thin filament activation (Yang et al., 1998). A leftward shift in the force-pCa relationship produced by RLC phosphorylation is similar to that produced by decreasing the distance between thick and thin filaments by osmotic compression (via dextran), or increasing sarcomere length (Yang et al., 1998; Allen and Moss, 1987). Considering this effect is abolished at saturating levels of Ca^{2+}, and at

longer sarcomere lengths (Allen and Moss, 1987; Yang et al., 1998), RLC phosphorylation may only induce significant enhancements in force at lower Ca^{2+} concentrations and shorter lengths.

The force force-frequency relationship is also a fundamental component of contraction as it represents the force generated by a muscle over a range of stimulation frequencies. This relationship depicts the uniform change in force due to concomitant changes in stimulation frequency. While held isometrically, a muscle will progressively produce greater force as the stimulus frequency increases (Brown et al., 1998). Stimulations may range from a single twitch to fully-fused tetani, all of which correspond with a Ca^{2+} transient and contractile response; with voluntary recruitment of muscle occurring with stimulation frequencies resulting in incompletely fused tetanic contractions (MacIntosh and Willis, 2000). As a result, one may consider the force-frequency relationship analogous to the force-pCa relationship as determined by measurements of mean free intracellular Ca^{2+} in intact single fibers (Balnave and Allen, 1996). Thus, the average free Ca^{2+} concentration increases as well. Similar to the force-pCa and length-tension relationships, the force-frequency relationship is susceptible to modulation under various conditions. Fatiguing stimuli will elicit a rightward shift in this relationship, resulting in less force produced by a stimulus. Depending on the type of fatigue, force decrements will be noticeable at different point along the curve. For example, during low frequency fatigue (LFF) a loss in force is most evident at low frequencies of stimulation. Balog (2010) suggests that a work induced decrease in the ratio of force production in response to 20 or 30 Hz stimulation versus 100 Hz can be used to define LFF. Considering the sigmoidal appearance of the force-frequency curve,

lower activation frequencies fall along the steep portion of the curve, therefore a shift in either direction will have a significant effect on enhancing, or depressing force. Conversely, phosphorylation of the RLC may enhance force output in response to a submaximal stimulus (Manning and Stull, 1982; Moore and Stull, 1984). This effect is most prominent at low frequencies of stimulation as it may compensate for reduced sensitivity to Ca^{2+} associated with fatigue. This may be attributed to the fact that at higher stimulation frequencies the amount of Ca^{2+} available is not limiting during LFF, therefore force output will not be inhibited (Allen et al., 2008; Fitts 2008). Vandenboom et al., (1993) suggested that PTP was not evident for frequencies of stimulation up but not above 20 Hz in isolated muscles at room temperature. As a result, RLC phosphorylation elicits its greater effects at low stimulation frequencies. MacIntosh and Willis (2000) suggests that the magnitude of potentiation will decrease as the plateau of both the force-frequency, and force-pCa relationship is approached. Thus, force potentiation will have a reduced effect as the contraction amplitude approaches maximum force, however 20 Hz may not necessarily represent the upper limit for potentiation. For example, Roszek et al., (1994) and St. Pierre and Gardiner (1985) demonstrated potentiation at 37° C, with intermittent contractions at 40 Hz in rat gastrocnemius muscle. Bevan et al., (1993) also found cat tibialis posterior muscle to have similar properties. MacIntosh and Willis (2000) report potentiation to be evident in Sprague-Dawley rats during brief intermittent contractions for stimulations resulting in near saturating Ca^{2+} concentration (i.e., 70 -80 Hz). It is important however to consider the effect of increasing temperature on such observations of potentiation. The aforementioned studies examined potentiation at ~ 25° C, while the latter implemented higher bath temperatures. The effect of RLC

phosphorylation is greater at more physiological temperatures (Rassier and MacIntosh, 2000), suggesting previous studies may be underestimating its role. Underestimation of observations can be attributed to the fact that peak unpotentiated twitch force and threshold duration for excitation increases with a decrease in temperature from 35° C to 20° C (Close and Hoh, 1968). In conjunction, potentiated twitch force increased ~ 2-fold at 35° C when compared to a normal twitch at a lower temperature in isolated rat EDL (Close and Hoh, 1968). The inverse relationship between temperature and force suggests that contraction-induced potentiation of intact mammalian skeletal muscle is augmented at elevated temperatures. This effect may be a result of the increased sensitivity to Ca^{2+} at higher temperatures where intracellular Ca^{2+} concentrations, and sensitivity are reduced (Moore et al., 1990). At lower temperatures Ca^{2+} transient are larger, and have a longer duration which may result in greater activation of the thin filament, as well as skMLCK. This may explain the 2-fold increase in P_t, and decrease in the magnitude of potentiation as temperature was decreased from 35° to 20° C in isolated rat EDL (Close, 1972).

An additional mechanical property of skeletal muscle that is critical to understanding dynamic function is the relationship between force and velocity of shortening. The force-velocity curve represents the relative force a muscle is capable of producing at various speeds of length changes. Accordingly power, which is defined as the rate of performing work, will be zero when the load is zero, as well as when the velocity of shortening is zero.

Fig. 8. Enoka (1996)- Variations in maximal force as a function of shortening velocity.
Represented is a typical force-velocity relationship. As the curve indicates, force is a function of the speed of muscle length change, and that this relationship differs when comparing shortening muscles (concentric) to lengthening muscles (eccentric).
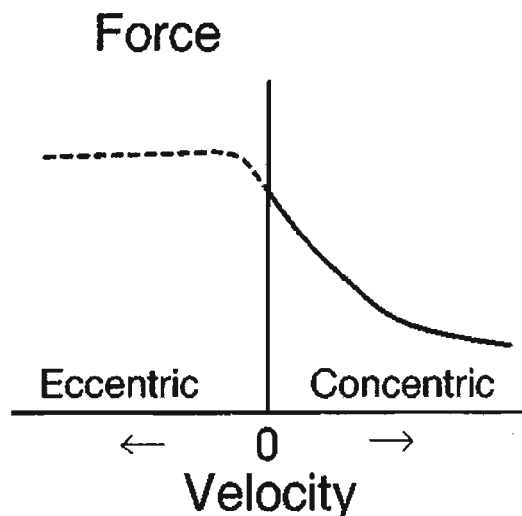
Various parameters dictate the shape and magnitude of this relationship. Maximal force produced is often attributed to the muscle cross sectional area. As a result, the larger the cross sectional area, the more force a muscle is capable of producing. Secondly, the maximal velocity of shortening is a function of fiber type and the number of sarcomeres in series (MacIntosh 2006, p. 170). Essentially, fast twitch fibers will have a faster shortening velocity than slow twitch fibers. Furthermore, fatigue and the buildup of metabolic by-products may also negatively influence the velocity of shortening. These factors, among others, coalesce to define the properties of the dynamic contractions. Upon observing the curve illustrated in figure 8 it is clear that greatest forces are produced eccentrically as the muscle contracts while lengthening. An isometric contraction represents the midpoint at which the muscle can produce high force without a change in length (depicted as the point closest to the Y-axis in Fig 8). At this phase the tension produced by the muscle is equal to the external load, resulting in no movement of

actin filaments. Figure 8 demonstrates the inverse relationship between speed of shortening and force output after isometric contraction, indicating that less force is produced as contraction velocity increases. Much like the aforementioned mechanistic relationships, the force-velocity curve is also susceptible to modulation due to RLC phosphorylation. When exposed to a low frequency CS, RLC phosphorylation led to an increase in shortening velocity for an absolute load in non-fatigued isolated muscle (Grange et al., 1995). An increase in velocity would result in an upward shift of the force-velocity curve, eliciting greater force at a given velocity. However, Karatzaferi et al., (2008) suggests that fatigue abolishes this effect. The authors demonstrated that at 30° C, low pH and elevated P_i levels coupled with RLC phosphorylation which increases with fatigue, work synergistically to inhibit the velocity of shortening (Karatzaferi et al., 2008). Furthermore, although velocity decreased in dephosphorylated fibers during fatigue, phosphorylated fibers experienced a two-fold greater decline. As a result, power output also decreased to a greater extent in phosphorylated fibers during fatigue. It has therefore been proposed that during fatigue *in vivo*, RLC phosphorylation may influence muscle mechanics by inhibiting velocity of contraction (Karatzaferi et al., 2008). This possible role is similar to that observed during fatigue when intracellular ADP concentration rises, preventing rapid dissociation of myosin heads from the thin filament.

Upon considering the plasticity of skeletal muscle under dynamic conditions it is necessary to also consider deactivation of the thin filament during active shortening; a circumstance which leads to transient impairments in force production. As a result, this history-dependent mechanism in skeletal muscle has been termed shortening induced deactivation (SID), and corresponds with increased $[Ca^{2+}]_i$ during muscle fiber shortening

(Vandenboom, Claflin & Julian, 1998; Jiang & Julian, 1999; Vandenboom, Hannon & Sieck, 2002). Essentially, SID refers to a reduction in the rate of force development after rapid shortening caused by decreased affinity for Ca^{2+} on Troponin binding sites (Edman, 1996). This concept suggests that SID allows for relative ease of thin filament sliding, enhancing the uninterrupted transmission of myosin heads without negative forces imposed by strongly bound crossbridges, as well as more rapid recruitment of force for subsequent contractions. Therefore, increases in shortening velocity result in a rightward movement down the force-velocity relationship, resulting in greater deactivation of the thin filament as well as deficits in force production.

2.6.0 Myosin regulatory light chain phosphorylation (Overview)

Early work by Close (1968) and Perrie et al., (1973) determined that the RLC of skeletal muscle myosin could be phosphorylated, and twitch force could be enhanced in response to repetitive stimulation. Since then, remarkable advancements have been made in understanding the molecular, and biochemical events that take place within striated skeletal muscle. Currently, it is well understood that the phosphorylation of myosin RLC modulates function by sensitizing the contractile apparatus to Ca^{2+} activation, thus augmenting force, work and power output. The following sections will examine this phenomenon in greater detail, reviewing the mechanism of RLC phosphorylation and affiliated post-translational modification of myosin.

2.6.1 Ca^{2+} and RLC phosphorylation

Ca^{2+} signals which govern skeletal muscle contraction also significantly contribute to skeletal muscle potentiation. A Ca^{2+} signal will initiate the cascade of enzymatically controlled reactions leading to the phosphorylation of the RLC subunit of mammalian skeletal muscle (Vandenboom and Houston, 1996). In vertebrate striated muscles, both thick and thin filament regulation is largely attributed to intracellular Ca^{2+} concentration. On the thin filament, Ca^{2+} binds to TnC causing Tm to roll off of actin binding sites, increasing the affinity of actin for myosin. This process ultimately leads to the ATP-dependent cycling of myosin crossbridges with actin, and the generation of force (Sweeney et al., 1993). Thick filament regulation, similar to thin filament, depends on the binding of Ca^{2+} to myosin to increase the actin-activated ATPase activity (Sweeney et al., 1993; Szent-Gyorgyi et al., 1973). Although the contraction and relaxation of striated muscle is thin filament regulated, muscle contractility may be modulated by Ca^{2+} dependent myosin RLC phosphorylation (Stull, Nunnally, Moore, and Blumenthal, 1985).

In addition to initiating contraction, Ca^{2+} has a critical role in the process of RLC phosphorylation. Ca^{2+} activates Ca^{2+}-calmodulin-dependent skeletal muscle myosin light chain kinase (skMLCK) (Stull et al., 1985). As a result, activation of skMLCK, and thus regulation of its activity, occurs via Ca^{2+} binding to calmodulin. Calmodulin is a ubiquitous protein that is activated upon binding up to four Ca^{2+} molecules. When intracellular Ca^{2+} concentration is low, the regulatory domain of MLCK binds to the catalytic domain to inhibit the kinase activity (Takashima 2009). However, upon Ca^{2+} binding to calmodulin, a Ca^{2+}- calmodulin complex binds to the regulatory domain of

MLCK, to release the regulatory domain from the catalytic domain, activating the kinase (Takashima 2009). Therefore, Ca^{2+}- calmodulin binding to skMLCK removes the inhibition, and activates the enzyme from its inactive form (Fig. 9) (Stull et al., 1986; Sweeney et al., 1993). Once inhibition has been removed, the enzyme can phosphorylate the RLC, its sole substrate (Sweeney et al., 1993; Takashima 2009). Correspondingly, in order for calmodulin to fulfill its duty in binding to skMLCK Ca^{2+} must be present. Activity of skMLCK has been reportedly enhanced ~ 1,000-fold in response to increases in Ca^{2+} concentration (Takashima 2009). Grange, Vandenboom and Houston (1993) also highlight the fact that at rest RLC phosphorylation levels are low because the skMLCK activating complex (Ca^{2+}-calmodulin) is poorly formed at low Ca^{2+} concentrations. This attributes to the approximate 10 % phosphorylation of the RLC observed during resting conditions (Moore et al., 1990), signifying that Ca^{2+} is the most important regulator of MLCK activity.

2.6.2 Role of skMLCK

Extensive studies have found skMLCK to be Ca^{2+}- calmodulin dependent, and capable of phosphorylating a specific class of myosin regulatory light chains (Stull et al., 1985). Although myosin light chain kinases are heterogeneous and belong to one of three classes; skeletal, smooth, or cardiac muscle/nonmuscle (Stull et al., 1986; Takashima 2009), all are specific for the phosphorylation of the RLC. Once activated, the resulting kinase activity is the transfer of one or more phosphates from the γ position on ATP to serine site 15 on the RLC of myosin (Sweeney et al. 1993; Levine et al., 1996; Zhi et al., 2005). This serine site is positively charged until neutralized by the negative phosphate (Sweeney et al. 1993; Levine et al., 1996).

skMLCK is a rapidly activated enzyme, with the ability to add a negatively charged phosphate to serine 15 of the RLC of myosin. Manning and Stull provide additional support with their observations that the phosphate content of myosin RLC increases at a rate consistent with maximal activation of skMLCK (Manning and Stull, 1979; 1982). Furthermore, P_t corresponded with highest levels of phosphate incorporation into the RLC, increasing from 0.10 to ~0.75 mol phosphate/mol RLC, respectively (Manning and Stull, 1979). This relationship was observed ~ 10-20 s after tetanic stimulation, with phosphate content decaying at a much slower rate. As evidenced by Manning and Stull, (1979), skMLCK activity reached its peak just seconds after the tetanic stimulation, and returned to baseline after ~20 s. The corresponding deactivation of the kinase results in the removal of phosphate from the RLC. A specific phosphatase, identified as myosin light chain phosphatase (MLCP), subsequently catalyzes the dephosphorylation and reverses the physiological effect of skMLCK activation (Morgan et al., 1976; Sweeney et al., 1993). This protein phosphatase functions at a relatively slow rate in fast twitch skeletal muscle, achieving baseline levels of phosphate content on the RLC after ~ 4-5 min in mammalian muscle at 37° C (Rassier and MacIntosh, 2000). Stull et al., (1985) suggests that the relatively high kinase activity and low phosphatase activity within fast twitch skeletal muscle differentiates it from slow twitch muscle. In slow twitch muscles, kinase and phosphatase activity is three times lower and four times higher than that reported in fast muscle, respectively. Ryder, Lau, Kamm, and Stull (2007) also reported that type I and IIa fibers in rodent muscle contain less skMLCK than type II fibers, therefore resulting in less phosphorylation with tetanic stimulation. This reduced kinase activity and elevated phosphatase activity attributes to the higher

stimulation frequency required to phosphorylate slow twitch muscle (greater activation of MLCK), to compensate for the much more rapid dephosphorylation rate (Stull et al., 1985). As a result, muscle fiber type has a profound impact influence of RLC phosphorylation. The potentiating influence is therefore absent or negligible in slow oxidative fibers, but profound in fast glycolytic fibers. It can thus be concluded that the phosphate content of the RLC which is governed by contraction in striated skeletal muscle is a function of the relative activities of myosin light chain kinase, and phosphatase.

Fig. 9. Manning and Stull, (1982)- Cascade of reactions regulating RLC phosphorylation
Calcium (Ca^{2+}) released during muscle contraction binds to calmodulin (CaM), thus forming a complex which activates myosin light chain kinase (MLCK) from its inactive form. Activated MLCK transfers a phosphate group (P_i) from ATP to the RLC of myosin. Myosin light chain phosphatase (MLCP) reverses the kinase activity by removing P_i from the RLC.
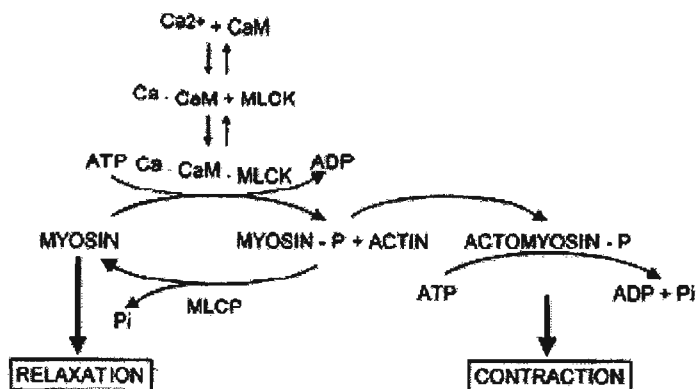
Despite the decline in kinase activity shortly after a tetanic stimulation, phosphate levels remain elevated, and then decay more gradually. Even though the amount of active kinase will progressively decline after tetanic stimulation at a slower rate than its activation, an additional twitch elicited before complete deactivation will increase the total amount of active skMLCK (Sweeney et al., 1993). Therefore, there is an observable

dependence of RLC phosphorylation on stimulation frequency and duration (Manning and Stull, 1979; 1982; Moore and Stull, 1984). At low but constant stimulation frequencies the RLC is phosphorylated in a time- and frequency- dependent manner, regardless of the fact that contractions are not fully fused (Moore and Stull, 1984). Sweeney et al., (1993) suggests that a state of equilibrium is maintained within the cell between rates of activation, and inactivation of the kinase with continuous stimulations at a low frequency. In contrast, brief high frequency tetanic stimulations have also been proven to induce a significant increase in RLC phosphate content in isolated mammalian striated skeletal muscle. Accordingly, the amount of phosphate incorporation on the RLC has been linked to the intensity of stimulation applied to the muscle. These values have been demonstrated to range from ~ 0.1 (resting) to ~ 0.5 (5 Hz, for 10 s) and ~ 0.75 (three 100 Hz, 500 ms volleys) (Vandenboom et al., 1997). As a result, the rate of phosphorylation is therefore dependent on stimulation frequency.

The modulatory basis of RLC phosphorylation stems from the resultant structural alterations within the contractile unit. Phosphorylation of myosin RLC places a negative charge on the phosphorylatable serine residue in the N-terminal region of the peptide (Sweeney et al., 1993; Levine et al., 1996; Zhi et al., 2005). This negative charge may result in stiffening of the myosin lever arm. It has been theorized that such stiffening would permit more efficient transmission of conformational changes at the active site of the myosin head down the lever arm, ultimately increasing the unitary step size of myosin (Levine et al., 1998). Conversely, in the unphosphorylated state the positively charged region of the RLC may form ionic interactions with negatively charged regions of either light, or heavy chains in neighboring myosin heads (Levine et al., 1996; Ritz-Gold et al.,

1980). Ultimately these interactions will attract the myosin heads, causing them to relax into ordered arrangements back on the thick filament surface, increasing the spacing between filaments (Fig 10. *position A*). Myosin binding sites on actin are thus less likely to be involved in actin-myosin interactions than in an unstable, phosphorylated state (Levine et al., 1996). It is therefore proposed that RLC phosphorylation "neutralizes" the attraction of RLC's to the thick filament backbone, effectively freeing myosin heads closer to myosin binding sites on the thin filament (Fig 10. *position B*).

Fig .10. Sweeney et al., (1993) – Posttranslational Modification of the Myosin II molecule
Illustrated are the thick (below) and thin (above) filaments of a contractile unit. Depicted is the transition of myosin heads from position A (resting/ unphosphorylated) to position B (weakly bound/ phosphorylated).
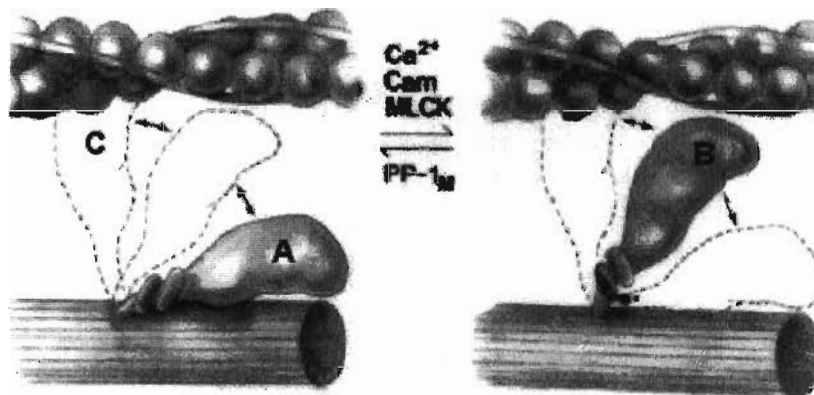
A- At rest, unphosphorylated
B- Myosin conformational change after RLC phosphorylation
C- Strongly-bound myosin head (force-producing interaction)

To summarize, relaxed (unphosphorylated) myosin heads remain in an ordered helical arrangement on the thick filament (Craig, Padron, and Kendrick-Jones, 1987). Contraction mediated phosphorylation of myosin is temporally associated with structural modifications which eliminate the organized arrangement of myosin heads, projecting them away from the thick filament backbone (Sweeney et al., 1993). As a result,

phosphorylated myosin has an increased f_{app} (Sweeney et al., 1990) which improves the rate of transition from non force generating to force generating states along the actin filament. The increase in f_{app} results in an increased probability of strong crossbridge formation, even at low levels of Ca^{2+} (Levine et al., 1996; MacIntosh, 2003). Therefore, RLC phosphorylation has been demonstrated to correspond with an increase in Ca^{2+} sensitivity of contractile proteins (Metzger et al., 1989; Sweeney and Stull, 1990; Szczesna et al., 2002), thus augmenting force output at suboptimal levels of Ca^{2+} activation.

2.6.3 Physiological effects of RLC phosphorylation

Although Ca^{2+} binding to the troponin-tropomyosin complex is the primary regulator of skeletal muscle contraction, RLC phosphorylation may play an important modulatory role. Based upon previous literature, RLC phosphorylation has a functional role in enhancing isometric twitch tension (Manning and Stull 1979; Manning and Stull 1982; Moore et al., 1984), improving the energy status of a cell (Crow and Kushmerick 1982), as well as increasing force production at lower levels of Ca^{2+} activation (Sweeney et al., 1990).

As previously discussed, the effect of releasing myosin heads from an ordered arrangement on the thick filament backbone contributes to the increased rate of strong crossbridge binding. When phosphorylated, the ordered arrangement of myosin was lost and heads appeared to project away from the thick filament backbone. RLC phosphorylation thus weakened interactions within the thick filament, facilitating the movement of myosin heads towards the thin filament (Levine et al., 1996). The

corresponding movement in myosin heads results in a greater population of bound crossbridges, increasing the rate of force development. Sweeney et al., (1993) suggests that potentiation of a twitch in mammalian skeletal muscle is characterized by an increase in the rate of force development, which contributes to an enhancement in peak force. The reported increases in muscle stiffness support such observations as the enhancement in active force would be a result of increased attached crossbridges, and therefore increase in the rate of force development. Analysis of chemically skinned skeletal muscle fibers has helped further verify the association between RLC phosphorylation, and force potentiation within skeletal muscle. Associated studies have determined that at less than physiological temperatures (15-25° C), myosin RLC phosphorylation has a minuscule effect on potentiating twitch force at a saturating Ca^{2+} concentration (Persechini et al., 1985; Metzger et al., 1989). Furthermore, maximal shortening velocity was unaffected by RLC phosphorylation, suggesting that the rate of crossbridge cycling was also unaffected. Results of the aforementioned studies demonstrated that RLC phosphorylation only elevates contractile performance at submaximal Ca^{2+} concentrations. The observed increase in force due to the phosphorylation of myosin RLC at low Ca^{2+} concentrations caused a shift in the force-pCa curve to a lower Ca^{2+} concentration, indicating an increase in the sensitivity of the contractile proteins to Ca^{2+} (Persechini et al., 1985; Sweeney and Stull, 1986; and Metzger et al., 1989).

Metzger et al., (1989) further analyzed the effect myosin RLC phosphorylation had on crossbridge interaction with actin in skinned single fibers. In agreement with Persechini et al., (1985), the authors determined that increasing the phosphate content of the RLC from 10 to 80 % had no effect on isometric force at saturating levels of Ca^{2+}

(i.e., pCa 4.5). However, at submaximal levels of Ca^{2+} activation (i.e., pCa 6.1) isometric force after phosphorylation of the RLC was markedly increased relative to the control values at Ca^{2+} levels associated with resting tension ($\sim$ pCa 9.0), which were unaffected by phosphorylation (Metzger et al., 1989). Furthermore, during the Ca^{2+} transient of a twitch an increased rate of crossbridge cycling resulted in a greater force output (Metzger et al., 1989). This provides evidence that force per attached crossbridge is not altered by phosphorylation; rather there are more crossbridges in force generating states contributing to force generation. Previous reports coincide with this observation (Persechini et al., 1985; Sweeney and Stull, 1986), suggesting that RLC phosphorylation induces a small but significant increase in steady-state isometric force at concentrations of Ca^{2+} below that necessary to elicit 60% of maximum isometric force. This will shift the steady-state isometric force-pCa relationship to the left, indicating an increased affinity of actin for myosin at its binding sites, as well as in the number of strongly bound crossbridges and sensitivity of the contractile apparatus to Ca^{2+} (Persechini et al., 1985; Sweeney and Stull, 1986; Metzger et al., 1989; Grange et al., 1993). Sweeney and Stull (1990) support these observations by concluding that RLC phosphorylation significantly affects f_{app}. Physiologically, the increased population of myosin heads in a force producing state increases the rate of crossbridge attachment at low levels of intracellular Ca^{2+}, an effect that is expressed as potentiation of tension development (Sweeney et al., 1993; Levine et al., 1996). It can thus be postulated that an increase in force at low levels of Ca^{2+} activation may not be due solely to recruitment of additional crossbridges, rather an increased accumulation of crossbridges in force generating states.

As evidenced by Yang et al., (1998), sarcomere length corresponds very closely with the effect of RLC phosphorylation. Decreasing the distance between the thick and thin filaments (i.e., sarcomere lengthening) decreased the effect of RLC phosphorylation on force potentiation in permeabilized rabbit psoas fibres (Metzger et al., 1989; Sweeney and Stull 1990). Upon reviewing the effects of RLC phosphorylation, decreased lattice spacing between thick and thin filaments will imitate structural changes observed during phosphorylation at shorter lengths. Therefore, RLC phosphorylation will provide most profound effects at shorter sarcomere lengths as increases in length will reduce the overall effect of augmented f_{app}.

2.7.0 Mammalian skeletal muscle studies

The following section will highlight various models used to study PTP. Of particular interest, the extensor digitorum longus (EDL) muscle is highly specific for fast myosin heavy chain isoforms. Specifically, Gorselink et al., (2002) determined that 12 week old C57Bl/6 mouse EDL is made up of ~ 8 % slow oxidative (type I), 18 % fast oxidative-glycolytic (type IIa), and 70 % fast glycolytic (type IIb) muscle fibers. Due to the well known properties of fast type IIb fibers, and their high kinase, low phosphatase activity, the EDL is an ideal muscle in which PTP can be studied. As a result, a majority of the literature in the following sections focuses on rodent fast twitch muscle.

2.7.1 Early *in vitro* isolated muscle research

Investigations with isolated rat EDL muscles at 23° C determined rates of RLC phosphorylation after a tetanic contraction. Manning and Stull (1979) suggested that the phosphate content of myosin RLC reached a maximum 20-25 s after the 1s isometric

tetanic contraction, thereafter declining steadily. P_t corresponded to phosphate content, achieving a maximal rate ~ 25 s after the conditioning stimulus, and then declined until reaching a steady state after ~ 5 min. Furthermore, kinase activity peaked 2-3 s after the tetanic conditioning stimulus, then began to decrease rapidly, achieving steady state after ~ 50 s (Manning and Stull, 1979; 1982). Potentiation of posttetanic twitch force was then counteracted by myosin light chain phosphatase, which dephosphorylated the RLC thus reversing the effect of the kinase (Morgan et al., 1976). It was observed that RLC phosphorylation and force potentiation occurred following stimulation, at frequencies eliciting non-fused contractions (Manning and Stull 1982). These observations coincide with additional work, (Moore and Stull, 1984; Vandenboom et al., 1997) demonstrating the dependence of RLC phosphorylation on stimulation frequency.

Previous work has thus established that crossbridge binding occurs sooner, and to a greater extent when the RLC is phosphorylated. This reaffirms that myosin RLC phosphorylation augments the rate of force development by an increase in the rate constant f_{app}. Considering that g_{app} is unaffected by RLC phosphorylation (Persechini et al., 1985; Sweeny and Stull, 1990), it can be concluded that RLC phosphorylation does not modulate maximal unloaded shortening velocity as it does not alter the rate at which myosin heads dissociate from the thin filament.

2.7.2 Dynamic properties of skeletal muscle

Although a skinned fiber model is ideal for examining myofibrillar properties and fine adaptations to intracellular Ca^{2+} concentrations, this model is not representative of *in vivo* conditions. Physiological conditions are poorly represented due to the absence of

various limiting factors such as temperature, and changes in fiber length. Such conditions will affect the force-pCa curve, altering Ca^{2+} sensitivity, among other detrimental effects. It is therefore important to incorporate these physiological conditions when defining the mechanism *in vivo*.

Grange et al., (1995) used a load clamp technique to assess the rate and extent of shortening in isolated mouse EDL when the RLC was phosphorylated by a conditioning stimulus at 25° C. Briefly, a muscle was held isometrically at a length associated with optimal twitch force (L_o) and then shortened against a load clamped to zero force. Results indicated that shortening after RLC phosphorylation caused a rightward shift in the force-velocity relationship, thus potentiating V_{max}, as well as the relative work and power a muscle is capable of producing. Furthermore, these effects corresponded with a 5-fold increase in RLC phosphate content (Grange et al., 1995). In part, potentiation of work could be attributed to the greater displacement of fibers when phosphorylated. This is made possible as the addition of a phosphate leads to repositioning of the myosin head away from the thick filament backbone to facilitate crossbridge attachment to actin in a strong binding state (Grange et al., 1995). This will result in an increase in f_{app}, leading to a greater population of cycling crossbridges contributing to force generation and sliding for a given load. Considering more work will be performed in the same time frame as in an unpotentiated state, power will also be greater as it is a function of the rate at which work is performed.

Grange et al., (1998) also investigated work and power during conditions simulating *in vivo* contraction. The authors examined augmented work and power output from a muscle rhythmically cycled over various sine excursions centered on L_o, while

stimulated with a single electrical pulse (1 Hz) in isolated mouse EDL at 25° C. Although work output fluctuated across work cycle frequencies, phases of stimulation and the total excursion amplitude, work was generally maximal for most phases at 7 Hz, where as power linearly increased with sine frequency. Once the speed at which maximal was work produced was determined, comparisons in contractile performance were made in both phosphorylated and non-phosphorylated states. Observations confirmed that a 5 Hz, 20 s conditioning stimulus resulted in a 3.7-fold increase in phosphate content on the RLC, which corresponded with potentiation of a single twitch yielding increases in force, as well as work and power output. The authors suggested that the relevance of observations demonstrating force potentiation are best revealed during dynamic conditions such as a work cycle, rather than at a single isometric length. Mean isometric twitch force and rate of force development were potentiated $\sim$ 14 and 12 % post-CS, respectively, along with a decrease in half-relaxation time. The decrease in half-relaxation time suggested that the rate and amount of Ca^{2+} released by the SR was attenuated after a conditioning stimulus rather than augmented. As a result, less Ca^{2+} was released per stimulation. It is therefore more likely that RLC phosphorylation rather than an increase in Ca^{2+} is the primary cause of twitch force potentiation (Grange et al., 1995; 1998). Coincident with the increase in RLC phosphate content, work and power output were potentiated from 25- 50 % across mean excursions of $\sim$ 5 – 13 % L_o (Grange et al., 1998). Collectively, the observations of Grange et al., (1998) provide important insight regarding RLC phosphorylation during contractions mimicking physiological muscle actions (i.e. locomotion), and that this modulatory mechanism may have greater significance during dynamic when compared to isometric contractions.

Additional investigations examining rat EDL muscle *in situ* at $\sim 37^\circ$ C provide supplementary evidence for the role of potentiation during dynamic contractions (Abbate et al., 2000; Abbate et al., 2001; MacIntosh and Bryan, 2002). Studies using isovelocity, and isotonic length changes have identified a significant increase in work and power output over a range of velocities using tetanic stimulations (Abbate et al., 2000; Abbate et al., 2001); as well as following repeated unfused tetanic stimulations over a prolonged duration (MacIntosh and Bryan, 2002).These results associate increases in work with an increase in phosphate content of the myosin RLC (Abbate et al., 2001). With greater displacement during shortening in the same time frame as unpotentiated muscles, more work and thus more power will be generated. It is therefore evident that RLC phosphorylation is beneficial to dynamic muscle contraction. Based on the force-velocity relationship, there is a correlation between RLC phosphorylation and the potentiation of work, power and displacement. RLC phosphorylation is capable of modulating both isometric and dynamic force output, suggesting that increased phosphate content of the RLC represents a reasonable mechanism by which work and power can be potentiated during cyclic contractions (Grange et al., 1998). What remains to be elucidated, however, is the degree to which this mechanism functions to enhance performance during dynamic contractions. Further insight regarding the speed dependence of potentiating work and power may help explain the functional relevance of RLC phosphorylation *in vivo*.

2.7.3 Genetic models

Altering the genetic makeup of C57BL wild type (WT) mice has led to the development of a method that further enhanced the study of potentiating contractile activity. skMLCK knockout mice, as well as skMLCK over expressers were developed

by modification of the MYLK2 gene which produces MLCK. As evident in Zhi et al., (2005), rationale for such genetic alterations stem from the basis of being able analyze potentiation in the presence, and absence of RLC phosphorylation. Zhi et al., (2005) demonstrated that MYLK2 gene inhibits RLC phosphorylation in response to electrical stimulation in rodent skeletal muscle. No significant increases in RLC phosphorylation were observed in skMLCK knock-out mice, while isometric twitch potentiation was also lower than that of control (WT) mice after a conditioning stimulus (Zhi et al., 2005; Gittings et al., 2011). Figure 11 illustrates the marked enhancement in isometric force after a conditioning stimulus known to phosphorylate the RLC, an observation that was absent in isolated EDL from skMLCK KO mice.

Fig .11. Gittings, W. (2009)- Force traces of isometric twitches from isolated KO / WT mouse EDL. The following representative traces compare isometric twitches (1 Hz) prior to, and following a brief tetanic stimulation (150 Hz) in WT (*left*) and skMLCK KO (*right*) mouse EDL
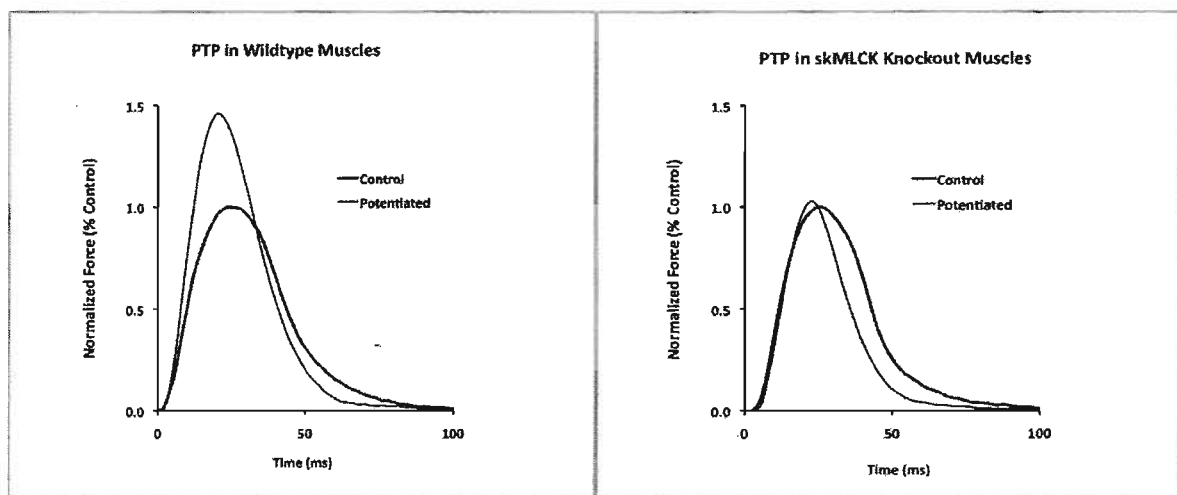
These observations are significant in identifying myosin RLC phosphorylation by skMLCK a primary step in potentiation of muscle force, due to previous stimuli in fast-twitch skeletal muscle fibers (Zhi et al., 2005). Furthermore, the low frequency method of stimulation (10 Hz, for 15 s) was similar to that used to elicit LFF in skeletal muscle

samples as previously mentioned (Vandenboom and Houston, 1996; Rassier and MacIntosh, 2000; Allen et al., 2008). If potentiation was observed in WT mice during these low frequency conditions in isolated muscle, twitch force potentiation may coexist with decreasing force output as a result of fatigue (Vandenboom and Houston, 1996). It can be concluded that RLC phosphorylation is not present in skMLCK knockout mice in response to tetanic stimulation. Although trace amounts of RLC phosphorylation were detected in KO's at the site phosphorylated by skMLCK, the authors suggested that other kinases may be capable of phosphorylating the RLC; however the effects are negligible. Conversely, during prolonged stimulation (10 Hz for 15 s), staircase potentiation was observed in both WT and KO muscles. Such investigations demonstrate that there may be alternate pathways of potentiating contractile output. Redundancy in this aspect therefore suggests the relative importance of this phenomenon *in vivo*, as even in the absence of skMLCK; potentiation of isometric twitch force was observed after repeated low frequency stimulation.

Following the work of Zhi and colleagues, Ryder et al., (2007) examined transgenic mice expressing a skMLCK Ca^{2+}-calmodulin biosensor. This study aimed to determine if skMLCK, or its activator Ca^{2+}-calmodulin limited twitch force potentiation. Results indicated that transgenic mice with up to 22-fold increases in skMLCK protein expression exhibited a more rapid rate of RLC phosphorylation, and force potentiation in mouse EDL in response to a conditioning stimulus than did wild type mice. Ryder et al., (2007) determined that skMLCK rather than Ca^{2+}- calmodulin was limiting for RLC phosphorylation and twitch force potentiation. These results lead to the suggestion that type IIb, but not type IIa or type I fibers contribute to force potentiation (Ryder et al.,

2007). Together, primary observations within the aforementioned studies suggest that skMLCK mediated RLC phosphorylation is the primary biochemical mechanism responsible for twitch force potentiation, however alternate means may exist (Zhi et al., 2005; Ryder et al., 2007).

2.7.4 Examining work and power output

A unique and functional component of skeletal muscle is its ability to shorten against a load, resulting in work. Josephson (1985; 1989; 1993) analyzed the mechanical performance of muscle during perturbations in length. During cyclic length changes, a muscle was either subjected to a single twitch, or a tetanic stimulation at predetermined time points. The resulting force-length plot forms a work loop, which is a graphical representation of work output. An appropriate means of analyzing the resulting work loop would be to divide the area into upper and lower segments, with each segment referring to work performed on the muscle, and work output by the muscle. The area beneath the lower limb of the loop, from minimal to maximal length, has dimensions of force x distance and is the work needed to stretch the muscle from its shortest to longest length (Fig. 13, *see Methods*) (Josephson 1993).

Although theoretically simplistic, the effects of cycle frequency on work and power are complex. Work per cycle initially increases, then declines at high cycle frequencies (Stevenson and Josephson, 1990). Josephson (1993) suggests that the decrease in work per cycle at high frequencies is a consequence of an increase in work performed on the muscle. Upon considering all mechanical factors contributing to contractile function, Josephson (1999) developed a list of primary determinants of muscle force, work and power: shortening velocity (i.e. force-velocity relationship), muscle

length (i.e. length-tension relationship), and the pattern of stimulation and time course of muscle activation. Josephson (1999) also suggested that the length-dependent changes in kinetics of muscle activation, as well as shortening induced deactivation will also play a significant role in shaping contractile performance. Cumulatively these factors will dictate the total force, work and power output of a muscle.

When plotting power with velocity and force the resultant relationship illustrates that as the rate of shortening increases, force produced and corresponding work and power outputs decrease uniformly (Fig. 12). Close examination of each variable may permit indication of a velocity at which optimal power output is attained. Therefore, when translating this relationship to a work loop model, power will begin to decline as work cycle frequency increases. This would be a result of a decrease in total work per cycle, ultimately affecting power (Josephson 1993). Fluctuations in temperature are also critical in determining peak power as the optimal frequency for power output increases with increases in temperature. As a result, careful consideration must go into examining power output via work cycles *in vitro* as many variables can affect contractile output.

Fig. 12. Josephson (1993)- Force-velocity-power relationship
Superimposed on the force-velocity relationship is power when fit to a curve (determined by multiplying force by velocity). It is evident that the capability to produce power increases with velocity until a peak or plateau is reached, thereafter this capability steadily declines.
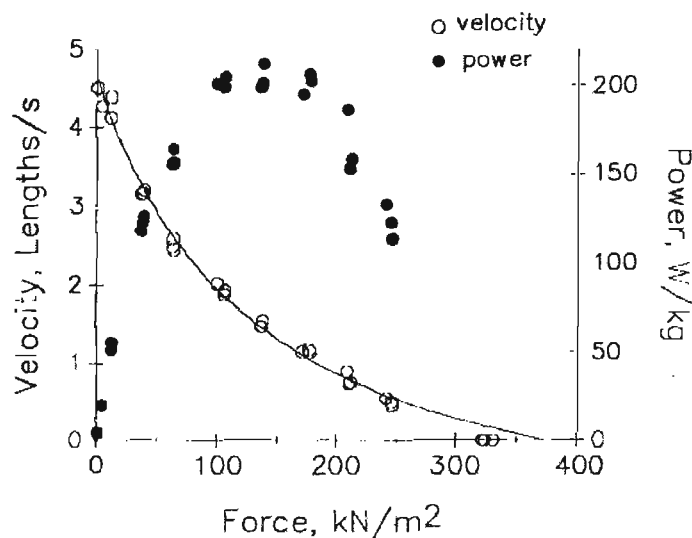
However, Stevenson and Josephson, (1990) suggested that a work cycle approach is suitable for representing muscles that are used cyclically, such as in locomotion or breathing. Specific variables such as cycle frequency, amplitude of shortening, and stimulation pattern have a natural correspondence with the variables that are important in modulating force and power output of muscle *in vivo* (Stevenson and Josephson, 1990). In comparison, Josephson (1993) suggests that maximal power output during isotonic and/or isovelocity length changes may overestimate the sustainable power available from a muscle during similar repetitive activations. Rationale for this stems from the fact that shortening velocity seldom remains constant throughout a shortening phase *in vivo*. Stimulation over a constant velocity or constant force would result in more work, and thus power. Furthermore, a common property of repetitively activated muscle is a sinusoidal shortening trajectory (Josephson 1993). Accordingly, the maximal power available from a muscle shortening with a sinusoidal trajectory is ~ 10-20 % less than

what would be obtained when shortening at an optimum velocity for the entire contraction (Josephson 1993). As a result, various discrepancies complicate the utilization of an isotonic or isovelocity contraction to represent repetitive activation *in vivo*.

2.7.5 Relationship to physiological function

Interest in the physiological relevance of RLC phosphorylation has markedly expanded with evolution in the understanding of this mechanism. It is undoubtedly attractive to consider the possibility of a group of potentiated motor units yielding augmented work and power output for the same level of neural input (Grange et al., 1998). To determine the magnitude of the potentiating influence during dynamic muscle contraction, it is critical to attempt to replicate the physiological conditions in which the contractions occur. Determination of work and power output from force-displacement, or force-velocity relationships do not adequately reflect performance *in vivo* (Grange et al., 1998). Correspondingly, the work loop approach is well suited for assessing work and power output from skeletal muscle during tasks such as running, swimming or flying (Josephson 1993). This model is derived from the nature of contraction *in vivo*, as during repetitive movements muscles attached to skeletal structures undergo repetitive length changes. Numerous factors such as the type of muscle examined, the solution and temperature in which the muscle sits, as well as the work cycle frequency and strain imposed all affect work and power output. As a result, great methodological concerns must be taken into consideration when using this model. However, the work loop approach offers a plausible means of extrapolating *in vitro* observations regarding RLC phosphorylation during dynamic contractions. As such, examination of both lengthening

(eccentric), and shortening (concentric) contractions are necessary as physiological performance is composed of agonist and antagonist muscle activation. For example, during locomotion muscles may act agonistically in initiating the stride or swing phase, however also have antagonist roles in stabilization during the landing or stance phase. It is therefore important not only to further elucidate the impact of RLC phosphorylation on concentric contractions, but eccentric as well.

2.7.6 RLC phosphorylation during eccentric contractions

Very little work has been published regarding the influence of RLC phosphorylation during lengthening contractions. As a result, the modulatory influence of this mechanism on eccentric contractions remains unclear. However, of the few reports that have investigated the influence of RLC phosphorylation during eccentric contractions, a negative effect has been established. Childers and MacDonald (2004) determined that RLC phosphorylation increases eccentric contraction induced injury in skinned fast-twitch fibers. Furthermore, Clarkson et al., (2005) suggested that single nucleotide polymorphisms for skMLCK are associated with increased sensitivity to exercise injury in humans. It has therefore been suggested that RLC phosphorylation renders a skeletal muscle more susceptible to injury after eccentric contractions as a result of the increased force, or perhaps by modulating the structural integrity of the myofibrillar lattice (Childers and MacDonald, 2004). Further elucidating this mechanism would understandably have clinical applications for special populations where individuals have disorders predisposing them to contraction induced injuries (i.e., Muscular Dystrophy). A more in depth examination regarding eccentric contractions and RLC phosphorylation is therefore warranted.

STATEMENT OF PROBLEM:

3.0.0 Purpose

What remains to be elucidated is whether contraction speed has an effect on the potentiation of work and power during an associated work cycle. Previous work has established that as muscle shortening velocity increases, absolute concentric force will decrease as demonstrated by the force-velocity relationship. Therefore, the aim of the present study was to observe relative changes in dynamic force, work and power output prior to and following tetanic stimulation as a result of altering the speed of shortening in fast twitch skeletal muscle during cyclic length changes. As a result, the primary objective was to assess the speed dependence of dynamic (i.e. concentric and eccentric) force, work and power associated with a conditioning stimulation known to phosphorylate the myosin RLC in fast-twitch skeletal muscle.

3.1.0 Hypotheses

- Potentiation of dynamic function is both speed (i.e. fast vs. slow) and direction (i.e. concentric vs. eccentric) dependent.

- Increasing work cycle frequency will augment the magnitude of potentiation of force produced, as well as relative work and power during concentric contractions. As a result, concentric activity will display a positive relationship with speed; as potentiation of contractile performance will increase as work cycle frequency increases.

- The magnitude of potentiation during eccentric contractions will not be greater than that of concentric or isometric contractions, displaying a decline in potentiation as work cycle frequency increases.

3.2.0 Rationale

In accordance with the fundamental principles of crossbridge binding and tension development, increases in the population of strongly bound crossbridges will in turn enhance active force production. Correspondingly, it can be assumed that eccentric contraction coincides with a greater population of strongly bound crossbridges as it is associated with greater force output than concentric or isometric contractions (Enoka, 1996; Brunello et al., 2007). Such characteristics are illustrated within the force-velocity relationship of skeletal muscle fibers as eccentric contractions correspond with higher force values than concentric (Fig 8.). A plausible explanation for this may in fact result from the increased activation of the thin filament due to an increased population of strongly bound crossbridges, as well as Ca^{2+} on thin filament binding sites while the muscle is lengthening as opposed to shortening (Yang et al., 1998; Gordon et al., 2000). This is evident as shortening reduces the number of actin bound crossbridges, and continues to decrease with increases in isotonic shortening speed in single frog fibers (Vandenboom, Hannon and Sieck, 2002). A decrease in strongly bound crossbridges is associated with the reduction in Ca^{2+} occupancy of TnC (Vandenboom et al., 1998). Rationale for the expected findings of the present investigations can therefore be based on the characteristics of the force-velocity relationship and the varying degrees of thin filament activation.

Although alternate mechanisms are possible, it is well accepted that RLC phosphorylation modulates contractile function to augment force production as a result of increased Ca^{2+} sensitivity, due to an increase in f_{app}. As a result, these observations can be attributed to the elevated population of myosin heads interacting with the actin filament. To fully grasp this concept, consider the model of crossbridge binding suggested by McKillop and Geeves, (1993). The authors suggest that initial binding of crossbridges positively influences additional binding along the thin filament, leading to greater activation. In turn, greater activation may translate into an increase in both the rate of force development as well as force production. Accordingly, +dF/dt must be inversely related to fiber shortening speed during concentric contractions. Such mechanistic factors are responsible for the steady decline in concentric force output as shortening velocity increases (see Fig 8.).

During eccentric contraction the opposite appears to be true, however. This may once again be attributed to a high level of thin filament activation as well as population of strongly bound crossbridges, as lengthening contractions are associated with a greater number of myosin heads contributing to force production (Brunello et al., 2007). To this end, it is predicted that increased muscle activation by RLC phosphorylation will result in the absence of eccentric force potentiation. This indicates that active lengthening mitigates the potentiation influence by increasing muscle activation independent of excitation-contraction coupling alone. Conversely, a concentric contraction is vulnerable to reductions in force production as a result of limited crossbridge binding, increased interfilament spacing and reduced +dF/dt (Vandenboom et al., 2002). Furthermore, as the speed of shortening increases it becomes more difficult for additional strong crossbridge

interactions between thick and thin filaments to occur as myosin heads are attaching/detaching at a rapid rate. As a result, it is expected that at this end of the force-velocity spectrum RLC phosphorylation will elicit its most profound effects.

Concurrent with the evidence provided above, thin filament activation may be modulated by the number of strong actin bound crossbridges during contraction. Under this model, it is conceivable that potentiation resulting from RLC phosphorylation is inversely related to thin filament activation. Thus, the mechanistic factors contributing to muscle activation levels may enhance, or mitigate the potentiation influence. Consistent with this, the greatest magnitude of potentiation would be observed during rapid shortening contractions, while such an influence would be negligible when a muscle is stimulated during rapid lengthening.

3.3.0 Assumptions

It is assumed that passive cycling of a muscle does not induce phosphorylation of the RLC in WT mice. This assumption is supported by the observations of Grange et al., (1998) who determined that isometric twitch properties (i.e. time to peak force (TPF), half relaxation time ($RT_{1/2}$), peak active force (F_{at}), and the rate of force development (dF/dt_{max})) were unaltered by work cycles at 7 Hz, with a sine excursion of 9 % L_o. Furthermore, it is also assumed that the strain amplitude used does not cause significant damage to the myofilament lattice. Brooks, Zerba, and Faulkner (1995) suggest that for single eccentric contractions a passive stretch of 50% beyond L_f (L_o x 0.44) strain or greater was necessary to produce significant damage. Considering the present study will

induce a stretch of ~ 5% L_o and cycle at frequencies up to 6.9 Hz, significant damage to the structural integrity of the contractile apparatus is not anticipated.

Although RLC phosphorylation has traditionally been accepted as the primary mechanism responsible for potentiation in fast twitch skeletal muscle, alternate mechanisms may also exist. MacIntosh (2010), and references therein, highlights these mechanisms suggesting that increasing peak free myoplasmic Ca^{2+} concentration, as well as the sequential elevation of oxidation then reduction potential in the cytoplasm may contribute to both staircase and PTP, respectively. Further investigation is required regarding the total contribution of these mechanisms, however. Thus, for the present study RLC phosphorylation will be considered the primary mechanism responsible for observations of augmented contractile performance.

3.4.0 Limitations

Although an *in vitro* experimental model has previously been used in numerous investigations, this model lacks certain aspects of *in vivo* conformity. For example the following experiments are conducted at sub-physiological temperatures (25° C). As previous studies have identified, the potentiating influence is greater at higher temperatures when compared to low temperatures (Lowy et al., 1991; Persechini et al., 1985). As a result, temperature can significantly affect contractile function (i.e., modifying symptoms of fatigue and/or potentiation). The present study may therefore underestimate the magnitude of potentiation observed at more physiological temperatures, and thus poses a potential limitation when drawing conclusions about *in vivo* function. Supplementary to this, the absence of an intact blood supply also detracts

from replicating *in vivo* conditions as the muscle is required to withdraw O_2 and essential substrates from the physiological solution in which it is incubated. To address this concern, an *in situ* model which offers physiological circulation could be used.

Although a work loop model is favourable for replicating physiological muscle actions such as locomotion, various discrepancies surround the work loop parameters. As such, selection of stimulation phase, sine excursion and work cycle frequency are factors that will significantly influence work and power output during a work loop. Generally, the optimum phase for work output is such that activation begins shortly before the end of the lengthening half cycle (Josephson 1993). Furthermore, as the work cycle frequency increases total cycle duration decreases. This may result in incomplete relaxation at the end of the shortening phase, therefore increasing the work required to re-lengthen the muscle, ultimately reducing net work (Josephson 1993). Collectively, selection of each parameter will dictate the amount of work and power developed. This may pose a potential limitation to yielding maximal contractile output if the aforementioned factors are not carefully considered.

An additional factor that must also be taken into consideration is the possible compliance of tendons within the muscle tendon unit (MTU). In this regard, compliance refers to the fact that a stretch imposed on the MTU versus the muscle fascicle alone may result in a varying degree of sarcomere length change and thus stress (Roberts and Azizi, 2010). Lichtwark and Barclay, (2010) suggest that the level of compliance within a tendon will have a significant impact on both peak and average power output of the muscle. Essentially, a more compliant tendon will result in less lengthening/shortening of the muscle fibers vs. the MTU. Therefore, the velocity at which the muscle fibers actually

shorten may be slower, and in more of a range that optimizes contractile output (i.e. ~ 25-39 % of V_{max}). Furthermore, shortening at a reduced speed would limit the level of thin filament deactivation associated with rapid shortening. As a result, despite taking care to limit the amount of tendon by tying the suture as close to the fascicle as possible, the variability in compliance may be a potential limitation in assessing performance of the muscle itself rather than the MTU as a whole.

METHODS

A large portion of literature exists examining the mechanical work output of a muscle during step length changes *in vitro*. However, measurements elicited while a muscle shortens under a constant load (isotonic), or velocity (isovelocity) fail to accurately represent the function of contracting muscle *in vivo*. By introducing phasic stimulation during a work loop model, the work cycle technique can be applicable to synchronous muscle, and utilized as a realistic method for estimating mechanical work and power output of muscle *in vivo* (Josephson 1985).

4.1.0 Experimental apparatus

Mouse EDL muscles were suspended in an oxygenated organ bath (Radnoti Glass Technology, Inc) containing a physiological solution maintained at constant temperature (25° C) using an Isotemp 3013S circulator (Fisher Scientific). Muscle stimulation was applied through flanking platinum electrodes driven by a Model 701B biphase stimulator (Aurora Scientific, Inc.). Isometric muscle length (i.e., not during dynamic length changes) was monitored using a horizontal stereo zoom microscope (Bausch & Lomb),

which can be manually controlled at increments of 0.01 mm using a sliding micrometer (Velmex, Inc). Contractile data were collected at 2000 Hz, using a 300C-LR servomotor acquired through a 604C analog to digital interface, and controlled by a dual-mode lever system (ASI). Data acquisition and immediate force analyses was performed using ASI 600a software (Version 1.60).

4.2.0 Wild type mice

Wild type (WT) C57BL/6 mice at age 10 weeks were purchased from Charles River Laboratories. Animals were housed in small groups and provided standard chow and water *ad libitum* and maintained at ambient room temperature on a 12 h: 12 h night: day cycle. All experiments were approved by the Brock University Animal Care and Use Committee (Protocol # 10-05-01).

4.3.0 Surgical procedures

Animals were sedated with an intraperitoneal injection of diluted Sodium Pentobarbitol (0.025 ml/g body weight, diluted with 0.9% saline) in a 1 ml syringe. EDL muscles were then surgically excised by isolating proximal and distal tendons with non-absorbable braided silk (4-0) sutures, and then separating the tendon-bony process union with a scalpel. One EDL was mounted on the experimental apparatus, while the other was maintained in an oxygenated physiological solution on ice. Viability of the second muscle is not a significant concern as Barclay (2005) suggested that a mouse EDL should sufficiently diffuse enough oxygen to remain viable while held in an oxygenated solution. The tyrode solution was continuously gassed (95% O_2, 5% CO_2) using a scintillated glass dispersion valve and maintained at 25° C. Final ionic concentrations of the solution was

(in mM): 121 NaCl, 5 KCl, 24 $NaHCO_3$, 0.4 NaH_2PO_4, 0.5 MgCl, 1.8 CaCl, 5.5 D-Glucose, and 0.1 EDTA. Following EDL extraction animals were euthanized by lethal injection of pentobarbital sodium into the heart (0.05ml/g body weight) and disposed of according to Brock University Animal Facility protocol.

4.4.0 General experimental protocols

The following experiments were conducted as a means of determining the relative potentiation of force, work and power in mammalian fast twitch skeletal muscle at various speeds of work cycle frequencies.

4.4.1 Preliminary procedures

After calibrating force and length of the servomotor, an EDL was suspended between two parallel platinum electrodes. Each experiment began with a preliminary sequence of protocols designed to ensure consistency of observations. Initially, L_o was roughly estimated by measurement through the stereo zoom microscope, and the EDL stimulated with two 500 ms (150 Hz) tetani, spaced 10 s apart to remove any compliance and possible slipping of the suture on the tendon. Muscles were then equilibrated for 45 min during which a 1 Hz, 100 ms twitch was elicited every 3 min, and voltage intensity of stimulation was gradually increased to ensure maximal excitation of all motor units. Such twitch pacing also permitted the observation of muscle viability throughout the equilibration protocol. Furthermore, muscle twitches in isolation had a negligible influence on RLC phosphorylation and fatigue, and were used to track the decay of twitch potentiation throughout the experimental design.

Following a 45 minute equilibration period, optimal length for isometric twitch force (L_o) was determined, after which each muscle underwent an experiment to assess the influence of a potentiating stimulus on both isometric (twitch and tetanic) and dynamic contractile function. Determination of L_o required linear length changes in which several 0.01 L_o length increments were elicited over a 2 s duration. A length-ramp occurred every 8 s, with a 1 Hz stimulus timed 5 s after each corresponding length change. Twitches were used rather than a tetanus because they are less energetically demanding, and most relevant to the stimulation patterns employed in the experiments (Crow and Kushmerick, 1982). At a muscle length of 1.1 L_o the protocol was complete, and the length at which active twitch force (passive force subtracted from total force) was maximal was considered L_o for the remainder of the experiment.

4.4.2 Experimental procedure

After equilibration and determination of L_o, dynamic function (i.e. concentric and eccentric output) was assessed using the work cycle technique. Various frequencies were incorporated to test the influence of different speeds of length change on the potentiation of dynamic function caused by a conditioning stimulus. Briefly, muscles were passively shortening or lengthening around L_o in a sinusoidal manner. Muscles initially cycled without receiving any stimulation for ~30 s, establishing work output of the passively moved EDL. As muscles continued to cycle, single twitch stimulations were intermittently applied every 5 s for ~ 30 s to determine active force, work and power. Sine wave excursion (peak to nadir) was equal to 5% muscle length, centered on L_o (± 2.5%). For each muscle, the magnitude of work was obtained at three different work cycle frequencies to mimic various speeds of physiological locomotion (1.5, 3.3 and 6.9

Hz). The order of sine frequencies was randomized to remove a potential order effect, ensuring that PTP was insensitive to the duration and order of the protocols. The timing of the single stimulus pulse during the sine cycle was coincident with L_o. The three different work cycle frequencies used (i.e. 1.5, 3.3 and 6.9 Hz) corresponded to muscle speeds of ~ 5, 12 and 25% of maximal shortening velocity (V_{max}), which will be examined more closely in the following sections.

4.4.3 Mimicking *in vivo* locomotion

Determination of work cycle frequencies was based on physiological locomotion in rodents. James et al., (1995) and Clarke and Still (1999) examined the biomechanics of locomotion in rodents through gait analysis and electromyography (EMG) activity. These authors determined that EMG activity of rat EDL begins after the foot has left the ground, and continues until just after the foot touches again (James et al., 1995). The predominance of EDL activity in late swing phase in rodents is similar to that of humans, functioning to maintain dorsiflexion of the foot and toes (Rodgers 1988). In addition, a minor phase of EDL activity also occurs during push off, co-contracting with other muscles of the lower leg to stabilize the ankle joint (Rodgers, 1988). EMG data were used to analyze ground contact times and various stride frequencies in rodents. As a result, a series of stride frequencies corresponding to various stages of locomotion was established. Briefly, a stride frequency of 2.87 Hz represented a slow walk, whereas 8.23 Hz was a flat–out gallop. Trot-to-gallop transition occurred at a stride frequency of 5.89 Hz, while the average pace of a walk was ~ 3.7 Hz (Clarke and Still, 1999). These findings are similar to that of Heglund et al., (1974). Thus, as stride frequency increased, the velocity of shortening also increased, translating into decreased total stride time.

Clarke and Still (1999) determined that average stride frequency in mice differed between forelimb (~ 263 ms) and hindlimb (~270 ms); with a slightly faster stride frequency in the forelimb. Each stride can be further broken down into stance and swing phases; as the stance phase represents when the limb is in contact with the ground, and swing refers to limb movement off of the ground. In light of such complex examinations of rodent gait mechanics, it has been suggested that there is an interdependence between temperature and stride frequency on power output (James et al., 1995). Taken together, there is a trend towards increased power output with increasing work cycle frequency and temperature to a more physiological range. However, this relationship will reach a plateau, thereafter decreasing work/power performed per cycle as a result of constraints imposed by the force-velocity relationship (James et al., 1995).

On the basis of this theoretical framework, the work cycle frequencies for this study have been determined. Accordingly, work cycle speeds were derived from previous studies (James et al., 1995; Grange et al., 1998; Clarke and Still, 1999), encompassing a range of physiological speeds of locomotion. To this end, slow, moderate and fast work cycle frequencies were selected as a means of observing the potentiating influence over various speeds of locomotion. Therefore, work cycle frequencies of 1.5, 3.3 and 6.9 Hz were chosen to mimic very slow, moderate and fast paced gait *in vivo*, respectively. It is also important to consider the velocity at which a muscle cycles *in vivo*, and how this can be incorporated in an *in vitro* design. Brooks and Faulkner (1988) determined that the V_{max} of a mouse EDL *in vitro* at $25°$ C is 10.4 fiber lengths sec $^{-1}$ (L_f/s) in young mice, and 9.8 L_f/ s in adult mice. In accordance with these values of V_{max}, James et al., (1995) report that young mice typically walk at shortening velocities of ~ 12-15 % of V_{max}; and

trot and velocities of $\sim$ 24-39 % V_{max}. When compared to the shortening velocity range of $\sim$ 23 – 35 % V_{max} which elicits optimal efficiency of filament sliding (Brooks and Faulkner, 1988), a trot may be the most economical form of ambulation. In the present study, the velocity of shortening was assessed as the muscle passed through L_o. Although cyclic length changes characterized by a work loop do not shorten or lengthen at a constant speed over the total excursion amplitude, length change speed immediately around L_o is relatively linear (Josephson 1985; 1989). The midpoint (L_o) of the lengthening and shortening phases was therefore representative of the peak velocity achieved throughout the entire sine excursion. Such observations determined that at work cycle frequencies of 1.5, 3.3 and 6.9 Hz, shortening velocity as the muscle passed through L_o corresponded to values of $\sim$ 5, 12 and 25 % of V_{max} (compared to published values of Brooks and Faulkner, 1988), respectively.

4.4.4 Determining work and power

As previously discussed, calculated work was a measure of force either produced by (concentric), or performed on (eccentric) a muscle over a specific change in length. By plotting force vs. length, the corresponding area under the curve represents total work. Josephson suggests that the area beneath the upper limb of the loop, from longest to shortest length, is the work performed by the muscle. Subtracting work input from output provides an area which is the net work performed within the cycle, and is usually expressed as Joules (J). Multiplying the net work per cycle (J) by the cycle frequency (time) determined the rate at which work was performed in Watts, which is also referred to as power (Josephson 1985).

Fig .13. Josephson (1985)- Determining net work production of a work cycle
When plotting force over length the area under the curve represents total work. When shortening the direction of length changes moves in a counterclockwise manner, indicating work is performed by the muscle. When lengthening the direction of length changes moves in a clockwise manner, indicating that work is performed on the muscle. By subtracting work output by work input net work per cycle can be determined.
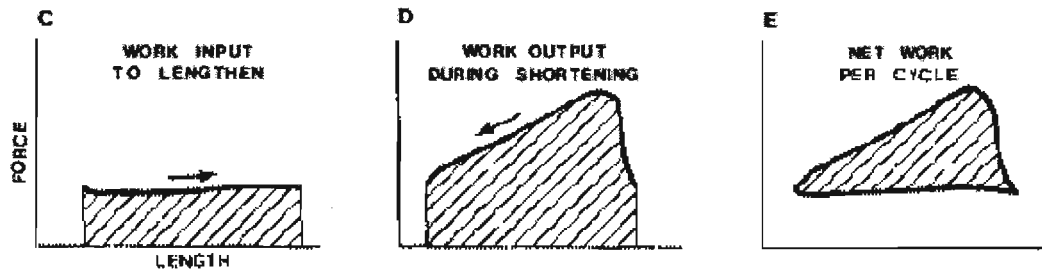
Work, and therefore power, were calculated used this approach. Data were imported into Microsoft® Excel, where the area under the curve was determined for both potentiated and unpotentiated work-loops. Subtracting passive from total work yielded a value which was made relative to wet muscle mass (J/Kg). Absolute work and power values were then compared before and after the conditioning stimulus to determination the relative change in both (potentiation).

4.5.0 Experimental timeline

The experimental procedures are best described in three distinct sequences (each sequence representing a new work cycle frequency), with each sequence further dissected into two phases (summarized in Fig. 15). Phase 1 (unpotentiated work cycles) of a sequence followed the equilibration/quiescent period, and refers to the muscle passively cycling at a specific work cycle frequency. As previously mentioned, 30 s of passive cycling was followed by 30 s of 1 Hz stimulations, spaced ~ 5 s apart; resulting in a total of 3 twitches during muscle shortening (concentric), and 3 while lengthening (eccentric). One twitch per cycle was timed to stimulate at a length that closely corresponded with L_o

during both shortening and lengthening portions of the work cycle. Thus, muscles were stimulated in such a manner that muscle length passed through L_o as it reached peak force. This also ensured that muscles were stimulated at a point which corresponded to the fastest shortening velocity during the work cycle. MacIntosh and Bryan (2002) have also incorporated such stimulation timing, despite the fact that it does not correspond with typical activation *in vivo* (Josephson 1993).

Phase 1 allowed for observation of the magnitude of unpotentiated force, work and power during a sine excursion (baseline). Upon completion of this phase ($\sim$ 1 min), the sine excursion ceased, and muscles were held isometric at L_o in preparation for a CS. The CS consisted of three 500 ms, 100 Hz tetani (Tetanus 1-3), elicited over a 10 s duration (see Fig. 14). This stimulation pattern results in maximal RLC phosphorylation, while minimizing fatigue (Vandenboom et al., 1997). In addition, a single twitch was elicited 5 s before Tetanus 1; and 15 s after Tetanus 3 to analyze absolute values of potentiated P_t. The duration of the entire CS protocol was $\sim$ 30 s, during which the myosin RLC was phosphorylated, and potentiation as well as fatigue were assessed.

Fig. 14- Example of CS protocol
Tetani were induced by a 100 Hz, 500 ms stimulation, each appropriated spaced 4.25 s apart. 5 s prior to, and 15 s following the tetanic stimulations are 1 Hz isometric twitches which assess the potentiation of isometric twitch force.
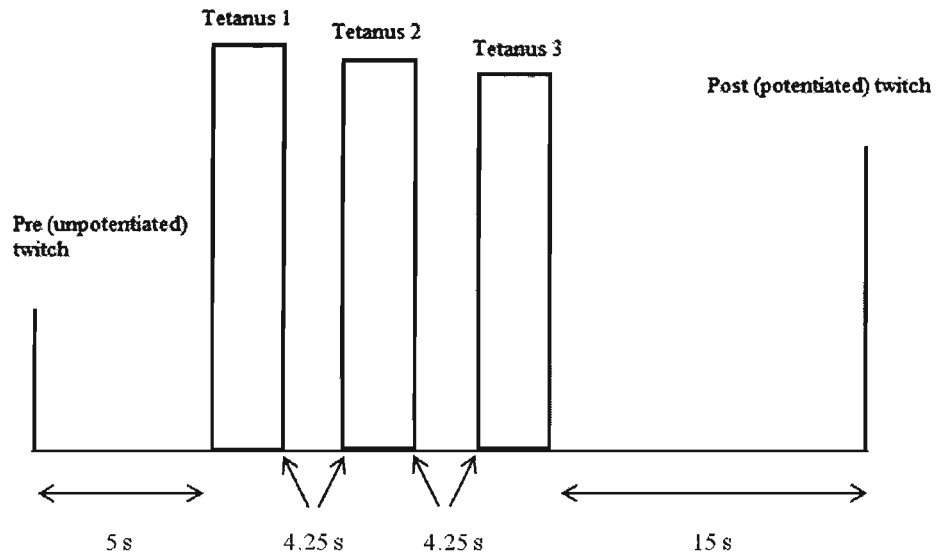
Phase 2 (potentiated work cycle); examined force, work and power output of a muscle following the CS and subsequent phosphorylation of the RLC. Following the CS (~17 s after the final tetanic stimulation) muscle length was immediately cycled around L_o using the same frequency and amplitudes as before the CS. Because of the rapid kinetics for the potentiation influence on muscle mechanics, only responses obtained within the initial 5 s of this phase were analyzed. Observations from these work cycles thus allowed direct comparisons to be made between eccentric and concentric force, work and power output before and after phosphorylation of the RLC. Therefore, this permitted the observation of the magnitude of potentiated work and power for each work cycle frequency.

The end of phase 2 marked the completion of one whole sequence. A quiescent period of 30 min followed phase 2, in which muscles held isometric at L_o were twitched

steadily. This rest period allowed phosphatases to dephosphorylate the myosin RLC, thus removing the potentiated effect (Morgan et al., 1976; Manning and Stull, 1979; Sweeney et al., 1993). EDL were stimulated with 1 Hz twitches every 2 min as a means of assessing the decay of isometric twitch force potentiation. The next phase commenced only when two consecutive twitches produced the same P_t as the initial (unpotentiated) twitch.

Followed the 30 min quiescent period, a transition was made to a new work cycle frequency. This transition marked the beginning of the next sequence which was identical to the last. This protocol (i.e., one sequence composed of two phases) was followed in its entirety for three different work cycle frequencies (1.5, 3.3, and 6.9 Hz) to assess the effect of potentiation on dynamic function at various speeds (order of work cycle frequencies randomized to prevent a potential order effect). See figure 15 for experimental timeline.

4.5.1 Analysis of potentiation/fatigue

Potentiation of both isometric and dynamic performance were assessed by subtracting the passive tension from total responses to stimulation of the muscle. This provided an active value representing peak force for a given stimulation, which was then compared by dividing the potentiated response by the unpotentiated response. Such comparisons provided a measure of the relative increase in contractile output. This decimal fraction therefore indicated of the amount of potentiation observed within the muscle.

Fatigue was assessed by evaluating the decrease in P_o during the CS protocol. This was accomplished by dividing peak force of the final tetanus by the first tetanus, thus providing a percentage indication of total contractile force depression (fatigue). These values were then compared throughout the experimental sequence to assess muscle viability.

4.5.2 Myosin RLC phosphorylation

In addition to contractile data, RLC phosphate content was assessed at four different time points on separate sets of muscles during the experiment. To obtain resting phosphorylation values, muscles were frozen immediately after equilibration (n = 8), as well as 30 min after the final CS (n = 5). Comparisons were thus made between resting phosphorylation levels prior to and following repeated bouts of contractile activity. In addition, phosphorylation induced by the high frequency conditioning stimulus was also assessed after a single CS (n = 7), as well as after the third and final CS (~ 1 hour apart) (n = 7). This permitted assessment of peak phosphorylation values, as well as muscle viability throughout the experimental timeline. Consistency among RLC phosphorylation levels, as well as isometric twitch force potentiation following each CS was therefore used as a measure of viability throughout the duration of the experiment. These data would therefore confirm that the RLC is repeatedly phosphorylatable, and that phosphorylation returns to baseline (resting) levels after a period on inactivity.

Muscles were appropriately freeze clamped and stored at -80° C in separate experiments. The aforementioned experiments are summarized below:

Exp#	Sample size(n)	Details
1	5	Prelim seq → Work cycles @ 3 sine frequencies + 3 rest periods → Freeze after final 30 min rest period . *Observe the return of RLC phos levels after a series of phosphorylation/ dephosphorylation protocols*
2	8	Prelim seq → Freeze muscle. (*Freezing immediately after equilibration protocol, prior to commencing sequence one*). *Determine initial resting RLC phosphorylation values*
3	7	Prelim seq → 1 CS → Freeze muscle ~15s post-CS (*Muscles frozen prior to commencing phase 2 within sequence one*). *Determination of peak RLC phosphorylation*
4	7	Prelim seq → Work cycles @ 3 sine frequencies + 2 rest periods → Freeze ~15s after final CS (*Frozen prior to commencing phase 2 within sequence 3*). *Assess viability of the muscle by comparing RLC phosphorylation after a single CS vs. three CS*

4.5.3 Determination of myosin RLC phosphorylation

After freezing, muscles were stored at − 80° C until shipped on dry ice to the laboratory of Dr. James Stull (University of Texas, Southwestern Medical Center, Dallas, TX). Muscles were homogenized in 10% trichloroacetic acid and 10 mM dithiothreitol at 0° C, and total proteins were collected by centrifugation at 3,000 rpm for 2 min in a table-top centrifuge. Protein pellets were solubilized into 8 M urea and then subjected to urea/glycerol-PAGE to separate phosphorylated and nonphosphorylated RLC as described previously (Ryder et al., 2007). Because the urea/glycerol-PAGE system

separates nonphosphorylated from monophosphorylated RLC, a direct quantitative measure of RLC phosphorylation in terms of percent or mol of phosphate/mol of RLC was provided. After separation, proteins were transferred to polyvinylidene difluoride membranes and probed with a polyclonal primary antibody raised in rabbits to purified skeletal RLC. Secondary antibody conjugated with horseradish peroxidase was then applied to the membranes. Quantitative measurements were processed on a Storm PhosphorImager (Molecular Dynamics; Sunnyvale, California) and analyzed by ImageQuant software.

4.6.0 Data analysis and Statistics

Statistical significance was determined using SPSS Inc. PAWS version 18.0 statistical analysis software. Correspondingly, a 2 x 4 Univariate analysis of variance (ANOVA) was used to test the hypothesis that there is a main effect for work cycle frequency and a conditioning stimulation (CS) on dynamic force. The dependent variables (i.e., force) was analyzed by comparing factor A (Stimulation: A1= pre-CS; A2= post-CS) against four levels of factor B (Speed: B1= Isometric; B2= 1.5 Hz; B3= 3.3 Hz B4= 6.9 Hz). Similarly, a 2 x 3 Univariate analysis of variance (ANOVA) was used to test the hypothesis that there is a main effect for work cycle frequency and a conditioning stimulation (CS) on dynamic work and power. Factor A was identical, however only three levels of factor B were included as there was no work calculated during isometric stimulations. If a main effect was significant, a Tukey HSD post-hoc analysis was used to determine differences between treatment means. For all statistical analyses, a P value of < 0.05 was considered significant.

A line graph and independent samples t-test were used in analyses which indicated a significant interaction, specifically selecting for cases that appear significantly different. Conclusions were thus drawn based on the significance of these observations.

For comparison of relative means, a one-way ANOVA was used, along with a Tukey HSD post-hoc analysis to determine whether work cycle frequency had a significant effect on the means, $(P < 0.05)$. To assess the relative difference in force and work between stimulations (i.e. concentric vs. eccentric) a similar 2 X 3 ANOVA was performed as mentioned above, however, factor A was changed to (type of stimulation: A1 = CON; A2 = ECC).

Fig. 15- Experimental timeline

Legend

Symbol	Meaning
∿∿∿∿	= sine excursion
———	= isometric period (at L_o)
₩	= twitch series during sine excursion (eccentric and concentric)
| |	= isometric twitches (detection of PTP)
■	= freeze muscle
UP WC	= unpotentiated work cycle
CS	= conditioning stimulation
POT WC	= potentiated work cycle
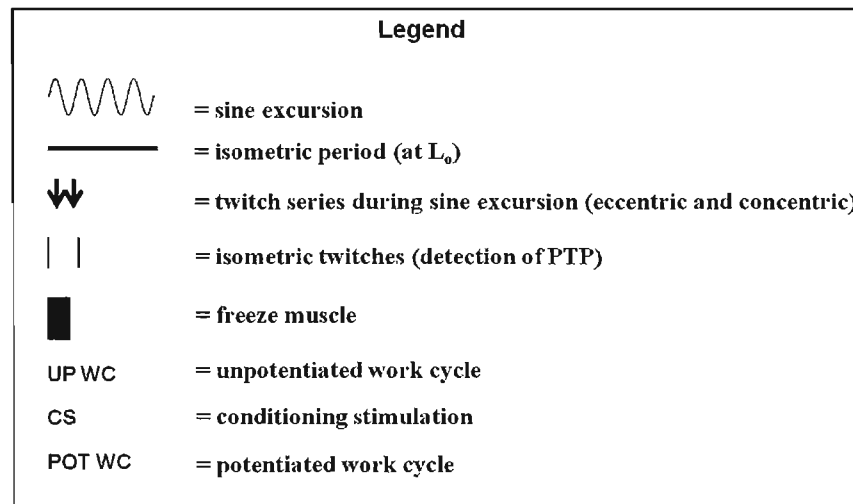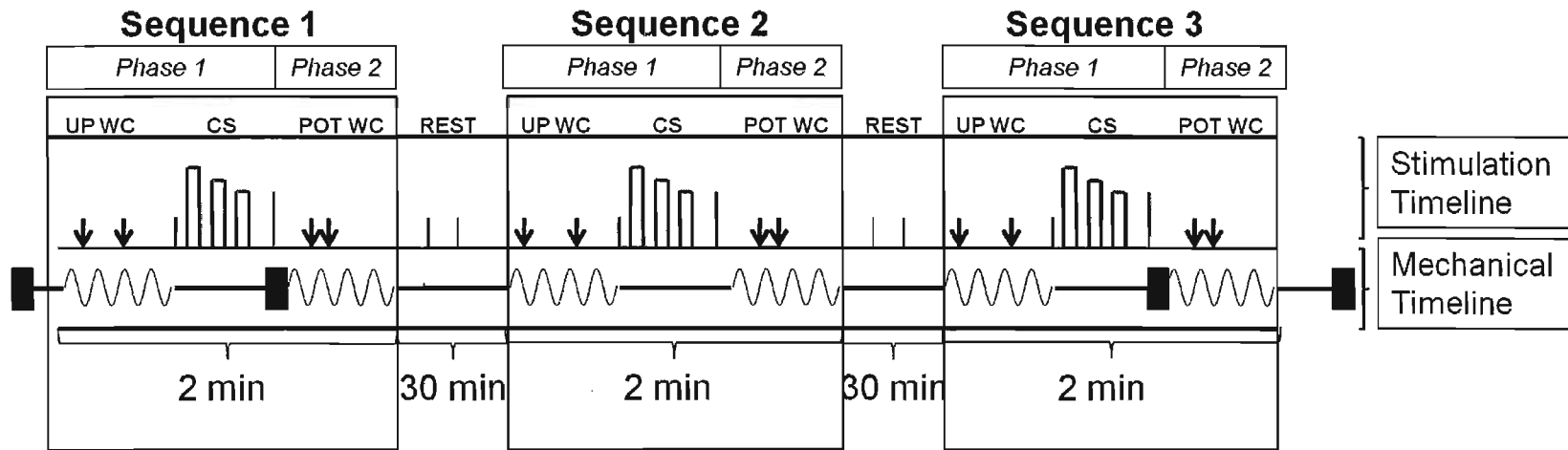
RESULTS:

5.1.0 Conditioning stimulus

Muscles were stimulated with a high frequency CS (Vandenboom et al., 1997) between pre- and post-measures of force, work and power to induce maximum potentiation of low frequency performance without causing substantial levels of fatigue. Pooled data for isometric twitch force demonstrated a consistent ($20 \pm 1\%$) increase in force compared to controls (Table 1). Furthermore, potentiation of isometric twitch force varied by less than 1% when compared at several points across the experiment. Conversely, the CS induced a negligible fatigue of peak tetanic force, with tetanus 3 being decreased by $\sim 4\%$ compared to tetanus 1 (i.e. 0.96 ± 0.002). In addition, tetanic forces recorded during each CS showed little variation when repeated throughout the experiment (no significant difference between CS; $P < 0.05$), suggesting the viability of the muscle after repeated stimulations.

5.2.0 RLC phosphorylation

Similar to previous reports (Zhi et al., 2005), the potentiation of twitch force observed was consistent with the $\sim$ 3-fold elevation in RLC phosphate content induced by the CS. Figure 16 demonstrates representative western blots, as well as summary data for experiments 1-4. RLC phosphorylation values for quiescent muscles frozen after equilibration (Exp.2), as well as those frozen $\sim$ 30 minutes after a CS (Exp.1) were 0.18 ± 0.02 and 0.17 ± 0.04 mol phos / mol RLC, respectively. In muscles frozen immediately following a conditioning stimulus at the beginning (Exp.3) and end (Exp.4) of an

experiment, RLC phosphorylation values were 0.47 ± 0.02 and 0.54 ± 0.04 mol phos per mol RLC, respectively. These data demonstrate that the conditioning stimulus had a similar effect in elevating RLC phosphate content throughout the duration of an experiment.
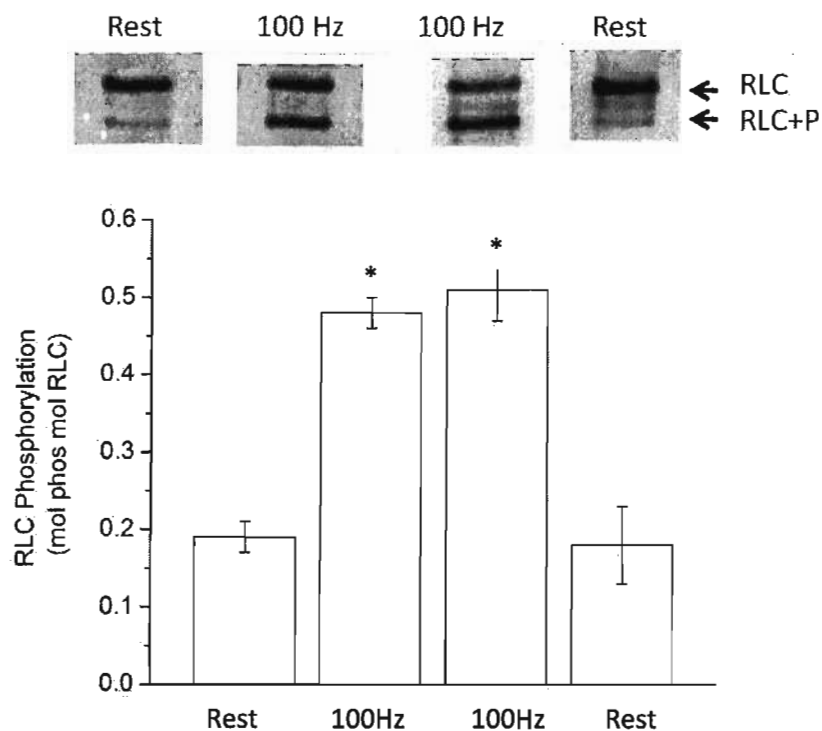
Fig. 16- Myosin RLC phosphate content- (Top) Representative blots show phosphorylated (P-RLC) and unphosphorylated (skRLC) bands in muscle samples prior to, and following a conditioning stimulus. Resting samples show low levels for RLC phosphorylation were obtained from quiescent muscles frozen at the beginning (far left lane) and the end (far right lane) of the experiment. Stimulated samples demonstrating high levels for RLC phosphorylation were obtained from muscles frozen immediately after the conditioning stimulus at the beginning (middle left) and the end (middle right) of the experiment. Lanes have been cut from different blots for the purposes of comparison. (Bottom) Summary of all blots showing RLC phosphorylation (expressed as mol phos per mol RLC as quantified by optical density) during experiments. * Stimulated value greater than resting value ($p < 0.001$). Values are mean $\pm$ S.E. ($n = 5 - 8$ per group).

5.3.0 Twitch force potentiation

To test the influence of passive cycling on contractile data collected, concentric and eccentric twitch forces were compared at the beginning and end of each work cycle train. These observations indicated that passive cycling had no significant effect on concentric, or eccentric twitch force at 1.5, 3.3 or 6.9 Hz. Passive cycling appeared to reduce final eccentric twitch force by $\sim$ 5% at 6.9 Hz; however, it was not significantly lower than the initial twitch (P = 0.572). Therefore, the speed of sinusoidal length change had no discernable effect on peak dynamic twitch force.

Analysis of dynamic twitch force output yielded results which were expected in relation to the known force-velocity properties of skeletal muscle. Table 1 represents twitch forces before and after application of a high frequency conditioning stimulus. As anticipated, absolute concentric force decreased and eccentric force increased as work cycle frequency increased from 1.5 to 6.9 Hz. Alternatively, isometric force remained constant when assessed throughout the experimental timeline, consistently potentiating $\sim$ 20 $\pm$ 1% following tetanic stimulation. A factorial ANOVA determined a main effect for both independent variables (speed and conditioning stimulation) on concentric force. Furthermore, Tukey's post-hoc analysis determined that significant decreases in absolute twitch force were apparent at each speed (in both UP and POT work cycles). As a result, both the CS and work cycle frequency had a significant effect on concentric force output; however, there was no significant interaction between the independent variables. Therefore, the CS which successfully phosphorylated the RLC of myosin corresponded with a significant increase in concentric force from pre-CS values for all work cycle

frequencies. Moreover, the magnitude of the force potentiating effect increased as work cycle frequency increased (Fig. 17).

Similar to concentric observations, there was a main effect of speed on eccentric twitch force; steadily increasing as work cycle frequency increased. However, the CS had no effect on increasing force post-CS vs. pre-CS ($P < 0.05$). Figure 17 demonstrates the relative change in dynamic force induced by the CS at each work cycle frequency (post-CS divided by pre-CS values). Upon comparing relative values, the differences between concentric and eccentric force become even more apparent. A clear increase above pre-CS values is illustrated for concentric force, while eccentric force remains relatively constant around pre-CS values. When compared to potentiated isometric twitch force, which remains constant, concentric force was potentiated to a greater extent at 3.3 and 6.9 Hz, but not 1.5 Hz (Table 1). Such observations suggest the existence of a minimum threshold work cycle frequency, below which the differences in potentiation between concentric and isometric forces are negligible. When normalizing dynamic force responses to isometric, a speed dependence for twitch force potentiation was evident (Fig.18), with the greatest separation in dynamic and isometric forces at the fastest work cycle frequency.

Table 1- Absolute forces before and after a conditioning stimulus

Freq.	Concentric		Eccentric		Isometric	
	Pre	Post	Pre	Post	Pre	Post
1.5Hz	57.1± 2.8	67.6± 3.4*	78.5± 3.7	82.9± 4.1	67.0± 3.2	79.9± 4.0*
3.3Hz	45.5± 2.2†	56.6± 2.9*†	95.4± 5.3†	96.8± 5.0†	67.3± 3.5	80.8± 4.3*
6.9Hz	28.2± 1.7‡	36.4± 2.2*‡	126.6± 7.4‡	120.6± 7.1*‡	66.2± 3.8	79.6± 4.5*

Means ± SEM; n = 9 for all observations. Forces expressed in mN and represent active force (total force minus the passive force). For dynamic forces, muscles were stimulated during shortening or lengthening phases of sinusoidal movement to produce concentric or eccentric force, respectively. In each case, force was measured as the muscle passed through L_o. Isometric data were obtained during separate, fixed length contractions at L_o. All pre and post – CS data were obtained ~5 - 10 sec before and ~ 15 - 20 sec after a conditioning stimulus. * post – stimulus value is significantly different than respective pre-stimulus value ($P < 0.05$); † significantly different from 1.5 Hz values ($P < 0.05$); ‡ significantly different from 1.5 and 3.3 Hz values ($P < 0.05$).
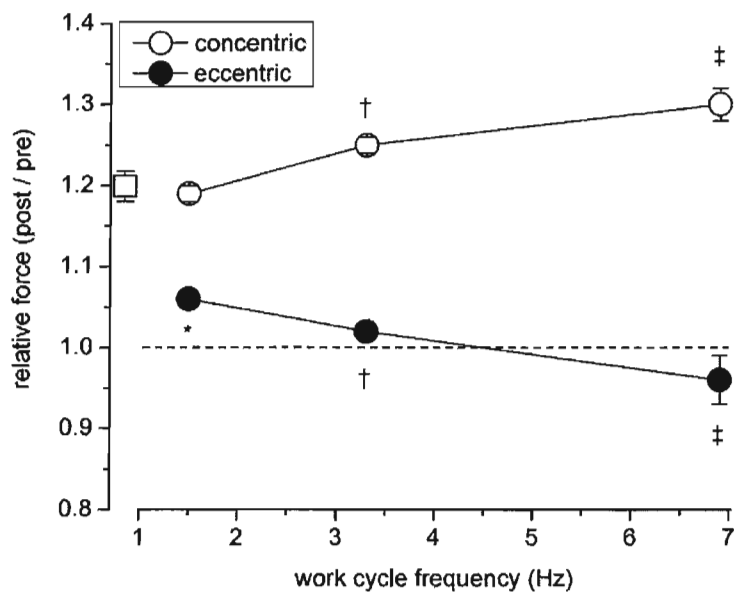
Fig. 17- Relative change in dynamic force as a function of work cycle frequency – For each parameter, relative change was calculated by dividing post stimulation values by pre stimulation values. All forces were determined at L_o. Square data point depicts relative isometric twitch force potentiation for reference. * sig. different than isometric value ($P < 0.05$); † 3.3 Hz sig. different than 1.5 Hz; ‡ 6.9 Hz sig. different than 1.5 and 3.3 Hz ($P < 0.05$). All concentric values were greater than corresponding eccentric values ($P < 0.05$). Based on data presented in Table 1.
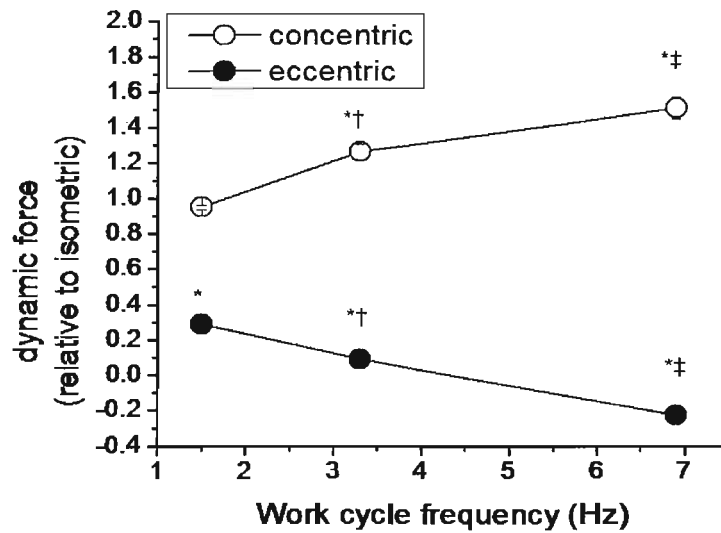
Fig.18- Dynamic forces normalized to isometric – Line graph showing potentiation of concentric and eccentric forces when normalized to the potentiation of isometric twitch force within each sequence. * concentric/eccentric sig. different than isometric (1.00) ($P < 0.05$); † 3.3 Hz sig. different than 1.5 Hz ($P < 0.05$); ‡ 6.9 Hz sig. different than 3.3 Hz.

5.4.0 Work and power

5.4.1 Concentric data

Tables 2 and 3 summarize work and power responses at each frequency for dynamic contractions. Recall that concentric and eccentric work / power values were produced by stimulating the muscle during sine shortening and lengthening. Given the corresponding output of force over a defined length, work was determined. A factorial ANOVA reported a main effect for speed (P = 0.000) but not the CS (P = 0.079) on concentric work/power output. A significant interaction was reported between independent variables, however, indicating that work output at a particular speed was dependent on the CS. A line graph identified an interaction at 6.9 Hz, illustrating that work was greater post-CS vs. pre-CS. An independent samples t-test later revealed that there was in fact a significant increase in concentric work post-CS over pre-CS (P < 0.05). In determination of where the effect of speed was significant, a post-hoc analysis revealed that work was significantly different between all work cycle frequencies, except for 3.3 and 6.9 Hz.

Table 2 - Concentric work and power during different frequency work cycles before and after a conditioning stimulus

	Work		Power	
Freq	*Pre*	*Post*	*Pre*	*Post*
1.5 Hz	0.62 ± 0.06	0.52 ± 0.04*	0.94 ± 0.08	0.79 ± 0.07*
3.3 Hz	0.94 ± 0.07†	0.99 ± 0.07†	3.11 ± 0.23†	3.25 ± 0.26†
6.9 Hz	0.85 ± 0.06†	1.18 ± 0.08*†	5.85 ± 0.40§	8.14 ± 0.58*§

Means ± SEM; n = 9 for all observations. Work expressed in joules (J) per kg wet weight muscle mass and represents the dimension of force x excursion per work cycle. Power expressed as watts (W) per kg wet weight muscle mass and represents the dimension of work per unit time (s). Muscles were stimulated during shortening phase of sinusoidal cycling to produce concentric force and work. Data obtained ~ 15 s before and ~ 20 s after a conditioning stimulus. * post – CS value significantly different than respective pre-stimulus value ($P < 0.05$); † significantly greater than 1.5 Hz values ($P < 0.05$); ‡ significantly different from 3.3 Hz values ($P < 0.05$); § significantly different from 1.5 and 3.3 Hz values ($P < 0.05$). For more details regarding calculation of work and power see Methods.

Representative work loop traces are depicted in Figure 19, demonstrating the influence of the CS on concentric work at each frequency (panels a-c). Considering the resultant area of the force-length plot represents work, Fig. 19 illustrates the changes in total work, and thus power, prior to and following a CS at each work cycle frequency. Despite the fact that concentric force significantly increased after a CS in all conditions (Table 1), post-CS work and power output decreased at 1.5 Hz and increased negligibly at 3.3 Hz. Only at 6.9 Hz was work and power significantly greater than pre-CS values. Figure 20 offers a closer examination of net work when plotting the difference between work in the potentiated versus unpotentiated state (delta work) over time. Panels A-C in Fig. 20 demonstrate the speed dependent balance between positive and negative work during muscle shortening at each condition. Fig. 20 (A-B) highlights the absence and negligible difference in work at 1.5 and 3.3 Hz. Most prominent is the significantly larger positive work area associated with the fastest work cycle frequency (Fig. 20- C). These observations further explain the difference in relative work output across each condition demonstrated in Figure 22. The dashed line represents a relative value of 1.0, indicating no change in work. Thus, an observable relationship exists between potentiation of work and speed of shortening. However, close examination reveals that a threshold frequency of ~ 2.5 Hz appears to be required in order to extract positive gains. Such observations aid in further elucidating why work and power only increased significantly from pre-CS values at 6.9 Hz (Table 2), as well as the frequency dependence for positive versus negative work which ultimately determines net work output.

Because power was determined as the rate at which work is performed, a similar relationship was found between absolute power and work cycle frequency (Fig. 23a).

Concentric power output was significantly influences by work cycle frequency, steadily

increasing as work cycle frequency increased. However, only at 6.9 Hz was power output

significantly greater post-CS in comparison to pre-CS.

(a)

(b)
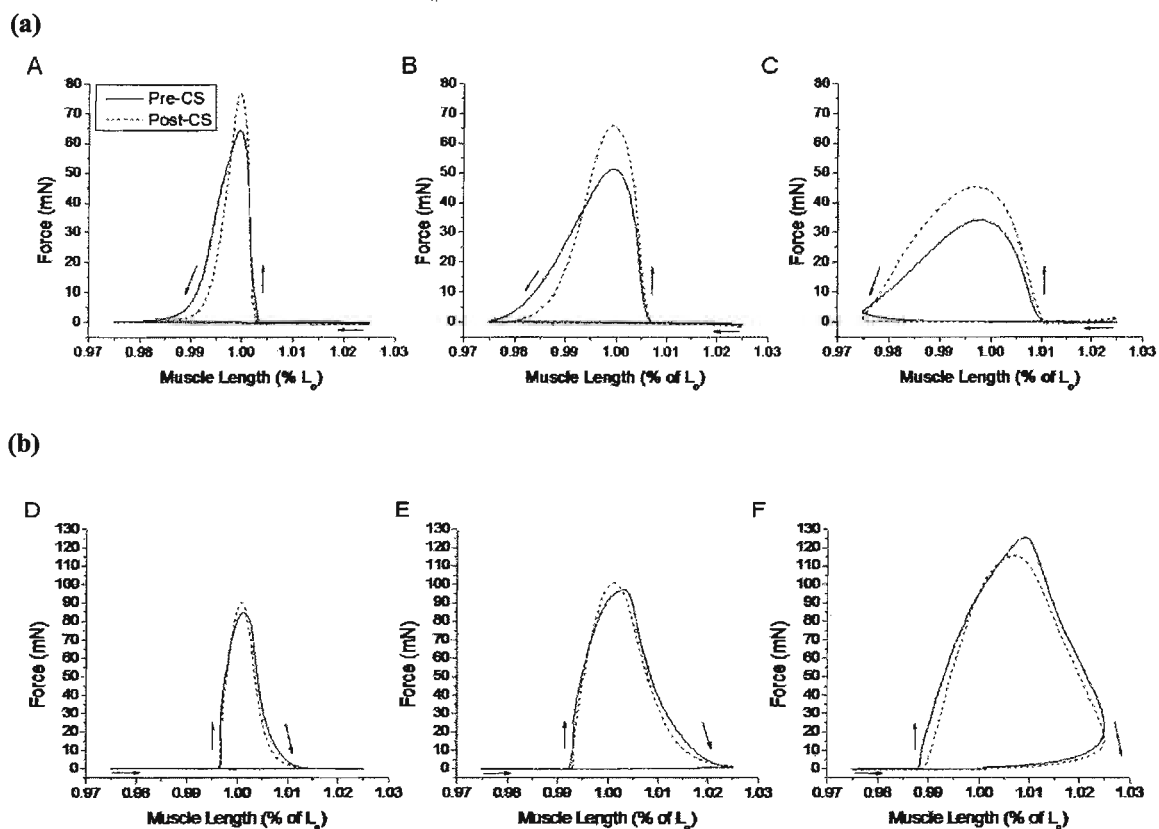
Fig. 19 – **Representative active (a) concentric, and (b) eccentric work loops-** Work loops of mouse EDL muscle *in vitro* (25° C) before and after a conditioning stimulus. Panels A-C (a) are representative work loops at 1.5, 3.3 and 6.9 Hz in response to a single stimulus pulse applied during shortening to produce concentric force at or near optimal length (L_o). Work loops were obtained ~ 20 s before and ~ 20 s after a conditioning stimulus. Here active concentric force plotted versus muscle length yields a counterclockwise loop (arrows), the area of which represents work. Panels D-F (b) are representative work loops at 1.5, 3.3 and 6.9 Hz in response to a single stimulus pulse applied during lengthening to produce eccentric force at or near optimal length (L_o). Work loops were obtained ~ 20 s before and ~ 20 s after stimulation. Active eccentric force plotted versus muscle length yields a clockwise loop (arrows), the area of which represents work. See Methods for details on sine-wave function and determination of dynamic work and power. All traces from same muscle.
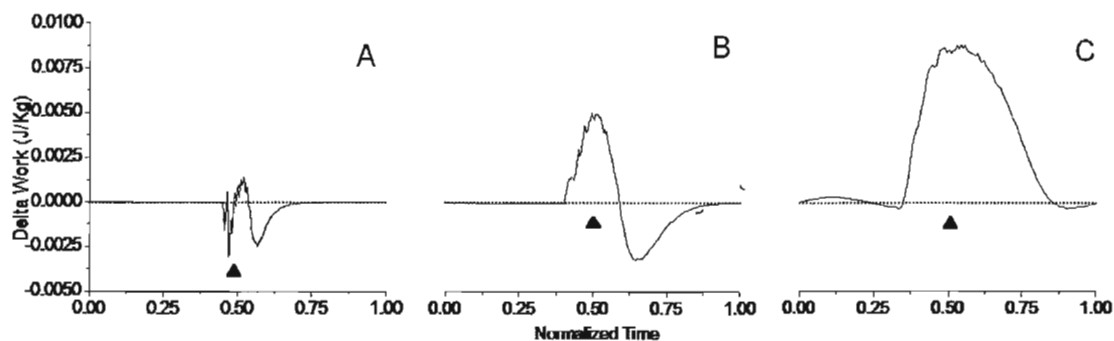
Fig. 20- Change in concentric work output over duration of stimulation- Representative records showing delta concentric work (potentiated – unpotentiated) vs. cycle time for 1.5 (A), 3.3 (B) and 6.9 Hz (C) work cycles. Solid triangle indicates L_0. The x-axis in each panel has been normalized to 1.00 to facilitate comparison, however actual time corresponded to $\sim$ 667, 303 and 145 ms for 1.5, 3.3 and 6.9 Hz work cycles, respectively. Negative work (area below line) is greater than positive work at 1.5 Hz, while positive work is greater than negative work at 6.9 Hz; positive and negative work were approximately equal at 3.3 Hz.

5.4.2 Eccentric data

Eccentric observations contrast those of concentric as the CS had no effect on augmenting total work or power output (Table 3). Despite a main effect for speed on eccentric work and power, significantly differing in each condition, respectively, pre-CS data were not significantly different from post-CS data. Also, no significant interaction was found between independent variables, indicating that the CS had no discernable effect on augmenting eccentric output at any work cycle frequency.

Table 3- Eccentric work and power during different frequency work cycles before and after conditioning stimulus

	Work		Power	
Freq	*Pre*	*Post*	*Pre*	*Post*
1.5 Hz	0.83 ± 0.07	0.73 ± 0.06	1.24 ± 0.11	1.09 ± 0.09
3.3 Hz	$1.96 \pm 0.17\dagger$	$1.78 \pm 0.15\dagger$	$6.54 \pm 0.54\dagger$	$5.86 \pm 0.48\dagger$
6.9 Hz	$3.43 \pm 0.32\ddagger$	$3.37 \pm 0.29\ddagger$	$23.67 \pm 2.1\ddagger$	$23.24 \pm 2.00\ddagger$

Means $\pm$ SEM; n = 9 for all observations. Work expressed in joules (J) per wet weight muscle mass. Power expressed as watts (W) per wet weight muscle mass. Muscles were stimulated during lengthening phase of work cycle to produce active eccentric force and work. Data obtained ~ 15 s before and ~ 20 s after a conditioning stimulus. * post – stimulus value different than respective pre-stimulus value ($P < 0.05$); † significantly different 1.5 Hz values ($P < 0.05$); ‡ significantly different from 1.5 and 3.3 Hz values ($P < 0.05$).

Figure 19 (panels d-f) offers a representation of the absence of potentiated work. Although absolute eccentric force significantly increased with work cycle frequency, relative potentiation of work output remained consistently low and/or negligible. Upon comparing relative work at each work cycle frequency (Fig. 22), eccentric work increased with increasing speed. This characteristic is similar to that of concentric work, however occurred at a much more gradual rate. Figure 21 suggests that such observations may be attributed to the dominance of negative work which combats positive work across all conditions. Distinct from concentric observations, negative work often prevailed over positive as a muscle lengthened regardless of work cycle frequency. As a result, net work output (positive work minus negative work) remained close to zero, indicating little or no work cycle frequency dependence for positive vs. negative work during eccentric work cycles. Therefore, as demonstrated in Table 3, as well as Fig.22, there was no significant increase in work and power following a CS for eccentric contractions.

Thus, despite the significant increase in absolute eccentric power as work cycle frequency increases (Fig. 23b), the relative change in power (as a function of work) was negligible as demonstrated in Figure 22. Upon examining absolute power output across each work cycle frequency, eccentric power was significantly greater than concentric at each work cycle frequency (P < 0.05).
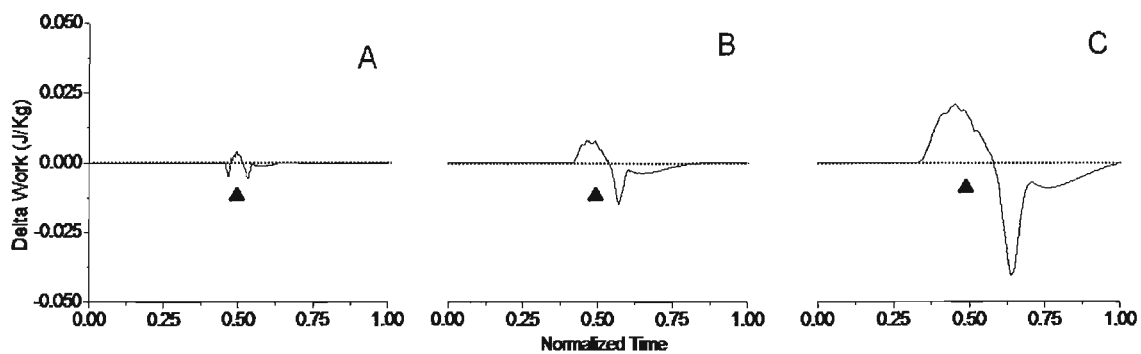
Fig. 21- Change in eccentric work output over duration of stimulation– Representative records showing delta eccentric work similar to that in Fig. 20. Solid triangle indicates L_o, with x-axis normalized to 1.00. Note that positive and negative work is approximately equal in all panels. For each trace, the zero - crossing is the point where positive work becomes negative work. All records are from the same muscle.
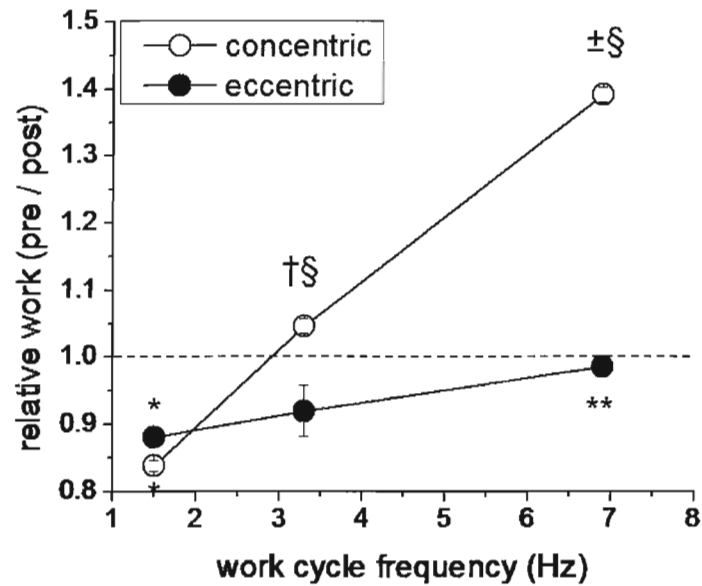
Fig . 22- Relative concentric and eccentric work as a function of work cycle frequency - For each parameter, relative change was calculated by dividing post stimulation values by pre stimulation values during each work cycle frequency. Figure is based on absolute data compiled in Tables 2 and 3. Note that all concentric values are different from 1.0 (dashed line represents no relative change in work) (P < 0.05). * sig. different than 1.00 (P < 0.05); † 3.3 Hz sig. different than 1.5 Hz; ** 6.9 Hz different than 1.5 Hz (P < 0.05); ‡ 6.9 Hz different than 1.5 and 3.3 Hz (P < 0.05); § concentric different than eccentric (P < 0.05).

(a)
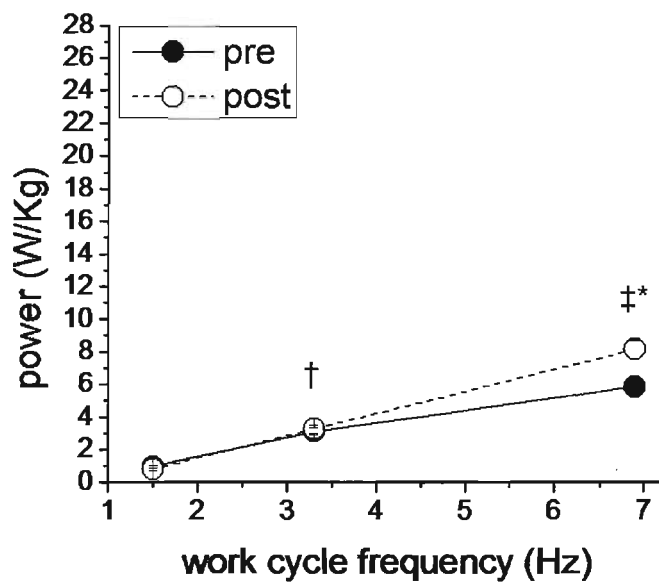
(b)
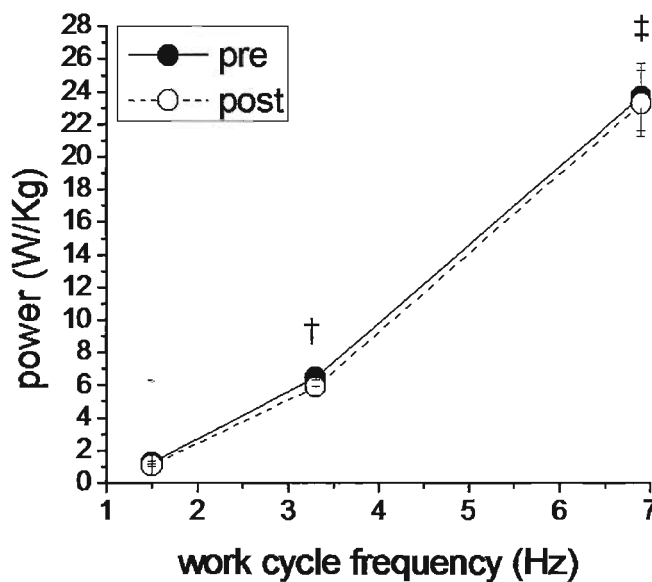
Fig. 23- **Absolute (a) concentric, and (b) eccentric power output** (as a function of work cycle frequency)- Both concentric (a) and eccentric (b) figures are represented along the same axes. * Post sig. greater than pre (P < 0.05); † 3.3 Hz sig. different than 1.5 Hz; ‡ 6.9 Hz different than 1.5 and 3.3 Hz (P < 0.05).

5.5.0 Maximal shortening velocity

Slack tests (*see Appendix C*) were performed on a small population of muscles (n = 3) in order to determine the unloaded shortening velocity (V_o) of mouse fast muscle incorporated within this study. Values were assessed as shortening speed in L_f/s, and in accordance with the work of Claflin and Faulkner (1985), unloaded shortening velocity was converted into maximal shortening velocity (V_{max}) as the ratio of V_o / V_{max} was reportedly 1.6 ± 0.1 when measured *in vitro* at $20°$ C. Data were in close association with the reported V_{max} values of 10.4, and 9.8 L_f/s assessed in young and adult mouse EDL, respectively, *in vitro* at $25°$ C (Brooks and Faulkner, 1988).

Table 4 – Shortening velocities of mouse EDL at $25°$ C

Sample size (n)	V_o	V_{max}
3	17.63 ± 0.78	11.02 ± 0.49

Means $\pm$ SEM; n = 3 for all observations. Table demonstrates calculated V_o and V_{max} values in fiber lengths per second (L_f/s). V_{max} was determined by dividing V_o by 1.6. Absolute values represent maximal unloaded shortening velocity (V_o), as well as the maximal shortening velocity of mouse EDL *in vitro*, $25°$ C.

DISCUSSION:

Current literature elucidates a strong relationship between phosphorylation of the RLC of myosin and potentiation of both isometric and dynamic (concentric) output. Uniform with this evidence is the understanding that such potentiation is limited or absent in slow twitch skeletal muscles; which demonstrate lower skMLCK activity (Moore and Stull 1984), as well as in skMLCK KO mice where the MLCK gene has been ablated (Zhi et al., 2005). Although alternate mechanisms of potentiation may be possible (i.e. increased free myoplasmic $[Ca^{2+}]$) (MacIntosh 2010), a basic assumption of the present investigation was that stimulation-induced elevations in RLC phosphate content (via high frequency CS) was the primary mechanism responsible for the potentiation of dynamic muscle function. Consistent with previous work, the introduction of a conditioning stimulus in the present study significantly increased phosphate content on the myosin RLC from resting values (~ 0.51 vs. ~ 0.19 mol P-RLC / total-RLC, pooled data). Following the CS protocol in each condition concentric force was significantly greater than pre-CS values, increasing ~ 19, 25 and 30 % from that of control at 1.5, 3.3 and 6.9 Hz, respectively. Although relative concentric work had decreased at 1.5 Hz (0.84 ± 0.01), and negligibly increased at 3.3 Hz (1.05 ± 0.01), work was significantly potentiated at 6.9 Hz (1.39 ± 0.01), thus highlighting a speed dependence for concentric performance following a CS. In contrast, the CS did not have an effect on potentiating eccentric activity as neither force, nor work/power were significantly increased at any work cycle frequency. As a result, the present observations revealed a profound hysteresis like effect, in which concentric output increased and eccentric output decreased, both proportionally with work cycle frequency. This therefore suggests that

contractile performance may be preferentially potentiated in a speed and direction dependent manner. These observations are in accord with previous work demonstrating that elevations in myosin RLC phosphate content increase steady state isometric force in response to submaximal, but not maximal, Ca^{2+} activation in skinned skeletal muscle fibers (Persechini, Stull and Cooke, 1985; Metzger et al., 1989; Sweeney et al., 1993). Moreover, recent work by Childers and McDonald (2004) showed that, in addition to enhancing steady state forces, phosphorylation of the RLC increases the maximally Ca^{2+} activated concentric force and work/power output of rabbit psoas skeletal muscle fibers by 20 - 25%. These results support a physiological role for RLC phosphorylation by showing that, unlike steady-state isometric force responses, dynamic performance is increased at higher Ca^{2+} activation levels.

Historically speaking, attempts at understanding muscle function during physiologically relevant tasks such as locomotion have relied on observations under constant velocities or loads. Although influential, by examining the force-velocity properties in isolation researchers failed to closely mimic the method of muscle activation as well as function *in vivo*. Thus, the emergence of a cyclic (work loop) model allowed such observations to be made over a natural range of motion, and at frequencies closely corresponding to physiological conditions. Such methods have since proven to be seminal in determining how muscles produce force, and how this translates to work and power output (Daniel 1999 and references therein). In using the work loop model, the purpose of this study was to investigate the speed dependence for the potentiation of mechanical function following a standard conditioning stimulus known to induce PTP of mouse EDL muscle *in vitro* (25° C) (Vandenboom et al., 1997; Xeni et al., 2011). Results indicated

that, although a shortening - speed threshold appears to be apparent, concentric force and work increased progressively with increasing shortening speed in the range of 1.5 to 6.9 Hz. In contrast, eccentric responses were relatively unchanged by the CS. These results highlight the possibility that contractile modulation by prior activation is "tuned" to enhance high power locomotor function. By converting potential energy into mechanical work when shortening, and acting as a physiological "brake" by generating high resistive forces during lengthening (Brunello et al., 2007), modification of skeletal muscle activity appears to be dependent on both the speed and type of contraction.

6.1.0 Work cycle technique

As previously discussed, the amplitude and frequency of work cycles used in this study fall within the range previously reported for mammalian skeletal muscle (Syme and Stevens 1989). Moreover, the work cycle frequencies utilized corresponded to slow, moderate and fast locomotion of rodents (James et al., 1995; Clarke and Still, 1999). Correspondingly, the force and work data reported in this study were consistent with several previous observations assessing performance using the work cycle technique (Grange et al., 1998; Xeni et al., 2011); however, some inconsistencies do exist (i.e. Brooks and Faulkner 1991; Lynch et al., 2001). Rationale for such discrepancies in work and power output between studies may be a result of varying methodologies for determining work (i.e. use of isovelocity length changes vs. work cycles, as well as tetanic stimulation frequencies vs. a single twitch. In addition, the aforementioned studies examined mice of different ages and/or strains which will have a significant effect of contractile performance.

Although previous investigations (James et al., 1995; Grange et al., 1998) have found a strain amplitude of $\sim \pm 5 \% L_o$ to be nearly optimal for power output, the underlying purpose of this study was to simply assess the speed dependence of potentiation. Hence, use of a smaller strain amplitude was not necessarily detrimental to the present results, as it still provided significant insight towards the mechanism of potentiation during repetitive activation simulating locomotion *in vivo*. Additional support for the selection of this strain amplitude lay in the examination of early pilot work. Previous observations demonstrated that passive tension responses were of equal, or greater magnitude than that of a stimulated response throughout the sinusoidal length change when strain amplitude was $10 \% L_o$ (peak to nadir). James et al., (1995) suggests that with increased passive forces in muscle there is a resultant decrease in power output due to the greater resistance to muscle lengthening. In an attempt to reduce passive forces strain amplitude was therefore lowered. While this removed the sine excursion from a typical working strain range of $\sim 13 \% L_o$ commonly observed in skeletal muscle (Burkholder and Lieber, 2001), the parameters employed in this study still demonstrated the basic characteristics of a work cycle model. Furthermore, although muscles are not stimulated *in vivo* at such low frequencies as in this study (i.e. 1 Hz), voluntary activation of skeletal muscle has been reported as an unfused tetanic stimulation (Rassier and MacIntosh, 2000). Considering the known effects of RLC phosphorylation on augmentation of submaximal contractile activity, potentiation may still be observed at voluntary activations frequencies *in vivo*. However, because physiological stimulation would occur at higher frequencies, the magnitude of potentiation observed would be less than that found at 1 Hz stimulations. As such the present investigations, although not

exactly physiological, are still relevant in further elucidating the mechanisms behind the potentiating influence during *in vivo*-like conditions.

6.2.0 The potentiation influence

The present study observed a speed-dependent, direction-dependent increase in concentric work and power output, which was coincident with a 3-fold elevation in RLC phosphate content. This is consistent with previous studies using rodent hind limb muscle models *in situ* (Abbate et al., 2000; 2001; MacIntosh and Bryan 2002). Previous investigations have reported an increase in the magnitude and velocity of shortening, resulting in augmented work and power output during isotonic/isovelocity muscle length changes after previous activation. The magnitude of augmented work and power reported in these studies were proportional to increases in muscle shortening speed. Thus, it is evident that skeletal muscle is more sensitive to the potentiation mechanism as shortening speed increases, observations that are consistent with the present findings that concentric work and power was greater as work cycle frequency increased. Rationale for this outcome may originate from observations in single fibers from frog (Edman, 1975) and mouse (Vandenboom et al., 1998) skeletal muscle, demonstrating thin filament deactivation during shortening. Essentially, thin filament deactivation refers to the mechanism which results in a decreased affinity for Ca^{2+} on Troponin binding sites, thus reducing thin filament activation. Correspondingly, this may sensitize the contractile apparatus to the effects of RLC phosphorylation; where increased Ca^{2+} sensitivity, as well as the increase in transition of crossbridges to a strong force generating state (well documented in skinned fiber studies Persechini et al., 1985; Metzger et al., 1989; Sweeney and Stull, 1990) function to augment force production. Pursuant to such

evidence, augmented contractile performance at higher velocities of shortening will thus induce a greater magnitude of potentiated work and power when compared to slower velocities. Evidence for this was well demonstrated within the results of the present investigation as relative potentiation of concentric work and power was ~ 66% greater in the fastest condition when compared to the slowest (Fig. 22). It is important to recall that activation of the thin filament is controlled by the binding of Ca^{2+} to the TnC, as well as the feed-forward effects of strongly bound crossbridges. Briefly, strong binding promotes the formation of additional strongly bound crossbridges at adjacent sites along actin, thereby further activating the thin filament secondary to Ca^{2+} binding. Considering eccentric activity often corresponds with greater average force output than that observed during concentric or isometric (Faulkner, Brooks and Opiteck 1993), a greater level of thin filament activation would be expected. Correspondingly, Lombardi and Piazzesi (1990) observed an increase in muscle fiber stiffness during lengthening contractions, representing an increase in attached crossbridges and thus thin filament activation in comparison to isometric conditions. As a result, the contractile apparatus would be less sensitive to the potentiating influence, suggesting that a conditioning stimulation will have a minimal effect on potentiating work and power. Consistent with this, results indicated a marked reduction in the magnitude of eccentric work and power potentiation observed across each condition, demonstrating a decreased sensitivity to the potentiating influence. Thus, potentiation of contractile performance appears to be a function of crossbridge activation, demonstrating a relationship with the activation state of the contractile apparatus.

6.3.0 Dynamic force, work and power

In the present study work cycle frequency significantly influenced contractile performance. Increases and decreases in force associated with eccentric and concentric contractions, respectively, depict the speed dependent properties of skeletal muscle as described by the force-velocity relationship. Under such parameters, the increases in work cycle frequency and thus velocity of muscle length change, corresponded with significant increases in force during lengthening stimulations, and decreases when stimulated during shortening. However, upon assessing the relative difference between conditions, PTP of dynamic twitch force was only significant post-CS for concentric, but not eccentric contractions. Despite the marked increase in force; concentric work and power output only increased significantly from pre-CS measures in the fastest condition (6.9 Hz). Close examination of figures 19 and 20 help provide an explanation for such observations. Representative work-loops shown in Fig 19 (a) display a distinct "crossover" point during relaxation where post-CS force is reduced compared to pre-CS force. The corresponding area under the curve prior to and following the crossover point thus signifies the differences in net work and power per work cycle. If the crossover point occurs earlier in the relaxation phase (i.e. closer to L_o) and the area under the curve is greater for pre-CS measures, total work and thus power output will also be greater pre-CS. With the proposed influence of a crossover point in mind, only at 6.9 Hz was work and power significantly greater than pre-CS values as the crossover occurred late enough (near complete relaxation) to maximize the area under the curve for post-CS measures. Therefore, at fast shortening speeds the potentiation of concentric force translated into augmented work and power output, where as slower frequencies failed to reproduce such

observations. This may in fact be a result of rapid shortening (i.e., 6.9 Hz) broadening the peak of the twitch such that the area under the curve is larger, providing more positive work. Conversely, at slower speeds the twitch reaches its peak and relaxes over a much smaller length, thus limiting work output. Figure 20 further emphasizes why work and power was not found to be greater than pre-CS values by illustrating the change in work over the duration of stimulation. The magnitude of negative work is greater than that of positive at 1.5 Hz, and approximately equal at 3.3 Hz. Only at 6.9 Hz was the amount of positive work enough to overcome that of negative work.

In contrast, panels d-f of figure 19 (b) (eccentric observations) reveal that the crossover points are much closer than in panels a-c, with a smaller difference in area under pre vs. post-CS curves. Therefore, the location of the crossover was less of an influence during eccentric stimulation, and the failure to observe significant increases in work and power can be attributed to the fact that the CS had a negligible effect on augmenting post-CS force. Figure 21 reveals the predominance of negative work over positive work for all conditions, further demonstrating why a significant increase in work and power was not observed.

6.4.0 Physiological significance

Specific results reported in this investigation may be relevant to physiological function. When considering the stretch-shortening cycle in skeletal muscle, higher force output during concentric contraction will in turn elicit greater work and power output. Josephson (1993; 1999) among others have previously identified that as stride (work cycle) frequency increases, stride duration decreases. This will result in the hind limb

having to support more of the mouse's body weight, as demonstrated by an increase in ground reaction force from ~ 50 to ~ 65 % of body weight when stride frequency increased from~ 2.6 to 5.4 Hz (Clarke, Smart and Still, 2001). Therefore as work cycle frequency increases and stride duration decreases, a muscle will have to generate greater force during the push off phase to compensate for the increased percentage of body mass being supported. As a result, even a small increase in force output at fast speeds of shortening (due to potentiation) may allow; a) greater stabilizing forces to be generated; as well b) more power to translate an object through space. Recalling that the EDL primarily functions late in the swing phase, and also has a minor role in the push-off phase during gait potentiation may be a useful compensatory mechanism for optimizing performance in the face of fatigue during prolonged submaximal activation (i.e. high speed locomotion). Mechanistically, the aforementioned scenario would result in a rightward shift of the force-pCa curve, indicating a decreased sensitivity to Ca^{2+}, and thus a reduction in thin filament activation and force production. However, the well characterized leftward shift in the force-pCa relationship, and increase in f_{app} affiliated with RLC phosphorylation would offer an acute compensatory mechanism by which performance would be restored to, or near, pre fatigue levels. Physiologically, the importance of this potentiating influence becomes greater as stride frequency increases, and contractions shift further along the force-velocity relationship toward significant reductions in force output.

From a performance standpoint, increasing concentric power may thus prove to be advantageous. However, maximizing net work and power is not always favourable. Such circumstances may simultaneously increase the work required to re-lengthen a muscle

following contraction, increase the amount of work performed on the muscle during lengthening, and may ultimately increase the damage endured by the muscle as a result of high force lengthening contractions. Therefore, it would be counterproductive for a muscle to produce more work in this aspect as this modulation would increase the work required of antagonist muscles to re-lengthen the potentiated agonist muscle, in effect creating a "futile cycle". In addition Childers and McDonald (2004) determined that RLC phosphorylation mediated enhancement of maximally Ca^{2+} activated force increased eccentric contraction induced injury. Thus, the appealing observations regarding the conflicting response of potentiation during concentric/eccentric contraction may be valuable in optimizing function during physiological actions such as locomotion. This would supplement work and power output during shortening, while averting significant muscle damage and/or injury.

Considering muscle strain injuries are of the most frequent injury in sports, and eccentric contraction induced injuries are a major contributor to muscle strain (Black and Stevens, 2001 and references within), a physiological means of reducing such injury is rather significant. In the present study, the presence and coincident absence of a potentiation effect on concentric and eccentric forces are therefore particularly relevant during high frequency work cycles, where concentric force is reduced and eccentric force increased.

6.5.0 Prior activation and myofilament structural integrity

Eccentric contractions are often associated with disruption of sarcomeres, and cytoskeletal elements involved in force transmission, as well as excitation-contraction

coupling impairments and damage to the muscle membrane. Thus, it is important to consider such factors as they may have a marked effect on force production. Prior to reviewing this, however, it is critical to recognize differences associated with different muscle fiber types. Fast glycolytic skeletal muscle fibers are more susceptible to eccentric contraction induced injury than slow oxidative fibers (Lieber et al., 1991). Physiologically the low oxidative capacity of fast twitch fibers may predispose them to injury during repeated eccentric contractions (Patel et al., 1998). This is believed to result from depletion of high energy phosphates and subsequent formation of actin-myosin crossbridges in the rigor state (Koh, 2008). Therefore, stretch induced by eccentric contractions in the rigor state leads to muscle injury. Conversely, slow oxidative fibers contain elevated levels of specific cytoskeletal proteins that may provide structural support for sarcomeres, thus protecting a muscle fibers structural integrity during lengthening.

Concomitantly, myofibrillar damage following eccentric contraction in fast twitch fibers has been previously associated with sarcomeric disruptions such as Z-disc streaming (Friden et al., 1983), as well as degradation of cytoskeletal components like desmin (Leiber et al., 1996) and dystrophin (Lovering and De Deyne 2004); leading to the loss of membrane integrity. Despite such observations made *in vivo* and *in vitro* (in both human and animal models) suggesting that sarcomere disruption is a primary cause for immediate deficits in force production, one could also argue that structural damage is exacerbated with time (hours to days following activity), becoming more evident while force deficits remain unchanged or improve (Koh, 2008). As a result, the concept that immediate loss in function following eccentric activity stems from impairments in

excitation-contraction coupling becomes increasingly attractive. Warren et al., (1993) demonstrated that force impairment following eccentric activity in isolated rat muscle is not due to disruption of myofibrillar force generating structures, rather, due to disruption at the level of excitation-contraction coupling, as observed after caffeine supplementation. Additional support for this has been provided by studies examining Ca^{2+} release during stimulation in single fibers (Balnave and Allen, 1995), as well as whole muscle (Ingalls et al., 1998), suggesting that force deficits may be due to alteration of the T-tubule structures. Upon taking all factors into consideration, conclusions remain equivocal as to whether disruption at the level of the sarcomere, or neuromuscular junction (i.e. excitation – contraction coupling) is responsible for immediate force deficits. The present study did not assess the structural integrity of the myofilament lattice, nor did it attempt to address excitation-contraction coupling complications brought on by the experimental protocol as this was not the primary objective. Therefore, it is difficult to suggest whether the aforementioned factors are involved in the deficit of eccentric twitch force, and thus work and power following a conditioning stimulus, however it can be assumed that this contribution was minimal (see below).

Upon taking this into consideration, within the experimental protocol used herein, (i.e. low strain ± 2.5% of L_o), minimal fatigue was observed. The use of single twitch stimulations to reproduce dynamic and isometric contractions, in conjunction with a total of ~ 20 or fewer eccentric stimulations across the entire experimental timeline suggests that muscle fatigue is not a primary concern. Contractile data demonstrating consistency of isometric P_t (pre/post-CS) throughout the experiment (~ 64% of values within 1 SD of the means), as well as P_o supports this argument. In addition, the conditioning stimulus

had only a minor effect on fatiguing peak tetanic force; with P_o for the final tetanic stimulation being decreased by ~ 4% when compared to the first stimulus. Considering that fatigue was mostly absent in this study, the deficit in eccentric performance was likely attributed to alternate mechanisms. One possible factor in regards to the present observations is the impact a conditioning stimulus may have on corresponding concentric and eccentric contractile performance. Observations from this study provide a scenario in which the conditioning stimulus plays a different role in modulating contractile performance depending on the nature of the contraction (eccentric vs. concentric). As a result, the potentiation influence may be "tuned" to the environment in which contraction is induced, demonstrating an acute modulatory effect which differs depending on the phase of stimulation. For example, following the conditioning stimulus, concentric work and power output potentiated ~ 40 % at 6.9 Hz; whereas eccentric work and power was lower than pre-CS values by ~ 2 %. This therefore highlights the hysteresis evident within the present observations. Hysteresis refers to systems which demonstrate a path dependence; suggesting that it is necessary to understand the history of the input in order to predict the path that will be followed. As a result, depending on the type of contraction (concentric vs. eccentric) and the speed at which the muscle is shortening or lengthening, the effect of previous contractile history in modulating performance will vary.

6.5.1 Possible mechanisms

Close examination of these observations suggests that muscle relaxation time may play a critical role in this regard. Previous work with intact cat muscle (37° C) (Brown and Loeb, 1998), and skinned rabbit psoas (15° C) (Patel et al., 1998) suggested that RLC phosphorylation reduces both the tetanic relaxation rate in whole muscle, as well as rate

of relaxation from steady state force at saturating Ca^{2+} activation. These results are in accord with recent reports from Gittings et al., (2011) which demonstrated that the half relaxation time from a tetanus in mouse EDL ($25°$ C) was greater after a tetanic potentiating protocol, and that relaxation time was significantly lower in EDL muscles from skMLCK KO mice. In contrast, half relaxation time from a single isometric twitch was significantly reduced, however, following the potentiating stimulation (Gittings et al., 2011). This observation corresponds with the present results as relaxation from concentric stimulations at slow and moderate work cycle frequencies was more rapid following the conditioning stimulation. As a result, this reduction in relaxation time from a single twitch stimulation accounts for the decrease in both total work performed by the muscle; as well as the work done on the muscle during lengthening after a concentric contraction. These observations suggest that a conditioning stimulation may increase the rate of relaxation in sub-maximally activated muscle, thus reducing the amount of work performed on the muscle during a subsequent contraction. Physiologically, during repetitive contractions rapid relaxation time associated with reduced work required to re-lengthen the muscle may facilitate biomechanical efficiency, as well as decrease the potential for muscle injury due to high forces exerted on the myofilament lattice while lengthening.

However, one must also consider the possibility that the muscle tendon or other series elastic components (i.e., titin) are affected by the repeated lengthening contractions. Several bodies of work provide compelling evidence suggesting that both repeated passive and active lengthening (Warren et al., 1993b, references therein) are associated with reductions in force output. Single fiber (Julian and Morgan, 1979;

Morgan 1990), as well as whole muscle reports (Black and Stevens, 2001; Roberts and Azizi, 2010) have demonstrated a nonuniformity in skeletal muscle while lengthening. Earlier work in single frog fibers suggested that nonuniform sarcomere length changes may result in "sarcomere popping" (see Julian and Morgan, 1979 for review). Consequently, increased sarcomere popping may increase total compliance within the contractile unit, ultimately reducing fiber stiffness (Morgan 1990). However, with a small stretch amplitude (i.e. 3% just-taut length) no significant increases, or decreases in fiber stiffness were reported (Morgan 1990). As a result, under low strain conditions as have been employed in this study, muscle fiber compliance may not be significantly affected.

A more recent report provides alternate evidence of disproportionate lengthening at various excursion lengths and velocities during length ramps *in situ*. Roberts and Azizi, (2010) suggested that series elastic components in turkey lateral gastrocnemius muscles may act as power attenuators during eccentric contractions by reducing peak forces, as well as fascicle lengthening velocity and peak power input to the active muscle itself. Interestingly, "shuttling" of mechanical energy through a tendon allowed active muscles to absorb energy at a lower rate than the maximal power input to the entire muscle-tendon unit (i.e. rapid lengthening caused a three-fold greater absorption of energy into the muscle-tendon unit than just the fascicle alone). Previous reports utilizing mammalian skeletal muscle have therefore developed the hypothesis that a majority of the stretch induced during rapid lengthening is localized primarily within the tendons. Thelen et al., (2005) also provides persuasive evidence in human hamstring by demonstrating that the peak rate of fiber lengthening, as well as fiber strain was reduced due to the stretch of simulated series elastic elements in the late swing phase during locomotion. As a result,

tendons receive a great transfer of potential energy with rapid lengthening, making up a majority of the imposed length change. In conjunction with observations from Roberts and Azizi (2010), by reducing the rate and magnitude at which a fascicle lengthens, series elastic components may act as an important protective mechanism of skeletal muscle and must therefore be considered in this discussion.

In the present investigation it is unknown whether the series elastic component played a significant role in attenuating power by absorbing energy during lengthening. Although care was taken to tie the suture as close to the muscle fascicle as possible, no conclusions can be made quantifying the series elastic contribution to these results. It is important, however, to highlight that the minimal strain placed on the muscle-tendon unit may limit larger energy transfers to series elastic elements. As a result, it is difficult to suggest what exactly contributed to the posttetanic force depression evident during eccentric stimulations. However, it is very possible that a muscle collectively employs various mechanisms to preserve contractile function, thus limiting damage and optimizing work performed. Redundancy in this aspect would suggest how critical energy transfer/absorption is during repetitive activities which mimic cyclic muscle actions (i.e. locomotion).

6.6.0 Summary

The present investigation provides a unique analysis of the potentiation influence on dynamic contractions. To this end, the magnitude of potentiation was explored in relation to both the speed, and type of contraction (i.e., con vs. ecc). Considering the activation status of the contractile apparatus varies depending on the nature of the

contraction, the thin filament will be more activated during eccentric than concentric contractions. Furthermore, when the velocity at which a muscle shortens is increased, the gap in activation levels becomes more apparent. In part, this can be explained by the characteristic deactivation of the thin filament as a rapidly shortening muscle is stimulated. Correspondingly, as thin filament deactivation increases (i.e., increasing work cycle frequency), the magnitude of potentiation observed in concentric force, work and power increased (fig. 24). In contrast, previous reports suggest that crossbridges of skinned skeletal muscle fibers demonstrate a conversion from a low to high force, and high stiffness state upon lengthening (Iwamoto, 1995); as well as increasing the population of bound crossbridges (Bagni, Cecchi and Colombini, 2005; Brunello et al., 2007) and thus activation. Under such circumstances, one would assume that the significance of augmenting the population of crossbridges in the strong binding state via RLC phosphorylation is negligible. Fittingly, the magnitude of potentiation observed in eccentric force, work and power was either insignificant, or not apparent in this study. In comparing relative eccentric force (pre / post-CS), a negative relationship was evident as force potentiation decreased with increasing work cycle frequency. Reasonable grounds therefore exist, suggesting that thin filament activation level is an important determinant in defining the potentiation influence in striated fast twitch skeletal muscle.
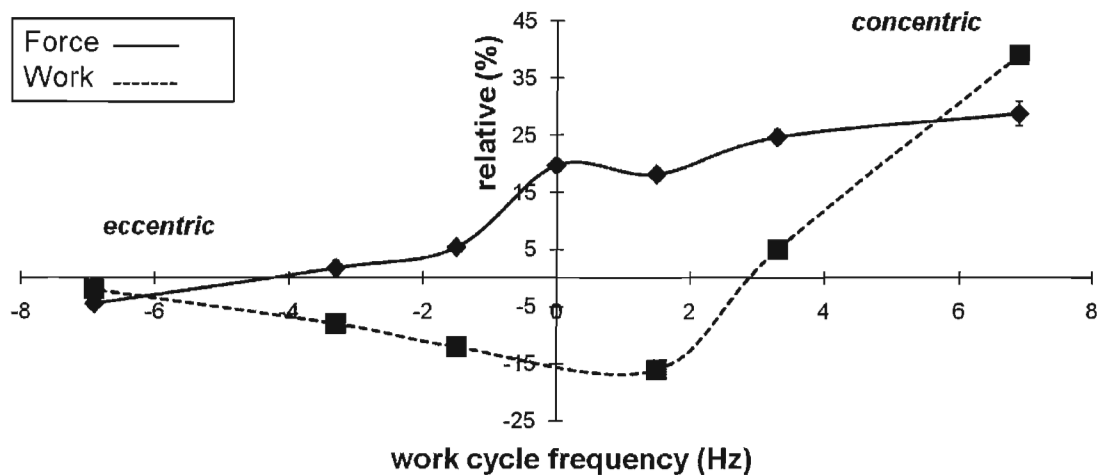
Fig. 24- Relative change in force and work – The relative change (post-CS / pres-CS) for both concentric and eccentric stimulations are plotted (eccentric values appear on the negative portion of the x-axis). Plotting the relative change pre-post (as a percentage) over work cycle frequency (Hz) highlights the speed and direction dependence of the potentiation effect. Concentric contractions at 6.9 Hz demonstrated the greatest relative increase in force and work/power in comparison to all other conditions. In contrast, eccentric contractions displayed negligible increases in force, work or power following a CS, thus demonstrating resistance to the potentiation effect.

6.7.0 Future considerations

- Supplementary to the present investigations, future studies should consider replicating these experiments using skMLCK KO mice. This would further elucidate the influence of potentiation during dynamic responses by examining these contractions in the absence of skMLCK. Such observations would provide novel insight as previous studies using the KO model focused specifically on isometric conditions.

- Although the highly speculative, it may be possible that RLC phosphorylation has a greater role in prevention/recovery from eccentric contraction induced damage. However, additional work is needed before any conclusions can be made. Should these observations be reproducible, this may have interesting ramifications on how RLC phosphorylation is perceived in vivo. Therefore, such ideologies provide rationale for future studies to explore the effects of RLC phosphorylation on eccentrically stimulated muscle in depth. Focus should be directed towards developing a model which minimizes fatigue while simultaneously injuring the muscle through eccentric contraction. A design which incorporates analysis of isometric P_o prior to and following a series of eccentric contractions would be favourable (see Warren et al., 1994). Furthermore, higher stimulation frequencies and greater strain should be incorporated to optimize the appearance of muscle damage. Biochemical analysis of markers of injury such as creatine kinase (CK) levels, and lactate dehydrogenase (LDH) should also be considered as a means of assessing the structural integrity of the myofilament lattice.

- In addition to further analyzing the eccentric observations from this study, it would be beneficial to establish exactly at what speed the potentiation threshold is reached during concentric contractions, and when this influence becomes more apparent than that of isometric contractions. To fit a proper speed-potentiation curve additional work cycle frequencies should be tested in a similar manner, as this would help "pin-point" a specific speed at which dynamic contractions yield a greater relative increase than isometric. There is a possibility that this relationship may be sigmoidal, in which there is little potentiation at low velocities, but significant potentiation at higher velocities. Regardless additional work is required before an accurate assessment can be made.

- As this study has provided insight towards the significance of RLC phosphorylation during dynamic contractions *in vivo*, additional steps can be taken in future studies. Incorporation of a more physiological strain amplitude and stimulation frequency would be among the most important modifications one should consider when progressing from the present study. However, this further complicates measures as the total work cycle duration shortens with increasing frequency. This limits the time for relaxation from higher frequency stimulation before the corresponding lengthening or shortening period has ceased. Increased relaxation times may therefore result in substantially higher forces being exerted on the muscle when re-lengthening after a concentric contraction, therefore increasing the risk of damage. Careful measures must be taken to ensure that stimulus timing and duration are appropriately implemented within the experimental design.

Conclusion

The influence of a CS on dynamic muscle function during work cycles appears to be highly speed and direction dependent. Thus, in agreement with the hypotheses formulated, increasing the speed of muscle shortening increased the relative potentiation of concentric force without, however, greatly altering eccentric responses. The present observations highlight complex interactions between concentric and eccentric force that preferentially increases net muscle work and power at high shortening speeds. This effect may modulate the dynamic function of skeletal muscle during locomotion *in vivo*. It is important to take such considerations into account as muscles are often perceived as motors with the sole purpose of producing mechanical energy. Such popularity surrounding the properties of a muscle while shortening has thus limited examination while lengthening. As a result, the behavior of muscle as it transcends concentric and isometric contractions and approaches the eccentric portion of the force-velocity curve is difficult to define. What is certain, however, is that skeletal muscles are necessary for absorbing energy during locomotion while decelerating, as well as in jumping or explosive movements. Correspondingly, this study revealed the contribution of prior activation history in optimizing contractile performance by augmenting force, work and power as the speed of contraction increases; while simultaneously eluding the damaging high forces associated with eccentric contractions from being exerted onto the muscle. To this end, an interesting observation from this study was the slight deficit in eccentric twitch force following a conditioning stimulus at 6.9 Hz. Although difficult to distinguish the exact mechanism responsible it is important to emphasize the fact that minimal strain was applied to the muscles with a limited number of eccentric contractions which is an

important consideration when assessing the magnitude of injury (McCully and Faulkner 1986; Brooks and Faulkner 1996).

This study employed relatively low muscle strain as well as a brief number of eccentric contractions, and exercised caution in tying sutures as close to the muscle belly as possible. When coupled with no significant deficit in P_o throughout the experimental protocol the possibility of other mechanisms (i.e. passive cycling reducing force) contributing to decreasing contractile function at fast speeds may be plausible. Aside from the observed deficit in peak force work and power output during eccentric contractions, the hysteresis-like effect evident in the present investigation highlights a selective enhancement of contractile output. This effect suggests that fast twitch skeletal muscles minimizes the potential for excessive negative work and/or muscle damage, while simultaneously maximizing its capacity to produce positive work during repetitive contractions.

REFERENCES:

Abbate, F., Sargeant, A., Verdijk, P., and de Haan, A. (2000). Effects of high-frequency initial pulses and posttetanic potentiation on power output of skeletal muscle. Journal of Applied Physiology, 88, 35-40.

Abbate, F., Van Der Velden, J., Stienen, J., and de Haan, A. (2001). Post-tetanic potentiation increases energy cost to a higher extent than work in rat fast skeletal muscle. Journal of Muscle Research and Cell Motility, 22, 703-710.

Allen, J., and Moss, R. (1987). Factors influencing the ascending limb of the sarcomere length-tension relationship in rabbit skinned muscle fibres. Journal of Physiology, 390, 119-136.

Allen, D., Lee., and Westerblad, H. (1989). Intracellular calcium and tension during fatigue in isolated single muscle fibres from Xenopus laevis. Journal of Phsyiology, 415, 433-458.

Allen, D., Lannergren, J., and Westerblad, H. (1995). Muscle cell function during prolonged activity: cellular mechanisms of fatigue. Experimental physiology, 80, 497-527.

Allen, D. (2001). Eccentric muscle damage: mechanisms of early reduction of force. Acta Physiologica Scandanavia, 171, 311-319.

Allen, D., Lamb, G., and Westerblad, H. (2008). Skeletal muscle fatigue: cellular mechanisms. Physiological Reviews, 88(1), 287-332.

Ashley, C., Mulligan, I., and Lea, T. (1991). Ca^{2+} and activation mechanisms in skeletal muscle. Quarterly Reviews of Biophysics, 24, 1-73.

Askew, G., and Marsh, R. (1998). Optimal shortening velocity (V/Vmax) of skeletal muscle during cyclical contractions: length-force effects and velocity-dependent activation and deactivation. The Journal of Experimental Biology, 201, 1527-1540.

Babault, N, Maffiuletti, N, and Pousson, M. (2008). Postactivation potentiation in human knee extensors during dynamic passive movements. Medicine and Science in Sports and Exercise, 40(4), 735-743.

Baker, D. (2003). The effect of alternating heavy and light resistances on power output during upper-body complex power training. Journal of Strength and Conditioning Research, 17(3), 493-497.

Bagni, A., Cecchi, G., and Colombini, B. (2005). Crossbridge properties investigated by fast ramp stretch of activated frog muscle fibers. Journal of Physiology, 565, 261-268.

Balnave, C., and Allen, D. (1995). Intracellular calcium and force in single mouse muscle fibers following repeated contractions with stretch. Journal of Physiology, 488, 25-36.

Balnave, C., and Allen, D. (1996). The effects of muscle length on intracellular calcium and force in single fibres from mouse skeletal muscle. Journal of Physiology, 492, 705-713.

Balog, E. (2010). Excitiation-contraction coupling and minor triadic protein in low frequency fatigue. Exercise Sport Sciences Reviews, 38, 135-142.

Baudry, S, Klass, M, and Duchateau, J. (2005). Postactivation potentiation influences differently the nonlinear summation of contraction in young and elderly adults. Journal of Applied Physiology, 98, 1243-1250.

Baudry, S, and Duchateau, J. (2007). Postactivation potentiation in human muscle: effect on the load-velocity relation of tetanic and voluntary shortening contractions. Journal of Applied Physiology, 103, 1318-1325.

Barclay, C. (2005). Modeling diffusive O2 supply to isolated preparations of mammalian skeletal and cardiac muscle. Journal of Muscle research and cell motility, 26, 225-235.

Bevan, L, Laouris, Y, Garland, S, Reinking, R, and Stuart, D. (1993). Prolonged depression of force developed by single motor units after their intermittent activation in adult cats. Brain Research Bulletin, 30, 127-131.

Biewener, A. (1998). Muscle function *in vivo*: A comparison of muscles used for elastic energy saving vs. muscles used to generate mechanical power. American Zoologist, 38(4), 703-717.

Bigland-Ritch, B., Jones, D, and Woods, J. (1979). Excitation frequency and muscle fatigue: electrical responses during human voluntary and stimulated contractions. Experimental Neurology, 64, 414-427.

Black, J., and Stevens, D. (2001). Passive stretch does not protect against acute contraction induced injury in mouse EDL muscle. Journal of Muscle Research and Cell Motility, 22, 301-310.

Blumenthal, D., Takio, K., Edelman, A., Charbonneau, H., Titani, K., Walsh, K., and Krebs, E. (1985). Identification of the calmodulin-binding domain of skeletal muscle myosin light chain kinase. Proceedings of the National Academy of Sciences USA, 82, 3187-3191.

Brenner, B. (1986). The cross-bridge cycle in muscle. Basic Research in Cardiology, 81, 1-15.

Brooks, S., and Faulkner, J. (1988). Contractile properties of skeletal muscles from young, adult and aged mice. Journal of Physiology, 404, 71-82.

Brooks, S., Faulkner, J., and McCubbrey, M. (1990). Power outputs of slow and fast skeletal muscle of mice. Journal of Applied Physiology, 68(3), 1282-1285.

Brooks, S., Zerba, E., and Faulkner, J. (1995). Injury to muscle fibers after single stretches of passive and maximally stimulated muscles in mice. Journal of Physiology, 488(2), 459-469.

Brown, I., and Loeb, G. (1998). Post activation potentiation- A clue for simplifying models of muscle dynamics. Amer Zool, 38, 743-754.

Brown, I., Cheng, E., and Loeb, G. (1999). Measured and modeled properties of mammalian skeletal muscle. The effects of stimulus frequency on force-length and force-velocity relationships. Journal of Muscle research and cell motility, 20, 627-643.

Brunello E, Reconditi M, Elangovan R, Linari M, Sun YB, Narayanan T, Panine P, Piazzesi G, Irving M, Lombardi V. (2007). Skeletal muscle resists stretch by rapid binding of the second motor domain of myosin to actin. Proc Natl Acad Sci USA, 104(50), 20114-20119.

Burkholder, T., and Lieber, R. (2001). Sarcomere length operating range of vertebrate muscles during movement. The Journal of Experimental Biology, 204, 1529-1536.

Cannell, M., and Allen, D. (1984). Model of calcium movements during activation in the sarcomere of frog skeletal muscle. Biophysics Journal, 45, 913-925.

Cazorla, O., Wu, Y., Irving, T., Granzier, H. (2001). Titin-based modulation of calcium sensitivity of active tension in mouse skinned cardiac myocytes. Circulation Research, 88, 1028-1035.

Childers, M., and MacDonald, K. (2004). Regulatory light chain phosphorylation increases eccentric contraction induced injury in skinned fast twitch fibers. Muscle and Nerve, 29, 313-317.

Chin, E. (2005). Role of Ca2+/calmodulin-dependent kinases in skeletal muscle plasticity. Journal of applied Physiology, 99, 414-423.

Choi, S., and Widrick, J. (2009). Combined effects of fatigue and eccentric damage in muscle power. Journal of applied Physiology, 107, 1156-1164.

Clarke, K., and Still, J. (1999). Gait analysis in the mouse. Physiology and Behaviour, 66(5), 723-729.

Clarke, K., Smart, L., and Still, J. (2001) Ground reaction force and spatiotemporal measurements of gait of the mouse. Behaviour Research Methods, Instruments and Computers, 33(3), 422-426.

Cleak, M., and Eston, R. (1992). Muscle soreness, swelling, stiffness and strength loss after intense eccentric exercise. Br Journal of Sports Medicine, 26(4), 267-272.

Close, R., and Hoh, J. (1968). The after-effects of repetitive stimulation on the isometric twitch contraction of rat fast skeletal muscle. Journal of Physiology, 197(2), 461-477.

Close, R. (1972). Dynamic properties of mammalian skeletal muscle. Physiological reviews, 52, 129-197.

Cooke, R, Franks, K, Luciani, G, and Pate, E. (1988). The inhibition of rabbit skeletal muscle contraction by hydrogen ions and phosphate. Journal of Physiology London, 395, 77–97.

Cooke, R, and Pate, E. (1985). The effects of ADP and phosphate on the contraction of muscle fibers. Biophysical Journal, 48, 789–798.

Craig, R., Padron, R., and Kendrick-Jones, J. (1987). Structural changes accompanying phosphorylation of tarantula muscle. Journal of Cell Biology, 105, 1319-1327.

Crow, M., and Kushmerick, M. (1982a). Myosin light chain phosphorylation is associated with a decrease in the energy cost for contraction in fast twitch mouse muscle. Journal of Biological Chemistry, 257, 2121-2124.

Crow, M, and Kushmerick, M. (1982b). Chemical Energetics of Slow- and Fast-Twitch Muscles of the Mouse. Journal of General Physiology, 79, 147-166.

Cuda, G., Pate, E., Cooke, R., and Sellers, J. (1997). *In vitro* actin filament sliding velocities produced by mixtures of different types of myosin. Biophysical Journal, 72, 1767-1779.

Curtin, N., and Edman, K. (1994). Force-velocity relation for frog muscle fibres: effect of moderate fatigue and intracellular acidification. Journal of Physiology, 475(3), 483-494.

Curtin, N., Gardner-Medwin, A., and Woledge, R. (1998). Predictions of the time course of force and power output by dogfish white muscle fibres during brief tetani. The journal of Experimental Biology, 201, 103-114.

Daniel, T., and Tu, M. (1999). Animal movement; mechanical tuning and coupled systems. The Journal of Experimental Biology, 202, 3415-3421.

Dawson, M., Gadian, D., and Wilkie, D. (1977). Contraction and recovery of living muscles studies by 31P nuclear magnetic resonance. The Journal of Physiology (London), 267, 703-735.

Debold, E., Dave, H., amd Fitts, R. (2004). Fiber type and temperature dependence of inorganic phosphate: implication for fatigue. American Journal of Physiology, 287, C673-C681.

Debold, E., Beck, S., and Warshaw, D. (2008). Effect of low pH on single skeletal muscle myosin mechanics and kinetics. American Journal of Physiology (Cell Physiol), 295, 173-179.

Debold, E., Turner, M., Stout, J., and Walcott, S. (2011) Phosphate enhances myosin powered actin filament velocity under acidic conditions in motility assay. American Journal of Physiology (Regul Integr Comp Physiol).

DeRuiter, C., Jones, D., Sargeant, A., and de Haan, A. (1999). Temperature effect on the rates of isometric force development and relaxation in the fresh and fatigued human adductor pollicis muscle. Experimental Physiology, 84, 1137-1150.

Dulhunty, A. (2006). Excitation-contraction coupling from the 1950's into the new millennium. Clinical and Experimental Pharmacology and Physiology, 33, 763-772.

Duthie, G, Young, W, and Aitken, D. (2002). The acute effects of heavy loads on jump squat performance: an evaluation of the complex and contrast methods of power development. Journal of Strength and Conditioning Research, 16(4), 530-538.

Dutka, T., and Lamb, G. (2004). Effect of low cytoplasmic [ATP] on excitation-contraction coupling in fast-twitch muscle fibres of the rat. Journal of Physiology, 560, 451-468.

Ebben, W. (2002). Complex training: A brief review. Journal of Sports Science Medicine, 1, 42-46.

Ebben, W, and Watts, P. (1998). A review of combined weight training and plyometric training modes: Complex training. Strength and Conditioning Journal, 20(5), 18-27.

Edman, K. (1979). The velocity of unloaded shortening and its relation to sarcomere length and isometric force in vertebrate muscle fibres. Journal of Physiology 291, 143-159.

Edman, K., Caputo, C., and Lou, F. (1993). Depression of tetanic force induced by loaded shortening of frog muscle fibres. Journal of Physiology, 466, 535-552.

Edman, K., (1996). Fatigue vs. shortening induced deactivation in striated muscle. Acta Physiologica Scandanavia, 156, 183-192.

Edwards, R., Hill, D., Jones, D., and Merton, P. (1977). Fatigue of long duration in human skeletal muscle after exercise. Journal of Physiology, 272, 769-778.

Enoka, R. (1996). Eccentric contractions require unique activation strategies by the nervous system. Journal of Applied Physiology, 81, 2339-2346.

Evans, A, Hodgkins, T, Durham, M, Berning, J, and Adams, K. (2000). The acute effects of a 5RM bench press on power output. Medicine and Science in Sport and Exercise 32(5).

Faulkner, J., Brooks, S., and Opitek, J. (1993). Injury to skeletal muscle fibers during contractions: conditions of occurrence and prevention. Physical Therapy, 73(12), 911-921.

Fitts, R. (1994). Cellular mechanisms of muscle fatigue. Physiological Reviews, 74, 49-94.

Fitts, R. (2008). The cross-bridge cycle and skeletal muscle fatigue. Journal of Applied Physiology, 104, 551-558.

Ford, L., Huxley, A., and Simmons, R. (1985) Tension transient during steady shortening of forg muscle fibers. Journal of Physiology, 361, 131-150.

Fowles, J., and Green, H. (2003). Coexistence of potentiation and low-frequency fatigue during voluntary exercise in human skeletal muscle. Canadian Journal of Physiology and Pharmacology, 81, 1092-1100.

Franks-Skiba, K., Lordelli, R., Goh, G., and Cooke, R. (2007). Myosin light chain phosphorylation inhibits muscle fiber shortening velocity in the presence of vanadate. American Journal of Physiology (Regul Integr Comp Physiol), 292, 1603-1612.

French, D, Kraemer, W, and Cooke, C. (2003). Changes in dynamic exercise performance following a sequence of preconditioning isometric muscle actions. Journal of Strength and Conditioning Research, 17(4), 678-685.

Friden, J., and Lieber, R. (2001). Eccentric exercise induced injuries to contractile and cytoskeletal muscle fibre components. Acta Physiologica Scandanavia, 171, 321-326.

Fryer, M., Owen, V., Lamb, G., Stephenson, D. (1995). Effects of creatine phosphate and Pi on Ca2+ movements and tension development in rat skinned skeletal muscle fibres. Journal of Physiology, 482, 123-140.

Gallagher, P., Herring, B., and Stull, J. (1997) Myosin light chain kinases. Journal of Muscle Research and Cell Motility, 18, 1-16.

Gandevia, S. (2001). Spinal and supraspinal factors in human muscle fatigue. Physiological Reviews, 81(4), 1725-1789.

Gilbert, G, and Lees, A. (2005). Changes in the force development characteristics of muscle following repeated maximum force and power exercise. Ergonomics, 48, 1576-1584.

Gittings, W., Huang, J., Smith, I., Quadrilatero, J., and Vandenboom, R. (2011). The effect of skeletal muscle myosin light chain kinase gene ablation on fatigability of mouse fast muscle. Journal of Muscle Research and Cell Motility, 5-6, 337-348.

Godt, R., and Nosek, T. (1989). Changes in the intracellular milieu with fatigue or hypoxia depress contraction of skinned rabbit skeletal and cardiac muscle. Journal of Physiology, 412, 155-180.

Gordon, A., Homsher, E., and Regnier, M. (2000). Regulation of contraction in striated muscle. Physiological Reviews, 80(2), 853-925.

Gorselink, M., Drost, M., de Brouwer, K., Schaart, G., van kranenburg, D., Roemen, T., van Bilsen, M., Charron, M., and van der Vusse, J. (2002). Increased muscle fatigue in GLUT-4 deficient mice. American Journal of Physiology (Endocrinol Metab), 282, 348-354.

Gossen, E, and Sale, D. (2000) Effect of postactivation potentiation on dynamic knee extension performance. European Journal of Applied Physiology, 83(6), 524-530.

Gourgoulis, V, Aggeloussis, N, Kasimatis, P, Mavromatis, G, and Garas, A. (2003). Effect of a submaximal half-squats warm up program on vertical jumping ability. Journal of Strength and Conditioning Research, 17(2), 342-344.

Grange, R, Cory, R, Vandenboom, R, and Houston, M. (1995). Myosin phosphorylation augments the force-displacement and force-velocity relationships of mouse fast muscle. American Journal of Physiology, 269, 713-724.

Grange, R., Vandenboom, R., and Houston, M. (1993). Physiological significance of myosin phosphorylation in skeletal muscle. Canadian Journal of Applied Physiology, 18(3), 229-242.

Grange, R, Vandenboom, R, Xeni, J, and Houston, M. (1998). Potentiation of *in vitro* concentric work in mouse fast muscle. Journal of Applied Physiology, 84, 236-243.

Greenberg, M., Mealy, T., Watt, J., Jones, M., Szczesna-Cordary, D., Moore, J. (2009). The molecular effects of skeletal muscle myosin regulatory light chain phosphorylation. American Journal of Physiology (Regul Integr Comp Physiol), 297, 265-274.

Gulick, A., and Rayment, I. (1997). Structural studies on myosin II: Communication between distant protein domains. BioEssays, 19(7), 561-569.

Heglund, Y., Taylor, C., and McMahon, T. (1974). Scaling stride frequency and gait to animal size: Mice to horses. Science, 186, 1112-1113.

Hodgson, M, Docherty, D, and Robbins, D. (2005). Post-activation potentiation. Sports Medicine, 35(7), 585-595.

Holmes, K., Angert, I., Kull, F., Jahn, W., and Schrider, R. (2003). Electron cryo-microscopy shows how strong binding of myosin to actin releases nucleotide. Nature, 45, 423-427.

Huxley, H. (1957). The double array of filaments in cross-striated muscle. Journal of Biophysical and Biochemical cytology, 31(5), 631-648.

Irving, M., Allen, T., Sabido-David, C., Craik, J., Brandmeir, B., Kendrick-Jones, J., Corrie, J., Trentham, D., and Goldman, Y. (1995). Tilting of the light-chain region of myosin during step length changes and active force generation in skeletal muscle. Nature, 375, 688-691.

Iwamoto, H. (1995). Strain sensitivity and turnover rate of low force crossbridges in contracting skeletal muscle fibers in the presence of phosphate. Biophysical Journal, 68, 243-250.

Iwamoto, H. (1998). Thin filament cooperativity as a major determinant of shortening velocity in skeletal muscle fibers. Biophysical Journal, 74, 1452-1464.

James, R., Altringham, J., and Goldspink, D. (1995). The mechanical properties of fast and slow skeletal muscle of the mouse in relation to their locomotry function. The Journal of Experimental Biology, 198, 491-501.

Jensen, R, and Ebben, W. (2003). Kinetic analysis of complex training rest interval effect on vertical jump performance. Journal of Strength and Conditioning Research, 17(2), 345-349.

Josephson, R. (1985). Mechanical power output from striated muscle during cyclic contraction. Journal of Experimental Biology, 114, 493-512.

Josephson, R. (1989). Power output from skeletal muscle during linear sinusoidal shortening. Journal of Experimental Biology, 147, 533-537.

Josephson, R. (1993). Contraction dynamics and power output of skeletal muscle. Annual Reviews in Physiology, 55, 527-546.

Josephson, R. (1999). Dissecting muscle power output. The Journal of Experimental Biology, 202, 3369-3375.

Julian, F., and Morgan, D. (1979). The effect on tension of non-uniform distribution of length changes applied to frog muscle fibers. Journal of Physiology, 293, 379-392.

Karatzaferi, C., Mybergh, K., Chinn, M., Franks-Skiba, K., and Cooke, R. (2003). Effect of an ADP analog on isometric force and ATPase activity of active muscle fibers. American Journal of Physiology, 284, 816-825.

Kennelly, P., Edelman, A., Blumenthal, D., and Krebs, E. (1987). Rabbit skeletal muscle myosin light chain kinase. The calmodulin binding domain as a potential active site directed inhibitory domain. Journal of Biological Chemistry, 263, 11958-11963.

Knuth, S., Dave, H., Peters, J., and Fitts, R. (2006). Low cell pH depresses peak power in rat skeletal muscle fibres at both 30° C and 15° : implications for muscle fatigue. Journal of Physiology, 575, 887-899.

Koh, T. (2008). Physiology and Mechanisms of skeletal muscle damage. In P. M. Tiidus (Editor), Skeletal Muscle Damage and Repair (pp. 3-12). Champaign/US: Human Kinetics.

Lamb, G., and Stephenson, D. (1991). Effects of Mg on the control of Ca2+ release in skeletal muscle fibres of the toad. Journal of Physiology, 434, 507-528.

Lannergren, J., and Westerblad, H. (1987). The temperature dependence of isometric contractions of single intact fibers dissected from a mouse foot muscle. Journal of Physiology, 390, 285-293.

Lamb, G. (2009). Mechanisms of excitation-contraction uncoupling relevant to activity-induced muscle fatigue. Applied Physiology, Nutrition and Metabolism, 34, 368-373.

Levine, R, Kensler, R, Yang, Z, Stull, J, and Sweeney, H. (1996). Myosin light chain phosphorylation affects the structure of rabbit skeletal muscle thick filaments. Biophysical Journal, 71, 898-907.

Lichtwark, G., and Barclay, C. (2010). The influence of tendon compliance on muscle power output and efficiency during cyclic contractions. The Journal of Experimental Biology, 213, 707-714.

Lindstedt, S., Reich, T., Keim, P., and LaStayo, P (2002). Do muscles function as adaptable locomotor springs? The Journal of Experimental Biology, 205, 2211-2216.

Lombardi, V., and Piazzesi, G. (1990). The contractile response during steady lengthening of stimulated frog muscle fibers. Journal of Physiology, 431, 141-171.

Lowy, J., Popp, D., and Stewart, A. (1991). X-ray studies of order-disorder transitions in the myosin heads of skinned rabbit psoas muscles. Biophysical Journal, 60, 812-824.

Lowey, S., Waller, G., Trybus, K. (1993). Skeletal muscle myosin light chains are essential for physiological speeds of shortening. Nature, 365, 454-456.

Lynch, G., Hinkle, R., Chamberlain, J., Brooks, S., and Faulkner, J. (2001). Force and power output of fast and slow skeletal muscles from mdx mice 6-28 months old. Journal of Physiology, 535(2), 591-600.

Lynch, G., and Faulkner, J. (1998). Contraction induced injury to skeletal muscle fibers: velocity of stretch does not influence the force deficit. American Journal of Physiology (Cell Physiol), 275, 1548-1554.

MacIntosh, B. (1991). Skeletal muscle staircase response with fatigue or dantrolene sodium. Medicine and Science in Sports and Exercise, 23(1), 56-63.

MacIntosh, B., and Bryan, S. (2002). Potentiation of shortening velocity during repeated isotonic contractions in mammalian skeletal muscle. European Journal of Physiology, 804-812.

MacIntosh, B. (2003). Role of calcium sensitivity modulation in skeletal muscle performance. News Physiology Science, 18, 222-225.

MacIntosh, B, and Willis, J. (2002). Force-frequency relationship and potentiation in mammalian skeletal muscle. Journal of Applied Physiology, 88, 2088-2096.

MacIntosh, B., Gardiner, P., and McComas, A. (2006). Skeletal muscle: form and function. USA: Human Kinetics.

MacIntosh, B., Taub, E., Dormer, G., Tamaras, E. (2008). Potentiation of isometric and isotonic contraction during high frequency stimulation. Pflugers Archive (European Journal of Physiology), 456, 449-458.

MacIntosh,B. (2010). Cellular and whole muscle studies of activity dependent potentiation. In D.E. Rassier (Ed.), Muscle biophysics: From molecules to cells (pp.315-342). Montreal, Quebec: Springer.

Manning, D., and Stull, J. (1979). Myosin light chain phosphorylation and phosphorylase. A activity in rat extensor digitorum longus muscle. Biochemical and Biophysical Research Communications, 90(1), 164-170.

Manning, D., and Stull, J. (1982). Myosin light chain phosphorylation-dephosphorylation in mammalian skeletal muscle. American Journal of Physiology, 242, C234-C241.

McCully, K., and Clarkson, P. (1986). Characteristics of lengthening contractions associated with injury to skeletal muscle fibers. Journal of Applied Physiology, 61(1), 293-299.

McKillop, D., and Geeves, M. (1993). Regulation of the interaction between actin and myosin subfragment 1: Evidence for three states of the thin filament. Biophysical Journal, 65(2), 693-701.

Metzger, J., and Fitts, R. (1987). Role of intracellular pH in muscle fatigue. Journal of Applied Physiology, 62, 1392-1397.

Metzger, J, Greaser, M, and Moss, R. (1989). Variations in cross-bridge attachment rate and tension with phosphorylation of myosin in mammalian skinned skeletal muscle. Journal of General Physiology, 93, 855-883.

Metzger, J. (1996). Effects of phosphate and ADP on shortening velocity during maximal and submaximal calcium activation of the thin filament in skeletal muscle fibers. Biophysical Journal, 70, 409-417.

Millar, N., and Homsher, E. (1990). The effect of phosphate and calcium on force generation in glycerinated rabbit skeletal muscle fibres. A steady state and transient kinetic study. Journal of Biological Chemistry, 265, 20234-23240.

Moore, R, and Stull, J. (1984). Myosin light chain phosphorylation in fast and slow skeletal muscle in situ. American Journal of Physiology and Cell Physiology, 247, 462-471.

Morgan, M., Perry, V., and Ottaway, J. (1976). Myosin light chain phosphatase. Bichemical Journal, 157, 687-697.

Morgan, D. (1990). New insights into the behavior of muscle during active lengthening. Biophysical Journal, 57, 209-221.

Morgan, D., Claflin, D., and Julian, F. (1996). The effect of repeated active stretches on tension generation and myoplasmic calcium in frog single muscle fibers. Journal of Physiology, 497(3), 665-674.

Morgan, D., and Proske, U. (2004). Popping sarcomere hypothesis explains stretch induces muscle damage. Proceedings of the Australian Physiological and Pharmacological Society, 34, 19-23.

Nosaka, K., and Clarkson, P. (1997). Influence of previous concentric exercise on eccentric exercise induced muscle damage. Journal of Sports Sciences, 15, 477-483.

Nicolopoulos-Stournaras, S., and Iles, J. (1984). Hindlimb muscle activity during locomotionin the rat. Journal of Zoology(London), 203, 427-440.

O'Leary, D, Hope, K, and Sale, D. (1998). Influence of gender on posttetanic potentiation in human dorsiflexors, Canadian Journal of Physiology and Pharmacology, 76, 772-779.

Parry, S, Hancock, S, Shiells, M, Passfield, L, Davies, B, and Baker, J.(2008) Physiological Effects of Two Different Postactivation Potentiation Training Loads on Power Profiles Generated During High Intensity Cycle Ergometer Exercise. Research in Sports Medicine, 16(1), 56- 67.

Patel, J., Difee, G., Huang, X., and Moss, R. (1998). Phosphorylation of myosin regulatory light chain eliminates force-dependent changes in relaxation rates in skeletal muscle. Biophysical Journal, 74, 360-368.

Pemrick, S. (1980). The Phosphorylated L2 light chain of skeletal myosin is a modifier of the actomyosin ATPase. The Journal of Biological Chemistry, 255(18), 8836-8841.

Perrie, W., Smillie, L., and Perry, S. (1973), A phosphorylated light chain component of myosin from skeletal muscle. Biochemical Journal, 135, 151-164.

Persechini, A., Stull, J., and Cooke, R. (1985). The effect of myosin phosphorylation on the contractile properties of skinned rabbit skeletal muscle fibers. Journal of Biological Chemistry, 260(13), 7951-7954.

Pinniger, G., Ranatunga, K., and Offer, G. (2006). Crossbridge and noncrossbridge contributions to tension in lengthening rat muscle: force-induces reversal of the power stroke. Journal of Physiology, 573(3), 627-643.

Prilutsky, B., Herzog, W., and Allinger, T. (1994). Force-sharing between cat soleus and gastrocnemius muscles during walking: explanations based on electrical activity, properties, and kinematics. Journal of Biomechanics, 27, 1223-1235.

Rassier, T., and MacIntosh, B. (2000). Coexistence of potentiation and fatigue in skeletal muscle. Brazilian Journal of Medical and Biological Research, 33, 499-508.

Rayment, I., Holden, H., Whittaker, M., Yohn, C., Lorenz, M., Holmes, K., and Milligan, R. (1993). Structure of the actin-myosin complex and its implications for muscle contraction. Science, 261(5117), 58-65.

Rayment, I. (1996). The structural basis of the myosin ATPase activity. The Journal of Biological Chemistry, 271, 15850-15853.

Rijkelijkhuizen, J., de Ruiter, C., Huijing, P., and de Haan, A. (2005). Low-frequency fatigue, post-tetanic potentiation and their interaction at different muscle lengths following eccentric exercise. Journal of Experimental Biology, 208, 55-63.

Risal, D., Gourinath, S., Himmel, D., Szent-Gyorgyi, A., and Cohen, C. (2004). Myosin subfragment-1 structures reveal a partially bound nucleotide and a complex salt bridge that helps couple nucleotide and actin binding. Proceeding of the National Academy of Sciences, 101, 8930-8935.

Rixon, K, Lamont, H, and Bemben, M. (2007). Influence of type of muscle contraction, gender and lifting experience on postactivation potentiation performance. Journal of Strength and Conditioning Research, 21(2), 500-505.

Robbins, D. (2005). Postactivation potentiation and its practical applicability: A brief review. Journal of Strength and Conditioning Research, 19(2), 453-458.

Roberts, T., and Azizi, E. (2010). The series elastic shock absorber: tendons attenuate muscle power during eccentric actions. Journal of Applied Physiology, 109, 396-404.

Rodgers, M. (1988). Dynamic biomechanics of the normal foot and ankle during walking and running. Physical Therapy, 68(12), 1822-1830.

Roszek, B, Baan, G, and Huijing, P. (1994). Decreasing stimulation frequency-dependent length-force characteristics of rat muscle. Journal of Applied Physiology, 77, 2115–2124.

Ritz-Gold, C. J., Cooke, R., Blumenthal, D. K., & Stull, J. T. (1980). Light chain phosphorylation alters the conformation of skeletal muscle myosin. *Biochemical and Biophysical Research Communications, 93*(1), 209-214.

Sale, D. (2002). Postactivation potentiation: role in human performace. Exercise Sport Science Review, 30(3), 138-143.

Sale, D.(2004). Postactivation potentiation: role in performance. British Journal of Sports Medicine, 38, 386-387.

Schiaffino, S., Gorza, L., Sartore, S., Saggin, L., Ausoni, S., Vianello, M., Gunderson, K., and Lomo, T. (1989). Three myosin heavy chain isoforms in type II skeletal muscle fibers. Journal of Muscle Research and Cell Motility, 10, 197-205.

Schneider, M., and Chandler, W. (1973). Voltage dependent charge movement in skeletal muscle: a possible step in excitation-contraction coupling. Nature, 242, 244-246.

Scott, W., Stevens, J., and Binder-Macleod, S. (2001). Human skeletal muscle fiber type classification. Physical Therapy, 81, 1810-1816.

Sobeszek, A. (1991). Regualtion of smooth muscle myosin light chain kinase, Allosteric effects and Co-operative activation by calmodulin. Journal of Molecular Biology, 220, 947-957.

Sonobe, T., Inagaki, T., Poole, D., and Kano, Y. (2008). Intracellular calcium accumulation following eccentric contractions in rat skeletal muscle *in vivo*: role of stretch-activated channels. American Journal of Physiology (Regul Integr Comp Physiol), 294, 1329-1337.

Squire, J., and Morris, E. (1998). A new look at thin filament regulation in vertebrate skeletal muscle. Federation of American Societies for Experimental Biology Journal, 12, 761-771.

Stevenson, D., and Wendt, I. (1984). Length dependence of changes in sarcoplasmic calcium concentration and myofibrillar calcium sensitivity in striated muscle fibers. Journal of Muscle Research and Cell Motility, 5, 243-277.

Stevenson, D., and Williams, D., (1982). Effects of sarcomere length on the force-pCa relation in fast and slow twitch skinned muscle fibers from the rat. Journal of Physiology, 333, 637-353.

St-Pierre, D, and Gardiner, P. (1985). Effect of "disuse" on mammalian fast-twitch muscle: joint fixation compared with neutrally applied tetrodotoxin. Experimental Neurology, 90, 635–651.

Steele, D., and Duke, A. (2003). Metabolic factors contributing to altered Ca2+ regulation in skeletal muscle fatigue. Acta Physiologica Scandenavia, 179, 39-48.

Stuart, D, Lingley, M, Grange, R, and Houston, M. (1988). Myosin light chain phosphorylation and contractile performance of human skeletal muscle. Canadian Journal of Physiology and Pharmacology, 66, 49-54.

Stull, J., Nunnally, M., Moore, R., Blumenthal, D. (1985). Myosin light chain kinases and myosin phosphorylation in skeletal muscle. Advances in Enzyme Regulation, 23, 123-140.

Stull, J., Nunnally, M., and Michnoff, C. (1986). Calmodulun-dependent protein kinases. The Enzyme, edited by Krebs, E and Boyer, P. Orlando: Academic 113-166.

Sweeney, H., and Stull, J. (1986). Phosphorylation of myosin in permeabilized mammalian cardiac and skeletal muscle cells. American Journal of Physiology, 250, 657-660.

Sweeney, H, and Stull, J. (1990). Alteration of cross-bridge kinetics by myosin light chain phosphorylation in rabbit skeletal muscle: implications for the regulation of actin-myosin interaction. Proceedings of the National Academy of Sciences USA, 87, 414-418.

Sweeney, H, Bowman, B, and Stull, J. (1993). Myosin light chain phosphorylation in vertebrate striated muscle: regulation and function, American Journal of Physiology, 264, 1085-1095.

Syme DA, Stevens DE (1989) Effect of cycle frequency and excursion amplitude on work done by rat diaphragm muscle. Can J Physiol Pharmacol 67: 1294-1299.

Szczesna, D., Zhao, J., Jones, M., Zhi, G., Stull, J., and Potter, J. (2002). Phosphorylation of the regulatory light chains of myosin affects Ca^{2+} sensitivity of skeletal muscle contraction. Journal of Applied Physiology, 92, 1661-1670.

Szent-Gyorgyi, A., Szentkiralyi, E., and Kendrick-Jones, J. (1973). The light chains of scallop myosin as regulatory subunits. Journal of Molecular Biology, 74, 179-203.

Takashima, S. (2009). Phosphorylation of myosin regulatory light chain by myosin light chain kinase and muscle contractions. Circulation Journal, 73, 208-213.

Takekura, H., Fujinami, N., Nishizawa, T., Ogasawara, H., and Kasuga, N. (2001). Eccentric exercise induces morphological changes in the membrane systems involved in excitatioin-contraction coupling in rat skeletal muscle. Journal of Physiology, 533(2), 571-583.

Thelen, D., Chumanor, E., Best, T., Swanson, S., and Heiderscheit, B. (2005). Simulation of biceps femoris musculotendon mechanics during the swing phase of sprinting. American College of Sports Medicine, 1931-1938.

Vandenboom, R, Grange, R and Houston, M. (1993). Threshold for force potentiation associated with skeletal myosin phosphorylation. American Journal of Physiology, 265, 1456-1462.

Vandenboom, R, Grange, R, and Houston, M. (1995). Myosin phosphorylation enhances rate of force development in fast-twitch skeletal muscle. American Journal of Physiology- Cell Physiology, 268, 596-603.

Vandenboom, R., and Houston, M. (1996). Phosphorylation of myosin and twitch potentiation in fatigued skeletal muscle. Canadian Journal of Physiology and Pharmacology, 74(12), 1315-1321.

Vandenboom, R., Xeni, J., Bestic, N. M., & Houston, M. E. (1997). Increased force development rates of fatigued mouse skeletal muscle are graded to myosin light chain phosphate content. The American Journal of Physiology, 272(6 Pt 2), R1980-4.

Vandenboom, R., Claflin, D., and Julian, F. (1998). Effects of rapid shortening on rate of force regeneration and myoplasmic [Ca^{2+}] in intact frog skeletal muscle fibers. Journal of Physiology, 511, 171-180.

Vandenboom, R., Hannon, J., and Sieck, G. (2002). Isotonic force modulated force redevelopment rate of intact frog muscle fibers: evidence for crossbridge induced thin filament activation. Journal of Physiology, 543, 555-566.

Vandenboom, R. (2004). The myofibrillar complex and fatigue: A review. Journal of Applied Physiology, 29(3), 330-356.

Vandervoort, A, and McComas, A. (1983). A comparison of the contractile properties of the human gastrocnemius and soleus muscles. European Journal of Applied Physiology, 51, 435-440.

Warren, G., Lowe, D., Hayes, D., Karwoski, C., Priot, B., and Armstrong, R. (1993). Excitation failure in eccentric contraction induced injury of mouse soleus muscle. Journal of Physiology, 468, 487-490.

Warren, G., Hayes, D., Lowe, D., Williams, J., and Armstrong, R. (1994). Eccentric contraction induced injury in normal and hindlimb suspended mouse soleus and EDL muscle. Journal of Applied Physiology, 77(3), 1421-1430.

Westerblad, H., and Allen, D. (1996). The effect of intracellular injections of phosphate on intracellular calcium and force in single fibres of mouse skeletal muscle. Pflugers Archive (European Journal of Physiology), 431, 964-970.

Westerblad, H., Lee, J., Lannergren, J., and Allen, D. (1991). Cellular mechanisms of fatigue in skeletal muscle. American Journal of Physiology, Cell Physiology, 261, 195-209.

Westerblad, H., and Allen, D. (1992). Changes of intracellular pH due to repetitive stimulation of single fibres from mouse skeletal muscle. Journal of Physiology, 449, 49-71.

Westerblad, H., Allen, D., Bruton, J., Andrade, F., and Lannergren, J. (1998). Mechanisms underlying the reduction of isometric force in skeletal muscle fatigue. Acta Physiologica Scandinavia, 162, 253-260.

Woodhead, J., Zhao, F., Craig, R., Egelmann, E., Alamo, L., and Padron, R. (2005). Atomic model of myosin filament in the relaxed state. Nature, 436, 1195-1199.

Wray, J. (1987). Structure of relaxed myosin filaments in relation to nucleotide state in vertebrate skeletal muscle. Journal of Muscle Research and Cell Motility, 8, 62

Wretling, M, Henriksson-Larsen K, and Gerdle, B (1997) Inter-relationship between muscle morphology, mechanical output and electromyographic activity during fatiguing dynamic knee extension in untrained females. European Journal of Applied Physiology, 76, 483–490.

Yang, Z., Stull, J., Levine, R., and Sweeney, H. (1998). Changes in interfilament spacing mimic the effects of myosin regulatory light chain phosphorylation in rabbit psoas fibers. Journal of structural Biology, 122, 139-148.

Young, W, Jenner, A, and Griffiths, K. (1998). Acute enhancement of power performance from heavy load squats. Journal of Strength and Conditioning Research, 12(2), 82-88.

Xeni, J., Gittings, W., Caterini, D., Huang, J., Houston, M., Grange, R., and Vandenboom, R. (2011). Myosin light chain phosphorylation and potentiation of dynamic function in fast mouse muscle. Pflugers Archiv (In Press)

Zhi, G, Ryder, J, Huang, J, Ding, P, Chen, Y, Zhao, Y, Kamm, K, and Stull, J. (2005). Myosin light chain kinase and myosin phosphorylation effect frequency-dependent potentiation of skeletal muscle contraction. Proceedings of the National Academy of Sciences USA, 102(48), 17519-17524.

Appendix A: Raw data

Table 1- Phosphorylation data – Table containing absolute data from all muscles used within the present investigations. *Phos. content* represent the ratio of phosphorylated RLC to total RLC (mol P-RLC / total-RLC per muscle sample).

Muscle #	Phos. content	Condition	Mean ± SEM
1	0.217	Frozen after 45 min equilibration (beginning of Exp.) *UNSTIMULATED*	0.17 ± 0.02
2	0.207		
3	0.183		
4	0.275		
5	0.086		
6	0.12		
7	0.165		
8	0.177		
9	0.496	Frozen ~ 17 s after first-CS *STIMULATED*	0.47 ± 0.02
10	0.455		
11	0.54		
12	0.366		
13	0.434		
14	0.548		
15	0.486		
16	0.58	Frozen ~ 17 s after third-CS *STIMULATED*	0.54 ± 0.02
17	0.61		
18	0.524		
19	0.517		
20	0.581		
21	0.552		
22	0.482		
23	0.157	Frozen ~ 30 min after final CS (end of Exp.) *UNSTIMULATED*	0.17 ± 0.05
24	0.185		
25	0.10		
26	0.087		
27	0.355		

Table 2- Mechanical data – Table containing absolute force data from isometric twitches ~ 5 s pre and ~ 15 s post-CS within each sequence. Relative data was determined by dividing post-CS by pre-CS values (represents the percent change in absolute force).

ISOMETRIC

Frequency	pre (mN)	post (mN)	relative
	74.1	89.69	1.21
	53.32	62.45	1.17
	61.06	74.39	1.22
	73.27	89.06	1.22
1.5Hz	52.92	63.2	1.19
	80.7	96.02	1.19
	73.89	88.25	1.19
	68.74	80.57	1.17
	65.14	75.62	1.16
	72.19	88.85	1.23
	52.03	61.82	1.19
	65.92	80.44	1.22
	77.2	91.64	1.19
3.3Hz	50.39	61.28	1.22
	77.12	93.95	1.22
	73.88	87.388	1.18
	71.47	85.71	1.19
	65.19	75.94	1.17
	70.03	87.56	1.25
	51.95	61.11	1.18
	63.26	78.2	1.24
	77.6	92.1	1.19
6.9Hz	48.68	59.24	1.22
	79.21	95.31	1.20
	73.96	87.28	1.18
	67.64	80.205	1.19
	63.45	75.27	1.19

Table 3- Mechanical data – Table containing absolute force data from concentric twitches during work cycle's ~ 5-10 s before, and ~ 15-20 s after the CS within each sequence. Relative data determined by dividing post-CS by pre-CS values (represents the percent change in absolute force).

CONCENTRIC

Frequency	pre (mN)	post (mN)	relative
	63.65	76.33	1.20
	45.31	52.36	1.16
	51.3	62.34	1.22
	62.47	75.61	1.21
1.5Hz	44.79	52.57	1.17
	68.35	80.79	1.18
	61.61	73.25	1.19
	58.76	67.97	1.16
	57.72	66.83	1.16
	50.5	64.89	1.28
	35.78	43.12	1.21
	43.59	54.91	1.26
	53.085	65.45	1.23
3.3Hz	33.93	42.49	1.25
	50.69	65.14	1.29
	46.83	58.045	1.24
	47.6	57.26	1.20
	47.72	58.09	1.22
	32.66	43.74	1.34
	22.48	27.56	1.23
	25.33	33.71	1.33
	35.45	44.24	1.25
6.9Hz	21.34	27.24	1.28
	33.17	42.74	1.29
	25.48	33.49	1.31
	27.26	34.86	1.28
	30.73	39.57	1.29

Table 4- Mechanical data – Table containing absolute force data from eccentric twitches during work cycle's ~ 5-10 s before, and ~ 15-20 s after the CS within each sequence. Relative data determined by dividing post-CS by pre-CS values (represents the percent change in absolute force).

ECCENTRIC

Frequency	pre (mN)	post (mN)	relative
	85.48	91.21	1.07
	63.44	65.80	1.04
	72.58	78.20	1.08
	84.98	92.44	1.09
1.5Hz	62.28	65.34	1.05
	94.81	99.51	1.05
	88.38	92.99	1.05
	80.80	83.19	1.03
	73.57	77.58	1.05
	97.73	102.30	1.05
	73.96	76.12	1.03
	94.66	96.02	1.01
	105.29	108.63	1.03
3.3Hz	71.27	73.24	1.03
	116.56	115.03	0.99
	111.38	110.85	1.00
	102.09	102.09	1.00
	85.33	87.27	1.02
	128.88	118.25	0.92
	98.62	97.89	0.99
	124.46	117.11	0.94
	142.72	137.74	0.97
6.9Hz	92.64	89.17	0.96
	153.83	148.14	0.96
	155.03	150.16	0.97
	130.48	117.79	0.90
	112.74	109.37	0.97

Table 5- Mechanical data – Table containing absolute work and power data from concentric contractions during work cycle's ~ 5-10 s before, and ~ 15-20 s after the CS within each sequence. Absolute work (J) and power (W) values were made relative to wet muscle mass in Kg. The relative difference (post / pre) represents the change in absolute force.

CONCENTRIC

Frequency	pre		post		relative
	work (J/Kg)	power (W/Kg)	work (J/Kg)	power (W/Kg)	
	0.68	1.02	0.58	0.87	0.85
	0.59	0.89	0.49	0.74	0.83
	0.70	1.05	0.57	0.86	0.82
	0.53	0.80	0.46	0.69	0.86
1.5 Hz	0.41	0.62	0.34	0.50	0.81
	0.81	1.22	0.72	1.07	0.88
	0.88	1.32	0.72	1.07	0.81
	0.53	0.80	0.44	0.66	0.82
	0.47	0.71	0.40	0.61	0.86
	1.07	3.55	1.10	3.65	1.03
	0.86	2.85	0.92	3.03	1.07
	1.10	3.62	1.13	3.72	1.03
	0.75	2.49	0.80	2.65	1.06
3.3 Hz	0.65	2.15	0.68	2.25	1.05
	1.15	3.81	1.27	4.19	1.10
	1.22	4.01	1.30	4.30	1.07
	0.89	2.94	0.90	2.95	1.01
	0.77	2.54	0.78	2.56	1.01
	1.01	6.95	1.42	9.83	1.41
	0.79	5.48	1.05	7.28	1.33
	0.96	6.60	1.32	9.08	1.38
	0.69	4.75	0.99	6.84	1.44
6.9 Hz	0.64	4.38	0.88	6.05	1.38
	1.04	7.16	1.45	10.04	1.40
	1.03	7.14	1.48	10.21	1.43
	0.69	4.78	0.96	6.60	1.38
	0.78	5.36	1.06	7.34	1.37

Table 6- Mechanical data – Table containing absolute work and power data from concentric contractions during work cycle's ~ 5-10 s before, and ~ 15-20 s after the CS within each sequence. Absolute work (J) and power (W) values were made relative to wet muscle mass in Kg. The relative difference (post / pre) represents the change in absolute force.

ECCENTRIC

| | pre | | post | | |
Frequency	work (J/Kg)	power (W/Kg)	work (J/Kg)	power (W/Kg)	relative
	0.88	1.32	0.80	1.20	0.91
	0.81	1.21	0.68	1.03	0.85
	0.92	1.38	0.74	1.11	0.81
	0.71	1.07	0.65	0.98	0.92
1.5 Hz	0.55	0.83	0.47	0.71	0.86
	1.09	1.63	0.99	1.49	0.91
	1.17	1.76	0.97	1.46	0.83
	0.71	1.07	0.64	0.96	0.89
	0.60	0.91	0.57	0.86	0.95
	1.99	6.57	1.88	6.21	0.95
	1.70	5.62	1.70	5.61	1.00
	2.29	7.56	1.98	6.52	0.86
	2.37	7.82	1.50	4.97	0.64
3.3 Hz	1.25	4.12	1.22	4.04	0.98
	2.39	7.89	2.26	7.47	0.95
	2.58	8.53	2.53	8.36	0.98
	1.75	5.76	1.65	5.45	0.95
	1.27	4.20	1.25	4.13	0.98
	3.87	26.70	3.58	24.73	0.93
	3.15	21.73	3.22	22.21	1.02
	4.21	29.03	3.99	27.55	0.95
	2.96	20.42	3.00	20.72	1.01
6.9 Hz	2.42	16.71	2.43	16.79	1.00
	4.48	30.88	4.46	30.79	1.00
	4.61	31.84	4.64	32.02	1.01
	3.06	21.14	2.83	19.55	0.92
	2.12	14.60	2.15	14.83	1.02

Appendix B: Representative traces

Fig 1- Representative workloops (passive tension included)

Illustrates representative concentric (A-C) and eccentric (D-F) workloops. Workloops were developed by plotting total force (mN) (passive response not subtracted) over muscle length (L_o). Arrows highlight the change total force response to concentric and eccentric stimulations as work cycle frequency increases.
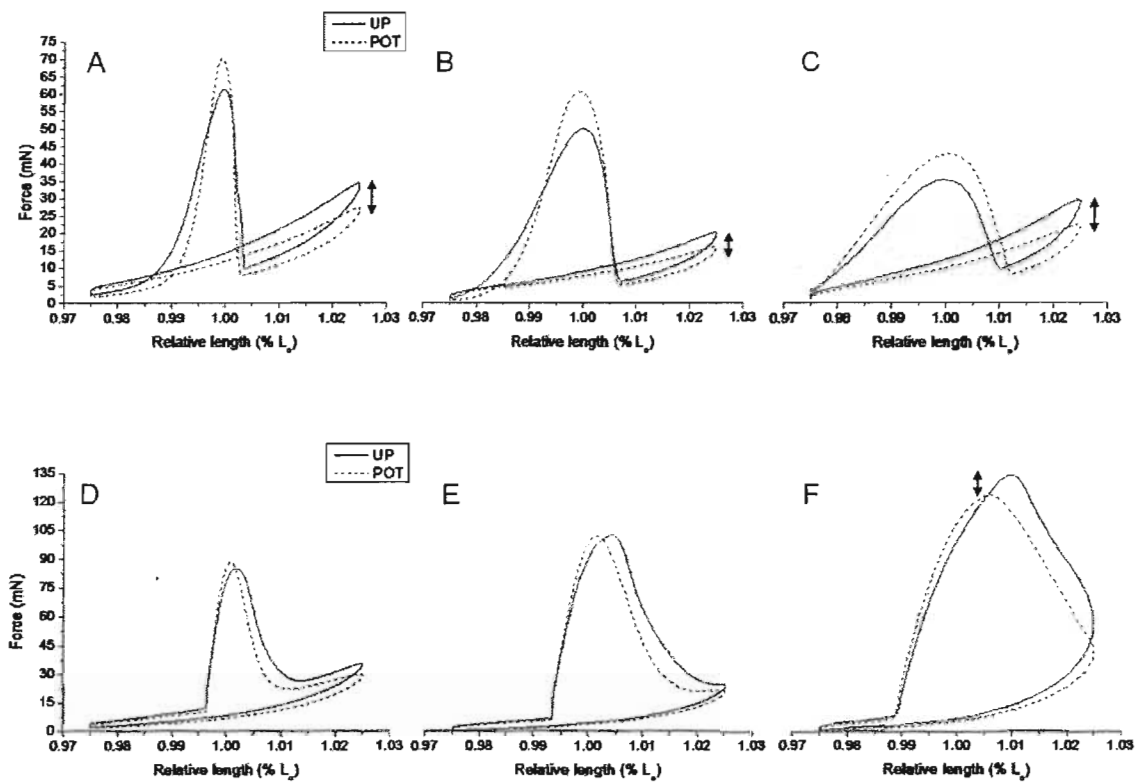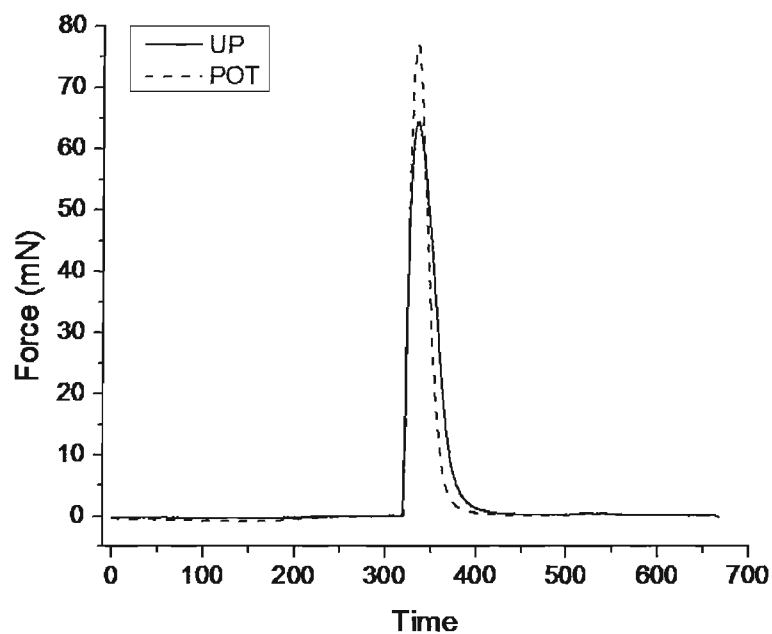
Fig 2- Representative force traces (A-F)

Representative concentric / eccentric force trace at each work cycle frequency, obtained by plotting force (mN) over time (ms). Demonstrated is the active force response from a 1 Hz stimulation, determined by subtracting the non-stimulated passive response from a stimulated response. Stimulations were timed in such a manner that peak twitch force occurred as the muscle shortened / lengthened through L_o.

(A) - Concentric force at 1.5 Hz

Representative concentric force trace at 1.5Hz, obtained by plotting force (mN) over time (ms).

(B) - Concentric force at 3.3 Hz
Representative concentric force trace at 3.3Hz, obtained by plotting force (mN) over time (ms).
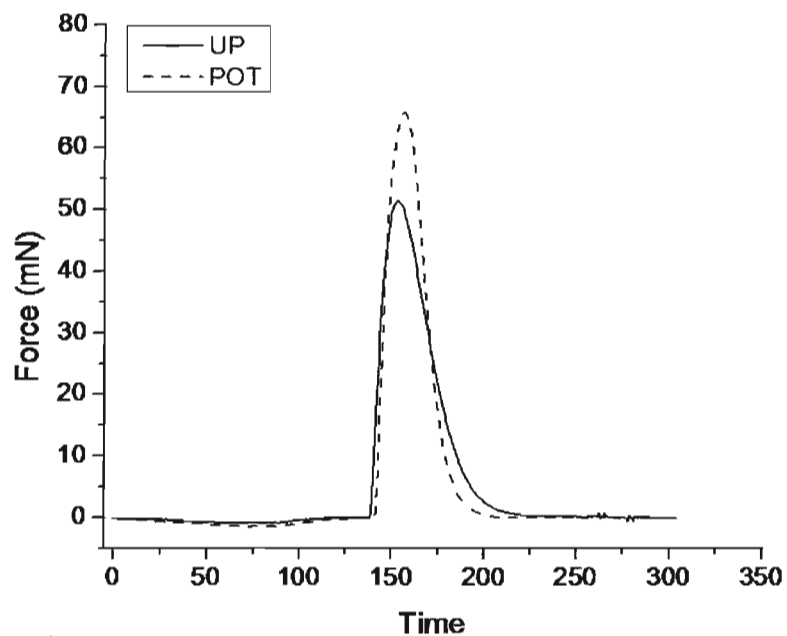
(C) - Concentric force at 6.9 Hz
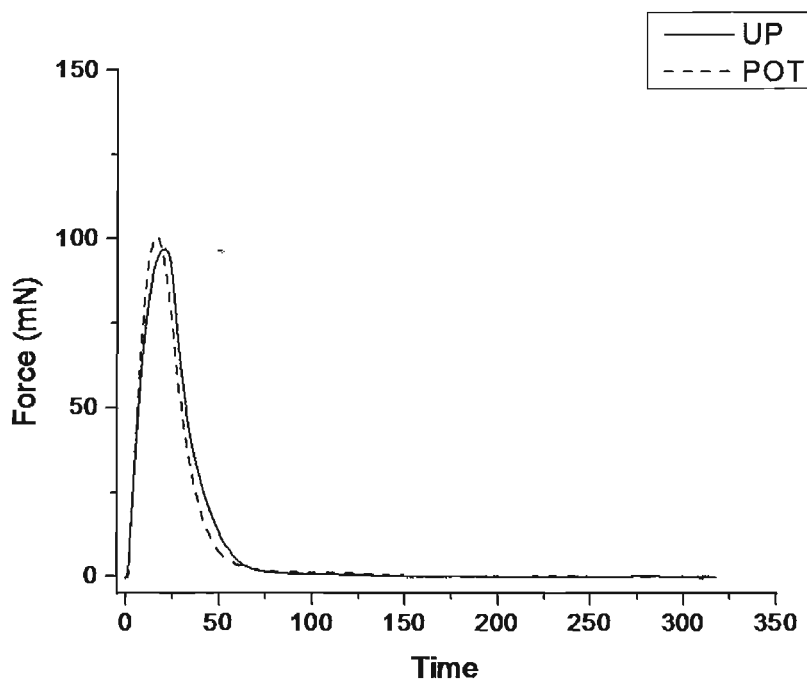Representative concentric force trace at 3.3Hz, obtained by plotting force (mN) over time (ms).
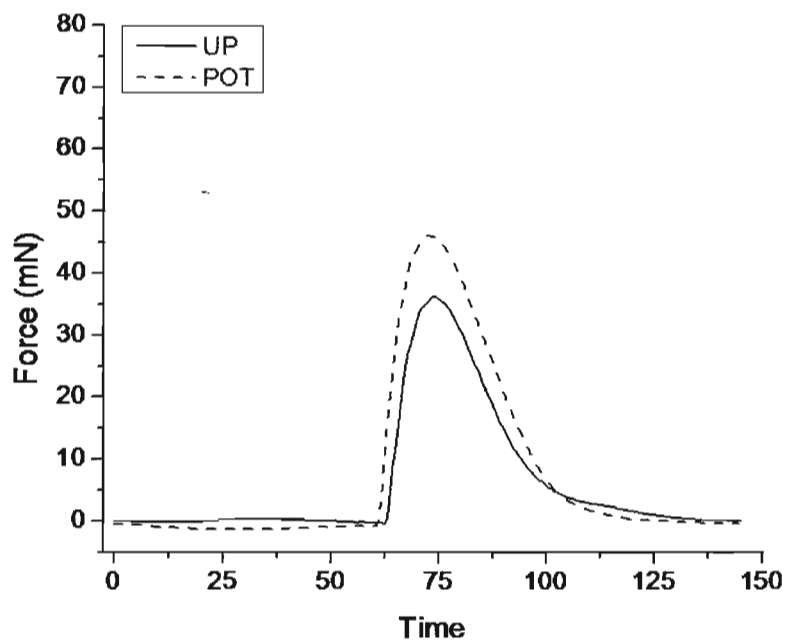
(D) - Eccentric force at 1.5 Hz

Representative eccentric force trace at 1.5 Hz, obtained by plotting force (mN) over time (ms).
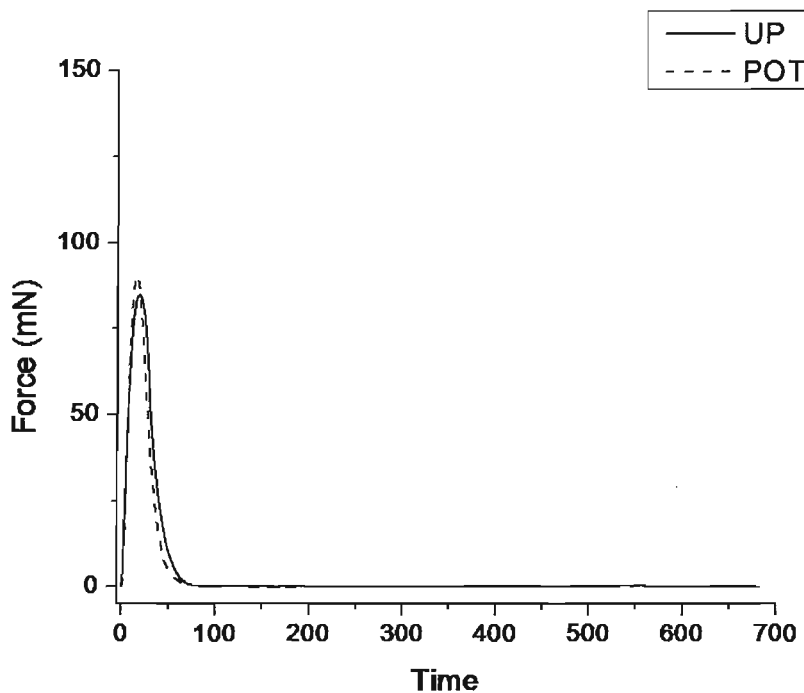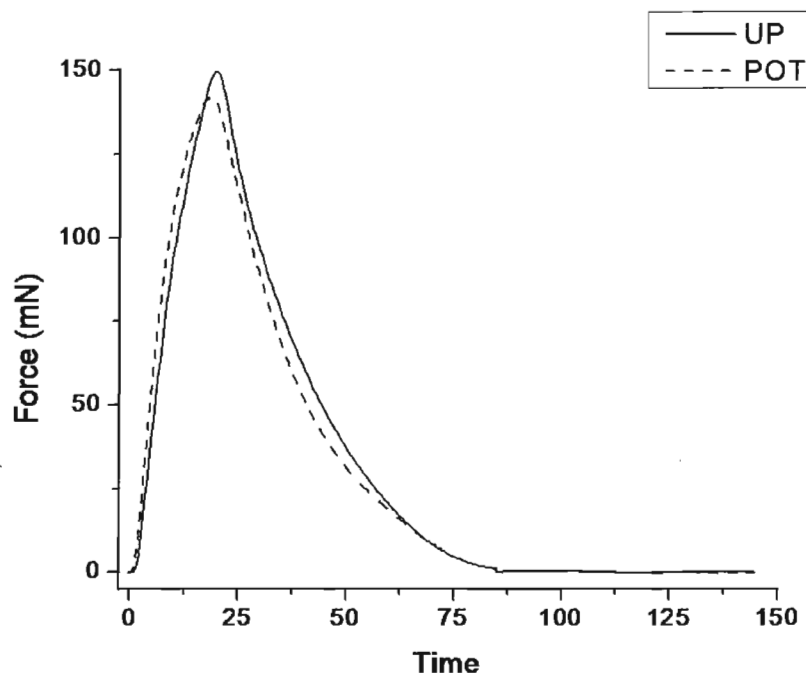

(E) - Eccentric force at 3.3 Hz

Representative eccentric force trace at 3.3Hz, obtained by plotting force (mN) over time (ms).

(F) - Eccentric force at 6.9 Hz

Representative eccentric force trace at 6.9Hz, obtained by plotting force (mN) over time (ms).

Appendix C: Slack test data

Slack tests for determination of unloaded shortening velocity

The slack test (Edman, 1979) is used as an indicator of a muscles capacity to maximally shorten the contractile apparatus during rest and fatigue conditions. Slack in the muscle sample is produced by rapidly shortening muscle length to a pre-determined position during a fused tetanic contraction. The time required for a contracting EDL to actively take up the compliance and produce measurable force is termed the slack time (ST). It has been shown that the size of the length step is positively correlated with slack time in a linear relationship (Edman, 1979). Slack test protocols will measure the slack time associated with five different length steps during sequential tetanic contractions and plotting these points. The slope of the linear regression fit to this data will determine the maximal unloaded shortening velocity. Length steps for the five tetani will be equal to 10, 12.5, 15, 17.5 and 20% of L_o. Slack time is therefore determined using a calculation-based method due to the difficult nature of determining the exact moment of force redevelopment. This calculation involves differentiation of the force-time function and subsequent quantification of 20% of the peak rate of force development (+dP/dt). The time that corresponds to 20% of peak +dP/dt is subtracted from the time at which the length step was initiated to calculate slack time (ST).

Fig. 3 (a) Representative slack test (Gittings, W. (2009). *The Influence of Myosin Regulatory Light Chain Phosphorylation on the Contractile Performance of Fatigued Mammalian Skeletal Muscle.* (Master's thesis).
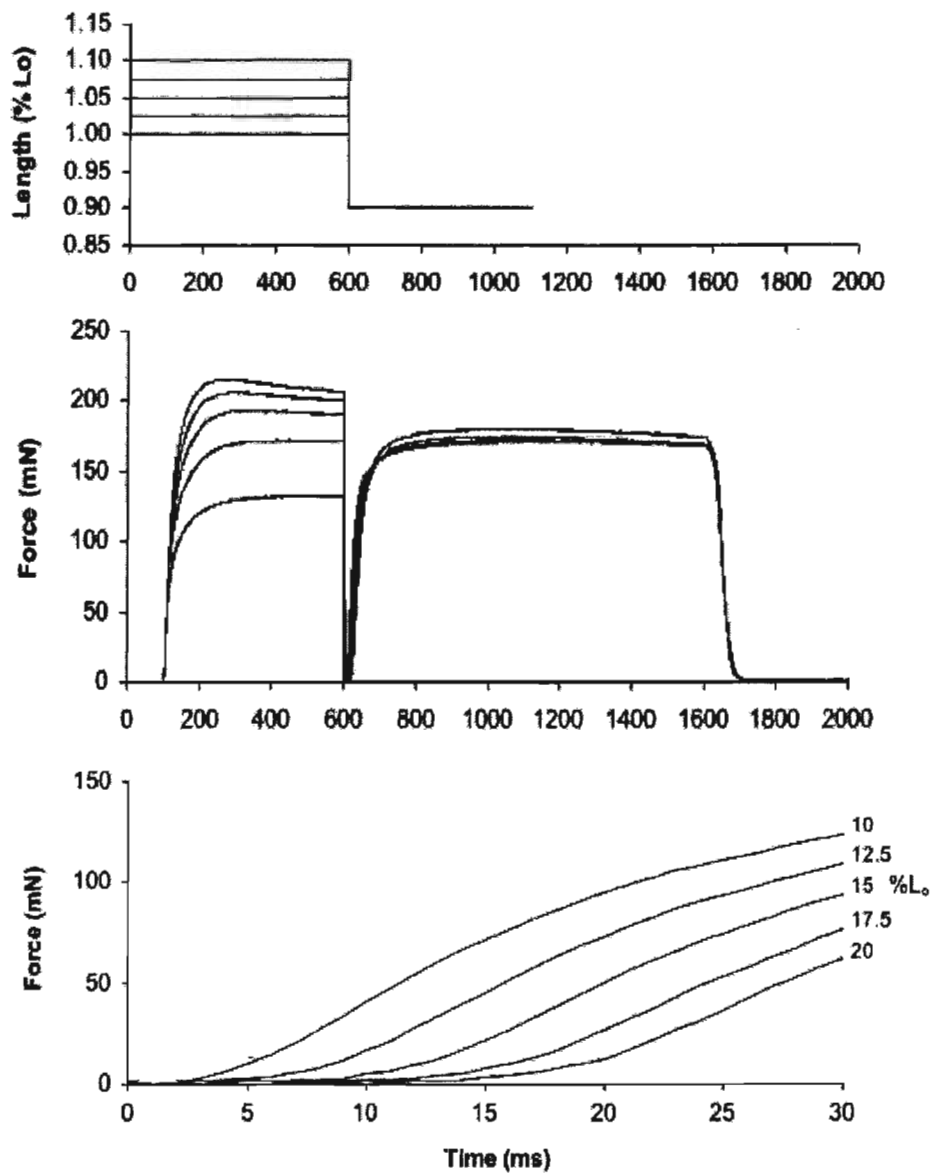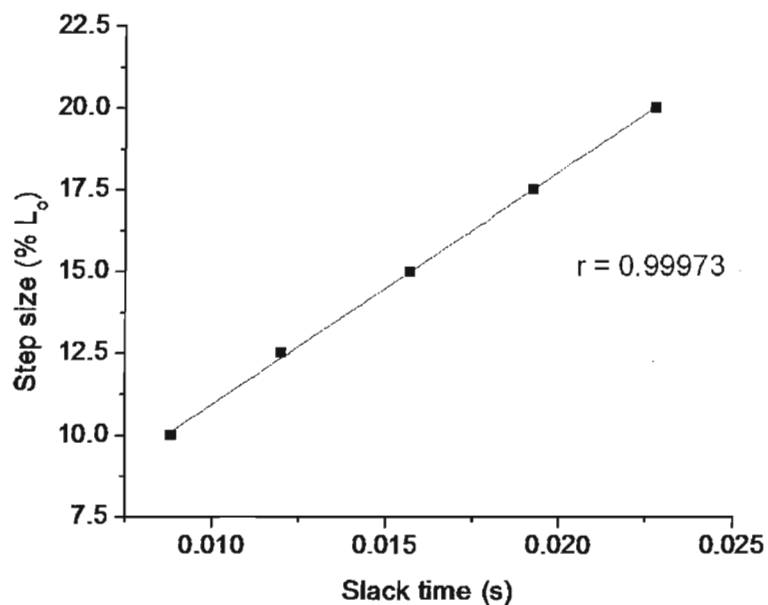
Fig. 3(b) Representative slack test results

Figure 3 (a and b) display a representative slack test from adult female mouse fast muscle. Fig. 1(a) was taken from Gittings (2009) Master's thesis as the identical protocol was employed in the present study. Fig. 1(b) demonstrates the correlation between step size and slack time for EDL *in vitro* (25° C). Plotted are the corresponding slack times (s) to predetermined length steps (% L_o) along with the respective Pearson's r-value. A value of 0.99973 demonstrates a strong positive linear relationship between the independent and dependent variables.